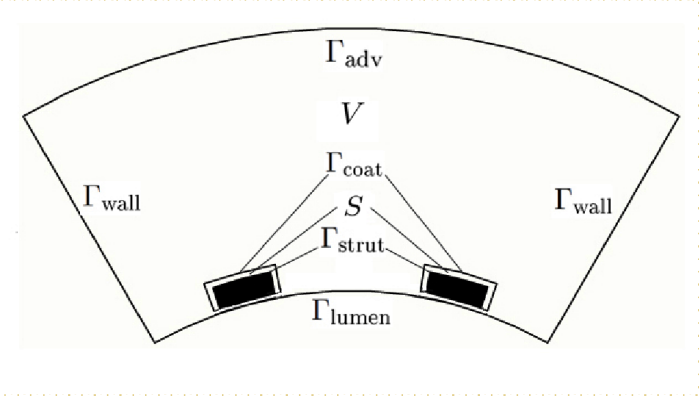

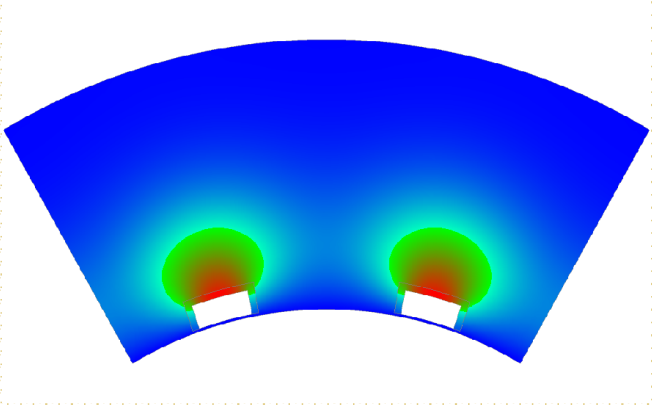

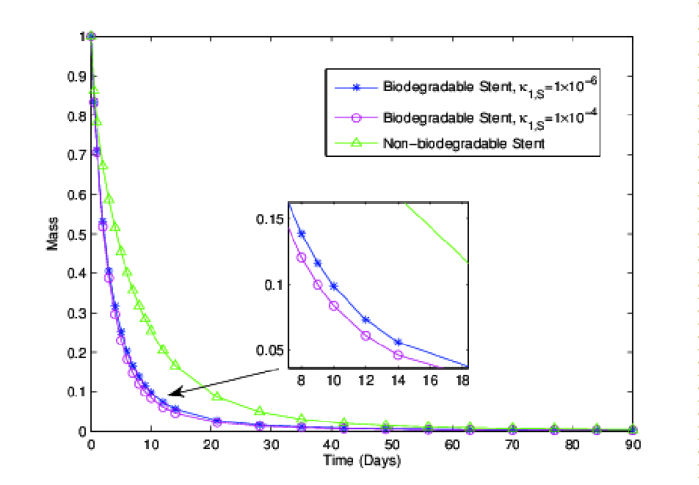

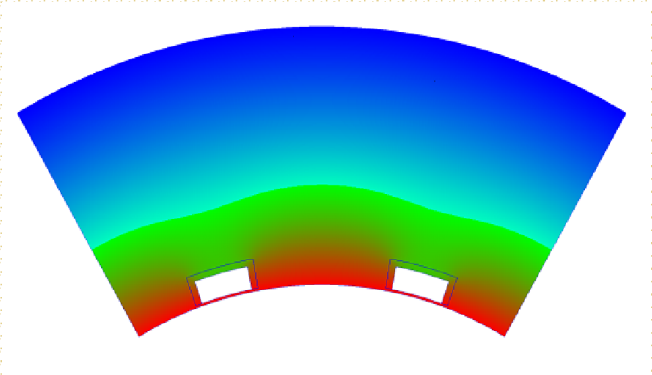

Jahed Naghipoor

NON-FICKIAN MODELS FOR BIODEGRADABLE DRUG ELUTING STENTS

Tese de Programa Inter-Universitário de Doutoramento em Matemática, orientada pelo Professor Doutor José Augusto Ferreira e Professora Doutora Paula de Oliveira e apresentada ao Departamento de Matemática da Faculdade de Ciências e Tecnologia da Universidade de Coimbra.

2014

· U C ·

UNIVERSIDADE DE COIMBRA

University of Coimbra

Doctoral Thesis

Non-Fickian Models for Biodegradable Drug Eluting Stents

Author:
Jahed Naghipoor

Supervisors:
Professor José A. Ferreira
Professor Paula de Oliveira

Tese apresentada à Faculdade de Ciências e Tecnologia da Universidade de Coimbra, para a obtenção do grau de Doutor - Programa Inter-Universitário de Doutoramento em Matemática

June 2014

Abstract

Mathematical modeling and numerical simulation of cardiovascular drug delivery systems have become an effective tool to gain deeper insights in the pharmacokinetics of therapeutic agents in cardiovascular diseases like atherosclerosis. Drug Eluting Stents (DES) which are tiny expandable mesh tubes coated by a polymer with dispersed drug, represent a major advance in the treatment of obstructed artery diseases.

The main objective of this thesis is to study a mathematical model that simulates "in vivo" drug delivery from a biodegradable DES. To study the complete problem of penetration of therapeutic agent from DES into the arterial wall, we progressively address more complex models.

The first model, presented in Chapter 2, will describe with details, in a simple two dimensional geometry, the biodegradation of polylactic acid (PLA), a material of choice in the design of DES, that degrades due to the penetration of plasma that breaks the polymer chains and reduces its molecular weight.

When drug diffuses from a polymer into a viscoelastic arterial wall, it is observed that the process can not be completely described by Fick's law of diffusion which was proposed by Adolf Fick in 1855. The reason lies in the fact that as drug diffuses into the arterial wall, it causes a deformation which induces a stress driven diffusion that act as a barrier to the drug penetration. Thus a modified flux should be considered, resulting from a sum of the Fickian flux and a non-Fickian flux.

To take into consideration this non-Fickian flux, we add a degree of complexity to the first model, by introducing in Chapter 3 the stress response of the arterial wall. It is a memory effect established by Maxwell-Wiechert model or Fung's quasilinear viscoelastic model.

To obtain a more realistic model of drug pharmacokinetics, the reversible nature of binding, between the agent and immobilized sites in the arterial wall, is considered in Chapter 4. The behavior of different families of drugs is compared.

Theoretical results concerning qualitative properties of the solutions and stability of the models are presented along the dissertation. From the numerical

viewpoint some aspects of clinical importance such as the influence of elastic modulus of the arterial wall, the effect of biodegradation of PLA, the permeability of the stent coating as well as the binding rates in the arterial wall will be addressed in this thesis.

A software package, to simulate the models in this dissertation, has been developed using freeFEM++.

Keywords: Non-Fickian coupled model, cardiovascular drug delivery, drug eluting stents, viscoelastic diffusion coefficient, numerical simulation.

Resumo

A modelação matemática e a simulação numérica do comportamento de sistemas de libertação controlada de fármacos constituem instrumento centrais na compreensão da farmacocinética de agentes terapêuticos nas doenças cardiovasculares, como por exemplo a aterosclerose. Os "stents" com libertação controlada de fármaco[1], que são tubos metálicos revestidos por um polímero que contem um fármaco disperso, constituem um tratamento de eleição em caso de obstrução de vasos.

O objectivo central desta tese é o estudo analítico e numérico de um modelo matemático que descreva a libertação de fármacos "in vivo", a partir de um "stent" com revestimento biodegradável. Para tal apresentamos ao longo da dissertação modelos progressivamente mais complexos, que culminam num sistema que descreve a biodegradação do polímero mas também propriedades dos tecidos vasculares como a viscoelasticidade e a ocorrência de afinidades entre o fárrmaco e o tecido vascular.

O primeiro modelo que estudamos, no Capítulo 2, descreve com detalhe a influência da biodegradação do ácido poliláctico (PLA), que é um dos polímeros mais usados no revestimento de *stents*. A degradação ocorre devido à penetração do plasma no *stent* com a consequente quebra das cadeias do polímero e a redução do seu peso molecular.

Quando o fármaco se difunde na parede vascular, que é viscoelástica, o processo não pode ser completamente descrito pela Lei de Fick, proposta por Adolf Fick em 1855. A razão reside no facto de o fármaco, ao difundir-se na parede vascular, causar uma deformação, que induz uma resposta do polímero sob a forma de uma resistência à penetração do agente terapêutico. No Capítulo 3 o fluxo Fickiano, considerado no modelo do Capítulo 2, é então modificado, pela introdução de um "anti-fluxo" de origem viscoelástica.

Para obter uma descrição mais realista da farmacocinética do agente terapêutico na parede do vaso incluímos, no Capítulo 4, a afinidade química entre o agente e o tecido vivo. O comportamento de fármacos hidrofílicos e hidrofóbicos é analisado.

[1]Drug Eluting Stents (DES) em língua inglesa

São apresentados nesta dissertação resultados teóricos relativos às propriedades qualitativas das soluções e à estabilidade dos modelos estudados. Do ponto de vista numérico são discutidos diferentes aspectos de importância clínica, como a influência do módulo de Young da parede vascular, as propriedades de degradação, a permeabilidade do revestimento polimérico e a afinidade do fármaco com a parede vascular.

Foi desenvolvida uma aplicação computacional, utilizando o "software" de livre acesso freeFEM++, para simular o comportamento dos modelos estudados nesta tese.

Palavras chave: Modelo acoplado não Fickiano, libertação controlada de fármacos no sistema cardiovascular, "stents" com libertação controlada de fármaco, coeficiente de difusão viscoelástico, simulação numérica.

Acknowledgments

Completing my PhD degree is probably the most challenging activity of my life thus far. The best moments of my doctoral journey have been shared with many people. It has been a great privilege to spend four years in the Department of Mathematics at University of Coimbra, and its members will always remain dear to me.

My first and foremost debt of gratitude must go to my supervisors, Professor José Augusto Ferreira and Professor Paula de Oliveira for making it possible to work on such a fascinating subject in the framework of my PhD thesis. They patiently provided the vision, encouragement and advise necessary for me to proceed through the doctorial program and complete my thesis.

I would like to thank Fundação para a Ciência e a Tecnologia (FCT) for the financial support under the scholarship SFRH/BD/51167/2010. My grateful thanks are extended to the Centro de Matemática da Universidade de Coimbra (CMUC) for supporting me in scientific events.

A special thank goes to my family. Words cannot express how grateful I am to my mother, father and siblings for their unbounded supports. I would also like to thank all of my friends who supported me in writing, and incented me to strive towards my goal. We had great moments together in Coimbra.

Last but not the least, I would like to express my heartfelt gratitude to my darling wife, Atefeh, for her unconditional love and unwavering supports.

Contents

List of Figures

List of Tables

Abbreviations

DES	**D**rug **E**luting **S**tent
BMS	**B**are **M**etal **S**tent
PLA	**P**oly**L**actic **A**cid
PLGA	**P**oly**L**actic-co-**G**lycolic **A**cid
QLV	**Q**uasi-**L**inear **V**iscoelastic
FEM	**F**inite **E**lement **M**ethod
VP	**V**ariational **P**roblem
FEVP	**F**inite **E**lement **V**ariational **P**roblem
IC	**I**nitial **C**ondition
BC	**B**oundary **C**ondition
IBC	**I**nterface **B**oundary **C**ondition
IBVP	**I**nitial **B**oundary **V**alue **P**roblem
IMEX	**IM**plicit **EX**plicit

Symbols

Symbol	Name	Unit
$\kappa_{1,S}, \kappa_{2,S}, \kappa_{1,V}$	Reaction rate	$\frac{cm^2}{g.s}$
$\kappa_{u,V}$	Association rate	$\frac{cm^2}{g.s}$
$\kappa_{b,S}$	Dissociation rate	$\frac{1}{s}$
M_W	Molecular weight	$\frac{g}{mol}$
α, β, γ	Autocatalysis rate	$\frac{s}{cm^2}$
k_S, k_V	Permeability	cm^2
μ_S, μ_V	Viscosity	$\frac{g}{cm.s}$
$C_{m,S}, C_V, C_{m,V}$	Concentration	$\frac{g}{cm^2}$
$D_{m,S}, D_V, D_{m,V}$	Diffusion coefficient	$\frac{cm^2}{s}$
$\gamma_{m,V}$	Transference rate	$\frac{cm}{s}$
P_c	Transference rate	$\frac{cm}{s}$

Chapter 1

Introduction and Problem Setting

In this thesis, we address the analytical and numerical study of the diffusion of a drug from a biodegradable stent and its release into a viscoelastic artery. The mathematical results established will be used to study the pharmacokinetics of drug eluting from a stent into the arterial wall.

In Chapter 1, we introduce biomedical concepts concerning the cardiovascular system and refer some treatments of cardiovascular diseases like atherosclerosis. We also establish the basic concepts to answer to the following questions:

- How can mathematical modeling clarify the mechanisms underlying the cardiovascular drug delivery systems?
- Why are drug eluting stents useful medical devices in cardiovascular drug delivery systems?
- What are the influences of the mechanical properties of the arterial wall and the affinities drug/vascular tissue, in the process of drug release by drug eluting stents?

Section 1.1 is devoted to controlled drug delivery and its application in medicine. In Section 1.2 we review the structure of the arterial system to study possible treatments of atherosclerosis. In Section 1.3 we investigate the application of cardiovascular stents (bare metal stents and drug eluting stents), their advantages

and failures for the treatment of the atherosclerosis. Polymer's degradation and its application in the cardiovascular stents will be also studied in this section. Mathematical models are briefly reviewed in Section 1.4.

1.1 *Controlled drug delivery*

Controlled drug delivery is the release of drug at a specified rate which is determined by the demand of the living system organ or tissue over a specified period of time ([43]). Since the sudden delivery of too much drug can be harmful and the release of too little amount of drug may limit its effectiveness, the control of the rate of drug release is a crucial issue.

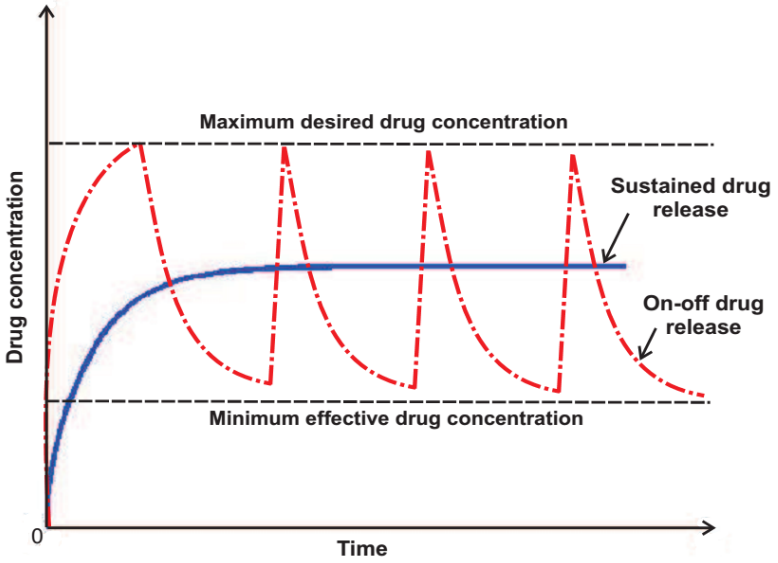

FIGURE 1.1: Profile of drug concentration in traditional release (red) and controlled release (blue) ([43]).

Traditional delivery systems are characterized by immediate and uncontrolled drug release kinetics. Accordingly, drug absorption is essentially controlled by the body's ability to assimilate the therapeutic molecule and thus, drug concentration in different body tissues, typically undergoes an abrupt increase followed by a similar decrease. As a consequence, it may happen that drug concentration

dangerously approaches the toxic threshold to subsequently fall down below the effective therapeutic level ([18]).

To predefine the performance of drug delivery systems, traditional delivery systems, as for example simple pills, have been replaced by controlled drug delivery systems (see Figure 1.1) to maintain drug concentration in target tissues at a desired value as long as possible and to help to control both under and overdosing ([18, 43]).

In controlled drug delivery systems part of the drug dose is initially released in order to rapidly get the drug effective therapeutic concentration. Then, drug release kinetics follows a well defined behavior in order to supply the maintenance dose, enabling the attainment of the desired drug concentration ([18]).

There is a huge literature in the field of controlled drug delivery. Some of these studies have an experimental character, others are completed with mathematical models. We mention without being exhaustive to [10, 12, 18, 22, 24, 35, 43].

1.2 *Arterial system: structural compounds and diseases*

The vasculature is a complex architecture of vessels that carry blood to and from the different organs of the body. The blood vessels may be classified based on their sizes, function and proximity to the heart. A vessel named *Artery* with 1 mm wall thickness and 4 mm lumen thickness is one of the thickest vessels of the arterial system which tolerate a pressure profile varying from 80 mmHg to 120 mmHg in each cardiac cycle.

Arteries are roughly subdivided into two types: elastic and muscular. Elastic arteries are located close to the heart, have relatively large diameters and are regarded as elastic structures. Muscular arteries are smaller, located at the periphery and are regarded as viscoelastic structures. Smaller arteries typically display more pronounced viscoelastic behavior than arteries with large diameters.

In what follows, we mention a few structural components of the arterial wall which are bio-mechanically relevant.

- **Endothelial cells** are cells in the arterial wall in direct contact with blood flow that have negligible mechanical properties. Its main action is the prevention of thrombosis (the formation of a blood clot) and the entry of blood

borne bacteria into the vascular wall. It can regenerate itself when it is injured;

- **Elastin** is a protein in connective tissue with high elastic properties and low stiffness. It allows tissues to resume their shape after stretching or contracting. It can stretch up to 60 percent and remain elastic to bear the load under physiological conditions;
- **Collagen** is a tortuous, thick fiber component of vascular wall with high stiffness. It is responsible for structural integrity of the vessel;
- **Smooth muscle cell** is a component that is responsible for active properties of blood vessel wall;
- **Ground substance** is a component that acts like a glue to keep all arterial components together.

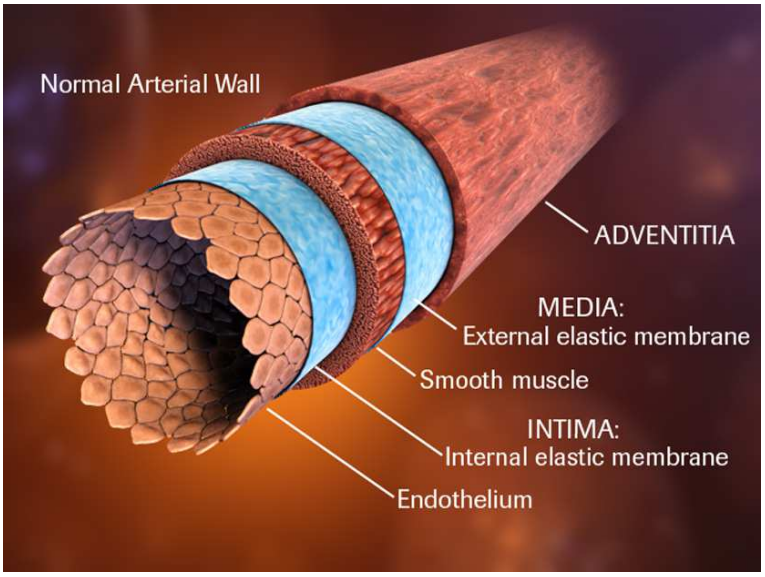

FIGURE 1.2: Layers of the arterial wall (http://www.3fx.com/Our-Work/Medical-Illustration.aspx).

Arterial walls are mainly composed of the three distinct layers named intima, media and adventitia (see Figure 1.2).

- **Intima** is the innermost layer of the artery and offers negligible mechanical strength in the healthy young individuals. It consists of an endothelial cell mono-layer that prevents blood, including platelets and other elements, from adhering to the lumenal surface. The mechanical contribution of the intima may become significant for aged arteries where the intima becomes thicker and stiffer;

- **Heterogeneous media**, the thickest layer of the artery, is composed by elastin (24%), vascular smooth muscle cells (33%), collagen (37%) and ground substances (6%). However, it behaves mechanically as a homogeneous material. Due to the high content of smooth muscle cells, it is the media that is responsible for the viscoelastic behavior of the arterial wall;

- **Adventitia** is composed of elastin (2%), ground substances (9%), fibroblast (9%) and collagen fibers (78%). At very high strains, the adventitia changes to a stiff tube which prevents the artery from overstretching and rupturing.

In the healthy young individuals, only the media and the adventitia are responsible for the strength of the arterial wall and play significant mechanical roles by carrying most of the stresses. At low strains (physiological pressures), it is chiefly the media that determines the properties of the arterial wall.

Other layers of arterial wall are as follow.

- **Endothelium**, a thin layer of cells with thickness $2\mu m$ that lines the interior surface of blood vessel and vessel forming, as an interface between circulating blood and the rest of the arterial wall;

- **Glycocalyx**, a thin layer of macromolecules with thickness $100nm$ to cover a plasma membrane of a single layer of endothelial cells;

- **Internal elastic lamina**, a layer of elastic tissue with thickness $2\mu m$ that forms the outermost part of the intima of blood vessels. It separates intima from media;

- **External elastic lamina**, a layer of elastic connective tissue lying immediately outside the smooth muscle of the media of the artery. It separates media from adventitia.

Cardiovascular diseases are among the leading causes of death in the industrialized world. Although since the 1970s, cardiovascular mortality rates have declined in many high-income countries, cardiovascular deaths have increased at a fast rate in low-income and middle-income countries ([40]). Among all cardiovascular diseases, atherosclerosis is the most common cardiovascular disease wherein some arteries start thickening until they eventually occlude. This process normally happens over a period of 50 to 60 years and seems to get particularly severe with age. In some cases, it begins in early life making primary prevention efforts necessary from childhood ([40]).

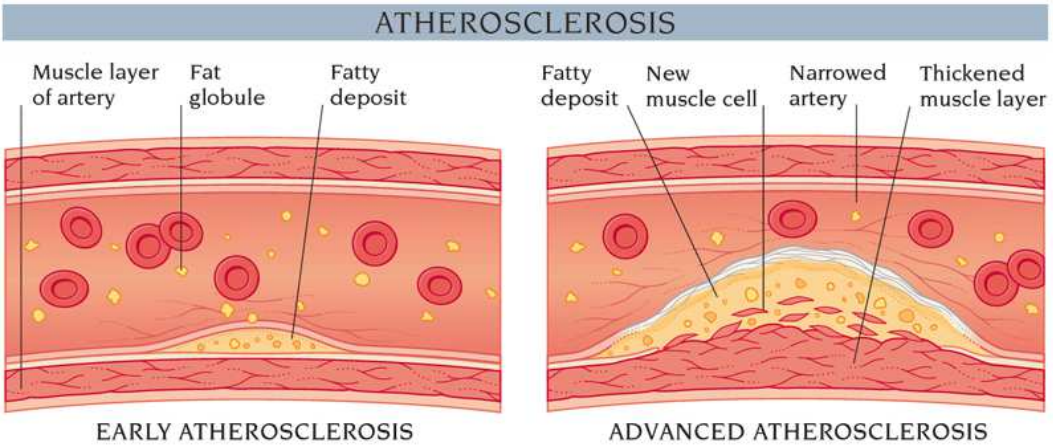

FIGURE 1.3: Atherosclerosis (http://www.nmihi.com/a/atherosclerosis.htm).

This disease is characterized by intramural deposits of lipids and proliferation of vascular smooth muscle cells. These changes are accompanied by loss of elasticity of the vessel wall and narrowing of the vascular lumen. Coronary atherosclerosis is clinically the most important aspect of atherosclerosis. As coronary arteries are relatively narrow, atherosclerosis could seriously reduce the blood flow through them. Initial and advanced atherosclerosis in the coronary artery are depicted in Figure 1.3.

To face with the pathology of atherosclerosis, different treatments have been developed during the years. The technology moves from invasive techniques to more safe and non invasive techniques.

Balloon angioplasty as it is shown in Figure 1.4, is the first technique of mechanically widening narrowed or obstructed arteries caused by atherosclerosis. An empty and collapsed balloon on a guide wire, known as a balloon catheter, is passed into the narrowed locations and then inflated to a fixed size using water pressures between 75 to 500 times of normal blood pressure. Inflated balloon dilates the blocked segment of the artery by compressing the atherosclerosis plaque and stretching of the arterial wall.

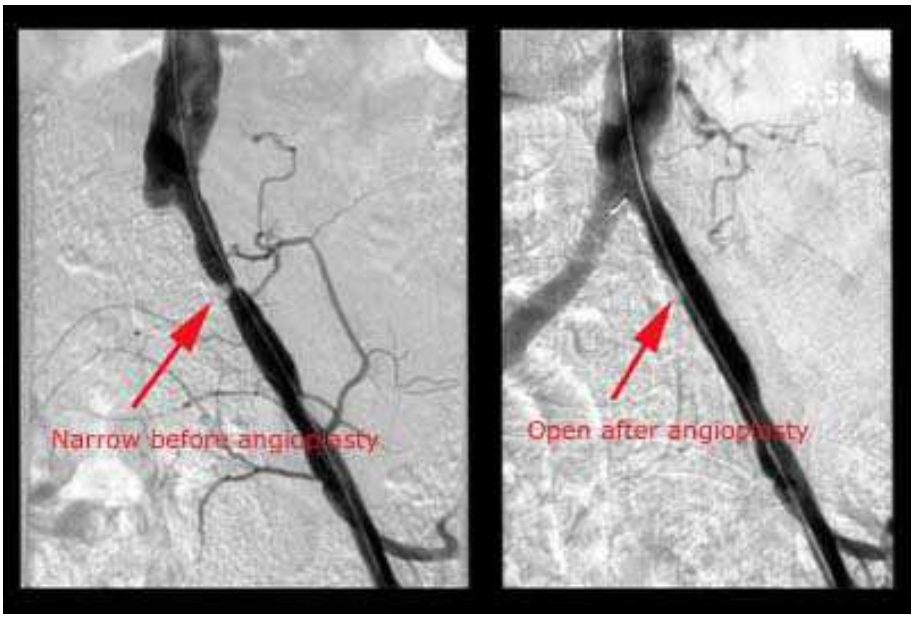

FIGURE 1.4: Balloon angioplasty (http://www.vascular.co.nz/angiogram.htm).

After many years of clinical experience and many catheter designs, angioplasty is still far from being perfect. A common problem called restenosis, re-narrowing the blood vessel, is being the main failure of the angioplasty. Restenosis occurs when blockage returns a few weeks after coronary angioplasty procedure. Although the initial success rate of the angioplasty for opening the blocked coronary arteries reached 95%, many studies reported acute blood clots in 3% to 5% and restenosis rates between 25% to 50% at 3 to 6 months after angioplasty ([39]). In this case, patient may require another angioplasty or a coronary artery bypass surgery. This procedure deeply injures the surface of the arterial wall so that deposition of proteins as well as platelets and inflammatory response stimulates the growing of a new plaque ([26]).

Problems like abrupt vessel closure and restenosis are being the main reasons of introducing new techniques like cardiovascular stents to overcome failures of the angioplasty ([39]).

1.3 *Cardiovascular stents*

A coronary stent is a tiny expandable mesh tube made by stainless steel which is delivered on a balloon catheter and implanted in the coronary artery, after balloon angioplasty, to help keep the artery open.

After the plaque is compressed against the arterial wall, the stent is fully expanded into position, thereby acting as a scaffold for the artery. The balloon is then deflated and removed and the coronary stent is left behind in the patient's artery. This technique results in a treatment option that requires much less recovery time when compared to balloon angioplasty ([39]).

In general, cardiovascular stents have two distinct and significant chronic failures:

- Immediately after deployment, thrombosis (acute blood clot) can occur due to the thrombogenic aspect of the stent promoting a foreign body response. This phenomena can be promptly treated with drug therapy;
- The other critical failure is in-stent restenosis which is the narrowing of a stented coronary artery due to the development of neo-intimal hyperplasia within the stent.

As it is already mentioned in Section 1.2, coronary balloon angioplasty is limited by abrupt closure and high percent of restenosis. Due to mentioned failures, bare metal stents (BMS) (Figure 1.5) were proposed to prevent these complications. However, they are associated with restenosis rates of $25\% - 30\%$ and also around $20\% - 25\%$ of bare metal stented arteries need a second procedure within 6 months. The other failure of BMS is that due to their microstructural properties, metals are not feasible materials to act as loadable drug carriers.

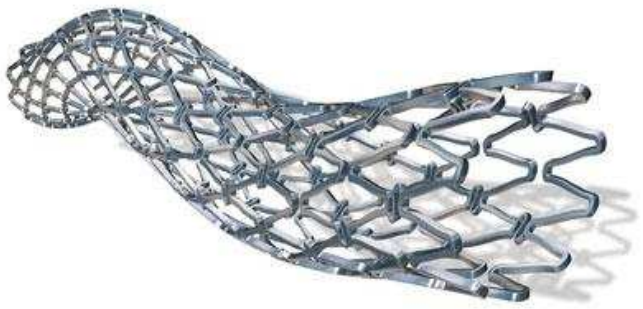

FIGURE 1.5: Bare metal stent (http://www.medgadget.com/2006/01).

All these drawbacks have encouraged significant efforts in the development of new stent materials, either used in coatings or in stents completely made of polymeric materials. Drug eluting stent (DES) is one of these new stent materials.

A DES is a stent that is coated by a polymer, containing an anti-proliferative agent, which is released gradually over the course of weeks to months after insertion of the stent. It will provide sustained inhibition of the neointimal proliferation as a response of vascular injury.

In $2002-2003$, DES were approved by regulatory bodies in Europe and also in the USA when initial studies showed a dramatic reduction in rates of restenosis compared to BMS.

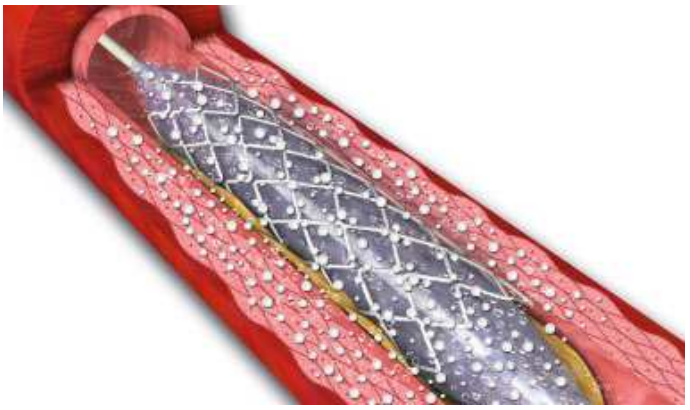

FIGURE 1.6: Drug eluting stent implanted in the blood artery (http://www.cxvascular.com/cn-latest-news/).

A DES (Figure 1.6) has three principal components: a stent platform (strut), a polymer coating and a drug. The drug is contained within the polymer coating and then diffuses into the arterial wall from the polymer source. The first DESs were designed with nondegradable polymer coatings; however, some of the newer DESs are manufactured with biodegradable polymer coatings ([43]).

Some benefits of DES are mentioned bellow:

- If a DES degrades in a controlled manner, the profile of released drug can be predicted;
- The gradual softening of DES leads to a smooth transfer of the load from the stent to the healing wall.

The primary pathophysiological mechanism of restenosis involves an exaggerated healing response of smooth muscle to vascular injury. In fact the injury made by angioplasty induces smooth muscle cells to proliferate and migrate to subintimal layer where the smooth muscle continue to migrate. These processes cause neointimal mass to expand and gradually encroach on the coronary artery.

It has been observed that smooth muscle cell derived from injuries of angioplasty show a higher migratory activity than cells made from primary injuries. Injuries with higher aggressive smooth muscle cells will develop more restenosis than an injury without such aggressive cells. Endothelial cells normally have some inhibitors like nitric oxide and heparin sulfate to inhibit smooth muscle cell proliferation. Their removal by angioplasty procedure contributes to a proliferative environment leading to restenosis.

As it is mentioned earlier, new generation DES are made of biodegradable polymers. A polymer is a large molecule made from many smaller units called monomers. The mechanical properties of a polymer are determined by many factors in addition to the monomer from which it is made. Properties such as stiffness, strength and degradation time are affected by the number of monomers within the chain (molecular weight) and the arrangement of the monomers. In general, the greater the molecular weight (longer chain of monomers), the greater strength and greater absorption time the polymer will have.

In DES, a polymeric material is used to coat the metallic struts, to serve as a drug carrier and to regulate and control the elution of the drug. Numerous polymers and co-polymers such as polylactic acid (PLA) and polylactic-co-glycolic acid (PLGA) have been studied experimentally and empirical models of drug release have been developed ([6, 8, 9]).

Studies to identify families of polymers that degrade predictably and disappear over time have become increasingly important. In the case of polymers used in drug eluting stents this aspect is crucial because the safe and predictable disappearance is one of the key factors in evaluating their performance.

Biodegradable polymers have hydrolysable bonds, making hydrolysis the most important mode of degradation. In biodegradable polymeric devices, the drug is released by the degradation and dissolution of the polymeric matrix, or by the cleavage of a covalent bond that binds the drug within the polymeric matrix.

Biodegradable polymers, however, are designed to slowly dissolve following implantation. Biodegradable polymers used in drug delivery must induce no undesirable or harmful tissue responses, and the degradation products must be nontoxic.

PLA is the polymer most commonly used for the production of biodegradable stents. Molecular weight of PLA is controlled by the quality of lactide used. The less water the lactide contains, the purer the PLA, with a higher molecular weight.

Pharmacological agents like dexamethasone, heparin, nitric oxide, paclitaxel and sirolimus have been investigated to inhibit restenosis by angioplasty procedure. These pharmacological agents have been used in stent coating in a number of commercial drug eluting stents. Recently, two more drugs, everolimus and zotarolimus, were added to the list of smooth muscle cell proliferation inhibitors used in drug eluting stents. Everolimus is being clinically investigated by Abbott Vascular, Santa Clara, CA, USA, with the XIENCE V^{TM} everolimus eluting coronary stent. The interesting fact about this drug is that it is used in conjunction with a new biodegradable polymer coating and give promising results in initial clinical studies.

In this dissertation, information from XIENCE V^{TM} everolimus eluting coronary stent investigated by Abbott Vascular is used to study the coronary drug eluting stent.

1.4 *Mathematical models for coupled cardiovascular drug delivery*

Mathematical modeling and numerical simulations of drug transport inside the arterial wall help to understand the efficacy of the treatment and can provide manufacturers with guidelines to optimize delivery from DES. During the last years, a number of studies have proposed mathematical models for coupled drug delivery in the cardiovascular tissues. We refer without being exhaustive to [2, 5, 24, 26, 33, 40, 43, 44, 46]. Most of these studies address the release of drug and its numerical behavior in one dimension, while the viscoelasticity of the arterial wall and the behavior of the biodegradable polymer are disregarded.

Pontrelli and de Monte ([31–33]) developed mathematical models for drug release through a DES in contact with the arterial wall as a coupled cardiovascular drug delivery system. They analyzed numerically and analytically the drug release from the coating into both a homogeneous mono-layer wall ([32]) and a heterogeneous multi-layered wall ([33]) in one dimension. Despite their interesting results, the biodegradation process of the carrier polymer, the penetration of the biological fluid into the coating and absorption of degraded polymer by the arterial wall have not been taken into account.

Prabhu and Hossainy ([34]) developed a mathematical model to predict the transport of drug with simultaneous degradation of the biodegradable polymer

in the aqueous media. They have used a simplified wall-free condition, in which the influence of the arterial wall is modeled through the coupling with a *Robin* boundary condition. An important feature of this model, which differentiates it from other models, is the reaction equations used to represent the polymer degradation. It is assumed that a set of oligomers can be identified as one compartment, characterized by a certain molecular weight range, for which their diffusion characteristics and degradation kinetics can be considered to be identical. The authors in [34] also consider that the diffusion coefficients depend on the concentration of PLA.

The model presented in Chapter 2 extends to two dimensions the one dimensional model proposed by Prabhu and Hossainy, and furthermore it uses a coupled stent-wall system instead of a simplified wall-free condition. The model is based on two sets of PDE's: one represents the kinetics of the drug and the degradation process in the stent and the other the kinetics of drug in the vessel wall. These equations are based on Fick's law and are described by

$$\begin{cases} \frac{\partial \mathcal{C}_S}{\partial t} + \nabla \cdot J_S = F_S, \\ \frac{\partial \mathcal{C}_V}{\partial t} + \nabla \cdot J_V = 0, \end{cases} \tag{1.1}$$

where $\mathcal{C}_S$ denotes a concentration (drug, PLA, oligomers, lactic acid and fluid) in the stent coating, while $\mathcal{C}_V$ represents the drug concentration in the arterial wall.

In system (1.1), $J_j,\ j = S, V$, represent Fickian mass fluxes in the stent and in the arterial wall, respectively, whereas F_S describes the degradation reactions. The system is coupled with the initial, boundary and interface conditions.

The results presented in Chapter 2 are extensions of the results included in the works:

- J. A. Ferreira, J. Naghipoor and P. de Oliveira, Numerical simulation of a coupled cardiovascular drug delivery model, Proceedings of the 13th International Conference on Computational and Mathematical Methods in Science and Engineering, CMMSE2013 (II), I. P. Hamilton and J. Vigo-Aguiar (editors), 642–653, 2013.
- J. A. Ferreira, J. Naghipoor and P. de Oliveira, Analytical and numerical study of a coupled cardiovascular drug delivery model, Journal of Computational and Applied Mathematics, 275 (2015) 433–446.

Arterial walls of the cardiovascular system are known to display a complex mechanical response under physiological conditions. The coronary artery has different portions of the layers, which mainly consist of elastin that is responsible for elasticity and smooth muscle cell and collagen in the media, which exhibit the viscoelastic behavior of the artery ([27, 29]).

Experiments like *creep tests* have demonstrated that the vascular tissue is viscoelastic ([16, 27, 41]). It is accepted that in the presence of small vascular deformations, linear viscoelastic models will adequately predict the process of drug penetration from stent into the arterial wall ([29]).

Classical Fickian diffusion equation does not account for the influence of viscoelasticity in the transport of molecules ([6, 10, 15, 16, 29]). From a mathematical viewpoint, a non-Fickian reaction-diffusion equation characterized by a modified flux could be an appropriate equation to simulate drug release.

The model presented in Chapter 3 is based on two sets of PDE's: one represents the kinetics of drug and degradation process in the stent and the other the kinetics of drug in the arterial wall. Equations in the stent are based on Fick's law while equations in the arterial wall are based on non-Fickian diffusion and are described by

$$\begin{cases} \frac{\partial \mathcal{C}_S}{\partial t} + \nabla \cdot J_S = F_S, \\ \frac{\partial \mathcal{C}_V}{\partial t} + \nabla \cdot \tilde{J}_V = F_V, \end{cases} \tag{1.2}$$

where $\mathcal{C}_S$ denotes a concentration (drug, PLA, oligomers, lactic acid and water) in the stent coating, while $\mathcal{C}_V$ represents the concentration of drug, lactic acid and water in the arterial wall. In equation (1.2), J_S represents a Fickian mass flux in the stent, while $\tilde{J}_V$ denotes a non-Fickian mass flux in the arterial wall. This flux describes the stress response of the vessel wall to the strain caused by the incoming drug. We assume that the transport of the drug and other available molecules, in the arterial tissue, takes place by non-Fickian diffusion and convection. Convection of molecules through the arterial wall is caused by the high pressure difference between the blood flow and the outer vascular tissue, adventitia, which results in blood plasma filtration across the arterial wall.

F_S and F_V in (1.2) describe the degradation reactions in the stent and in the arterial wall respectively. The velocities that define the convection terms are computed by *Darcy*'s law. The system is coupled with initial, boundary and interface conditions. The results presented in Chapter 3 are generalizations of the results included in the work:

- J. A. Ferreira, J. Naghipoor and P. de Oliveira, A coupled non-Fickian model of a cardiovascular drug delivery system, Preprint of Department of Mathematics of University of Coimbra, No. 14-13 (submitted).

In Chapter 4, we improve the model proposed in Chapter 3 to take into account the reversible nature of the binding between the drug and specific sites inside the arterial wall ([5, 26, 43, 44]).

The coupled non-Fickian nonlinear reaction-diffusion-convection model that describes the evolution of PLA and its compounds, the free drug and activated drug-binding site, is defined by

$$\begin{cases} \frac{\partial \mathcal{C}_S}{\partial t} + \nabla \cdot J_S = F_S, \\ \frac{\partial \mathcal{C}_V}{\partial t} + \nabla \cdot \tilde{J}_V = F_V, \\ \frac{\partial C_V}{\partial t} = G_V, \end{cases} \tag{1.3}$$

where $\mathcal{C}_S$ denotes a concentration (drug, PLA, oligomers, lactic acid and water) in the stent coating, $\mathcal{C}_V$ represents the concentration of lactic acid and water in the arterial wall while C_V represents the concentration of free and bounded drugs in the arterial wall. In system (1.3), fluxes J_S and $\tilde{J}_V$ are defined as in Chapter 3 and G_V stand for the reversible binding reactions.

The original results presented in Chapter 4 are a generalization of the following accepted paper:

- J. A. Ferreira, J. Naghipoor and P. de Oliveira, The effect of reversible binding sites on the drug release from drug eluting stent, Proceeding of 14th International Conference on Computational and Mathematical Methods in Science and Engineering, CMMSE2014 (II), I. P. Hamilton and J. Vigo-Aguiar (editors), 519-530, 2014.

Finally in Chapter 5 we summarize our conclusions and describe future works.

Chapter 2

A Nonlinear Coupled Model

In this chapter, we present an extension of the one dimensional model proposed by Prabhu and Hossainy in [34] whose aim was the study of drug release from a DES into the arterial wall. The main differences between our model and the model proposed in [34] are the fact that we consider a two dimensional domain and also the conditions that are used to couple the coated stent and the arterial wall. The main drawback of [34] is that the authors have considered that the coated stent was the only region of interest for studying the model and they represented the interaction between the arterial wall and the lumen by simple wall-free boundary conditions. An important feature of the model in [34], which differentiates it from previous similar models ([2, 5, 33, 46]) is the detailed equations that are used to represent the polymer degradation. Despite the accurate description of the phenomena in the coated stent, the authors have not studied the model from the theoretical and phenomenological viewpoints.

The main objectives of this chapter are studying the structure of the interface conditions in the coupling of two different physical domains as well as the biodegradation of the polylactic acid (PLA). Also the study of the two dimensional nonlinear coupled cardiovascular drug delivery system, from the numerical and theoretical viewpoints, will deserve our attention.

The chapter is organized as follows. Section 2.1 is devoted to the description of the model and its initial, boundary and interface conditions. In Section 2.2, we briefly explain the mass behavior of molecules in the phenomenological approach. In Section 2.3, we present the variational formulation of the model and an energy estimate is established. The stability of the proposed model is studied in Section

2.4 and by using an implicit explicit finite element method, we establish a semi-discrete variational form in Section 2.5 and a full discrete variational form in Section 2.6. Numerical simulations of the model and a sensitivity analysis of the parameters are discussed in Section 2.7.

2.1 *Description of the model*

We consider a stent S coated by PLA where the drug is dispersed and in contact with the arterial wall V. The stent will be slowly absorbed by the arterial wall as time evolves. In Figure 2.1 we represent a simplified physical model.

In the study of the model, the following assumptions are taken into account:

1. Despite the heterogeneity of the arterial wall (see Section 1.2), we assume that it is a homogeneous medium under a macroscopic view point;
2. The geometrical and mechanical effects of the stent strut (the metallic part of the stent) on the degradation of PLA and release of the drug are considered negligible;
3. The penetration of the oligomers and lactic acid into the arterial wall is considered negligible;
4. As the transport properties of the glycocalyx (the coverage of endothelium) are not clearly studied in the literature, we have considered its values in the endothelium layer.

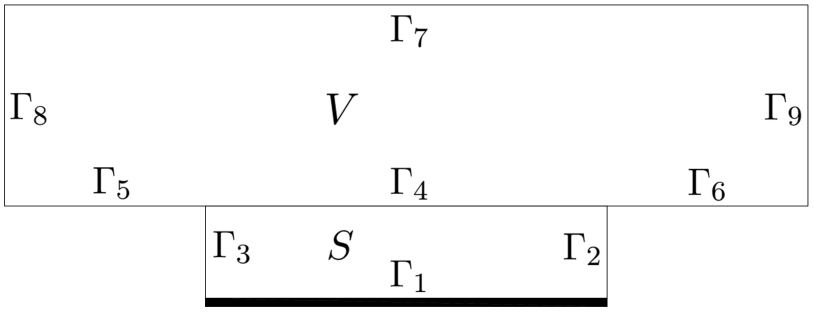

FIGURE 2.1: Polymeric stent S in contact with the vessel wall V.

In the stent S, Γ_1 is the boundary between the coated stent and the metallic part of the stent (stent strut) while Γ_2 and Γ_3 are the boundaries which separate the

coated stent and the arterial lumen. Γ_4 is an interface boundary which separates the coated stent from the arterial wall, V. Γ_5 and Γ_6 are the boundaries between the arterial wall and the arterial lumen while Γ_7 is the boundary between the arterial wall and the tissue (outer part of the arterial wall). Γ_8 and Γ_9 are virtual boundaries where conditions will be imposed.

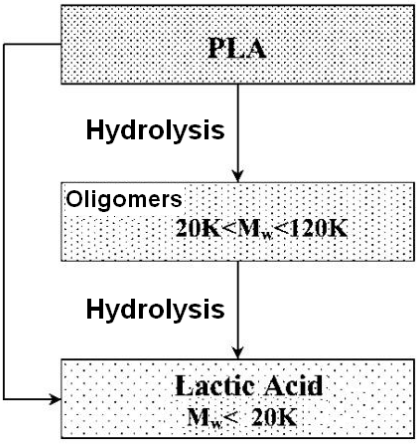

FIGURE 2.2: Schematic of the mathematical model for predicting degradation of PLA and drug release ([34]).

Mathematical modeling of drug delivery from a biodegradable coating into the arterial wall is relatively complex compared with modeling of drug release from a non-degradable polymer. In the case of a biodegradable coating, in addition to the physical mass transport process responsible for the drug release from the coating, the model has to account for the chemical processes responsible for the biodegradation.

In this thesis, we assume that two main reactions are responsible for the degradation of PLA into smaller molecules. As it is illustrated schematically in Figure 2.2, the first reaction is the hydrolyzing of the PLA producing oligomers which have smaller molecular weights M_W, $2 \times 10^4\ g/mol \leq M_W \leq 1.2 \times 10^5\ g/mol$. It is assumed that all of these oligomers have similar diffusivities when they diffuse through the coated stent. The second reaction is the hydrolyzing of the oligomers giving lactic acid with the molecular weight $M_W \leq 2 \times 10^4\ g/mol$. The lactic acid generated by this reaction is assumed to have a catalytic effect on further degradation of the PLA, which is represented by α and β in (2.4). These reactions are schematically represented by

$$\begin{aligned} C_{1,S} + C_{2,S} &\xrightarrow{\kappa_{1,S}} C_{3,S} + C_{4,S}, \\ C_{1,S} + C_{3,S} &\xrightarrow{\kappa_{2,S}} C_{4,S}, \end{aligned} \tag{2.1}$$

where $C_{1,S}, C_{2,S}, C_{3,S}$ and $C_{4,S}$ represent the concentrations of the water, PLA, oligomers and lactic acid in the coated stent, respectively (see Table 2.1). The constants $\kappa_{1,S}$ and $\kappa_{2,S}$ stand for the reaction rates of the first and second reactions respectively.

Molecule	Coated stent (S)	Vessel wall (V)
Water	$C_{1,S}$	-
PLA	$C_{2,S}$	-
Oligomers	$C_{3,S}$	-
Lactic acid	$C_{4,S}$	-
Drug	$C_{5,S}$	C_V

TABLE 2.1: Notation for the concentrations.

It should be noted that the effect of the extracellular enzymes in the degradation process is neglected in this model. As it is mentioned in [37], the degradation rates measured "*in vitro*" are essentially the same as that measured "*in vivo*". So the major route of degradation for PLA is most likely via non-enzymatic hydrolysis. It is also assumed that the drug does not react with PLA and its products.

Considering the notation $C^* = \big(C_{m,S}\big)_{m=1,\dots,4}$, the behaviour of the concentrations $C_{m,S},\ m = 1,\dots,5$, in the coated stent is described by the following nonlinear reaction diffusion equations

$$\frac{\partial C_{m,S}}{\partial t} = \nabla \cdot \big(D_{m,S}\nabla C_{m,S}\big) + F_{m,S}(C^*) \quad \text{in } S \times \mathbb{R}^+,\ m = 1,\dots,5, \tag{2.2}$$

where $C_{5,S}$ denotes the concentration of the drug in the coated stent. The reaction terms $F_{m,S},\ m = 1,\dots,5$, are defined by

$$F_{m,S}(C^*) = \begin{cases} -\sum\limits_{i=1,2} \mathcal{F}_{i,S}(C^*), & \text{m=1,} \\ -\mathcal{F}_{1,S}(C^*), & \text{m=2,} \\ \sum\limits_{i=1,2} (-1)^{i-1}\mathcal{F}_{i,S}(C^*), & \text{m=3,} \\ \sum\limits_{i=1,2} \mathcal{F}_{i,S}(C^*), & \text{m=4,} \\ 0, & \text{m=5.} \end{cases} \tag{2.3}$$

In (2.3), $\mathcal{F}_{1,S}$ and $\mathcal{F}_{2,S}$ are given by

$$\begin{aligned} \mathcal{F}_{1,S}(C^*) &= \kappa_{1,S}C_{1,S}C_{2,S}\big(1 + \alpha C_{4,S}\big), \\ \mathcal{F}_{2,S}(C^*) &= \kappa_{2,S}C_{1,S}C_{3,S}\big(1 + \beta C_{4,S}\big), \end{aligned} \tag{2.4}$$

where α and β are positive dimensional constants. The negative signs in (2.3) indicate the consumption of molecules while the positive signs indicate the production of molecules. For instance, the reaction term for the water is represented by

$$-\kappa_{1,S}C_{1,S}C_{2,S} - \kappa_{1,S}\alpha C_{1,S}C_{2,S}C_{4,S} - \kappa_{2,S}C_{1,S}C_{3,S} - \kappa_{2,S}\beta C_{1,S}C_{3,S}C_{4,S}. \quad (2.5)$$

The reaction term (2.5) indicates that PLA degrades into oligomers and lactic acid and also oligomers hydrolyze producing lactic acid. The negative signs in (2.5) indicate that the water is consumed during the time (see (2.1)). The other reaction terms in (2.3) have similar interpretations.

The diffusivities of the water, oligomers, lactic acid and drug will evolve with time. This variation occurs due to the progressive degradation of the polymer as well as due to the swelling of the polymer. It is therefore assumed that the diffusion coefficients increase exponentially with the extent of the hydrolysis of PLA ([34, 38]). The diffusivity coefficients in the coated stent are represented by

$$D_{m,S} = D^0_{m,S} e^{\alpha_{m,S}\frac{C^0_{2,S}-C_{2,S}}{C^0_{2,S}}} \quad \text{in } \bar{S}\times\mathbb{R}^+,\ m=1,\dots,5, \quad (2.6)$$

where $D^0_{m,S},\ m=1,\dots,5$, are the diffusivity of the respective species in the unhydrolyzed PLA and $C^0_{2,S}$ is the unhydrolyzed polymer concentration at the initial time.

For the arterial wall, the following simplified model

$$\frac{\partial C_V}{\partial t} = \nabla\cdot\left(D_V\nabla C_V\right) \quad \text{in } V\times\mathbb{R}^+, \quad (2.7)$$

with constant diffusion coefficient, D_V is assumed where C_V stands for the concentration of drug in the arterial wall.

Since the degradation starts at $t=0$, we assume that there are no initial oligomers and lactic acid in the coating. The drug and PLA are distributed uniformly. In the coated stent and the arterial wall, the initial conditions are defined by

$$\begin{cases} C_{1,S}(0) = C_{3,S}(0) = C_{4,S}(0) = 0,\ C_{2,S}(0) = C_{5,S}(0) = 1 \text{ in } S, \\ C_V(0) = 0 \text{ in } V. \end{cases} \quad (2.8)$$

Here and in what follows we denote by $v(t)$ a function that depends on x, y and t, that is for each t, $v(t):\bar{\Omega}\longrightarrow\mathbb{R}$, where $\bar{\Omega}$ represents $\bar{S}$ or $\bar{V}$.

We also assume that the boundary Γ_1, interface between the coating and the stent structure, is impermeable to the molecules present in the coated stent which means that no mass flux crosses it, that is

$$D_{m,S}\nabla C_{m,S}\cdot\eta_S = 0 \quad \text{on } \Gamma_1\times\mathbb{R}^+,\ m=1,\ldots,5, \tag{2.9}$$

where η_S is the unit exterior normal to Γ_1.

We assume that the blood flow in the arterial lumen does not significantly influence the drug release in the arterial wall. In Γ_2 and Γ_3, the boundary conditions are defined by

$$\begin{cases} D_{1,S}\nabla C_{1,S}\cdot\eta_S = \gamma_{1,S}(1-C_{1,S}) & \text{on } (\Gamma_2\cup\Gamma_3)\times\mathbb{R}^+, \\ D_{m,S}\nabla C_{m,S}\cdot\eta_S = -\gamma_{m,S}C_{m,S} & \text{on } (\Gamma_2\cup\Gamma_3)\times\mathbb{R}^+,\ m=2,\ldots,5, \end{cases} \tag{2.10}$$

where $\gamma_{m,S},\ m=1,\ldots,5$, represent transference coefficients.

We consider now the issue of finding effective coupling conditions across the interface Γ_4 which separates the coated stent and the arterial wall. The obvious condition to assign, at a permeable interface, is the continuity of the drug concentration and the other condition is the continuity of its flux, that is

$$\begin{cases} D_{5,S}\nabla C_{5,S}\cdot\eta_S = -D_V\nabla C_V\cdot\eta_V & \text{on } \Gamma_4\times\mathbb{R}^+, \\ C_{5,S} = C_V & \text{on } \Gamma_4\times\mathbb{R}^+, \end{cases} \tag{2.11}$$

where $\eta_S=-\eta_V$ on Γ_4. It is also assumed that Γ_4 is impermeable to PLA, lactic acid and oligomers.

In what concerns the interface boundary between intima and media, a *Robin* boundary condition of type

$$D_V\nabla C_V\cdot\eta_V = -\gamma_v C_V \quad \text{on } \Gamma_7\times\mathbb{R}^+, \tag{2.12}$$

is considered for the drug. The boundary condition (2.12) means that the drug can pass from intima to media.

A homogeneous Neumann boundary condition

$$D_V\nabla C_V\cdot\eta_V = 0 \quad \text{on } (\Gamma_8\cup\Gamma_9)\times\mathbb{R}^+, \tag{2.13}$$

is assumed for the virtual boundaries $\Gamma_8\cup\Gamma_9$.

The flux of drug from the arterial wall to the blood is given by

$$D_V \nabla C_V \cdot \eta_V = -\gamma_b C_V \quad \text{on } (\Gamma_5 \cup \Gamma_6) \times \mathbb{R}^+, \tag{2.14}$$

where γ_b is such that the endothelium layer offers a small resistance to the drug transport.

Summarizing, the boundary and interface conditions are defined by

$$\begin{cases} D_{m,S} \nabla C_{m,S} \cdot \eta_S = 0 & \text{on } \Gamma_1 \times \mathbb{R}^+, \ m = 1, \ldots, 5, \\ D_{1,S} \nabla C_{1,S} \cdot \eta_S = \gamma_{1,S}(1 - C_{1,S}) & \text{on } (\Gamma_2 \cup \Gamma_3) \times \mathbb{R}^+, \\ D_{m,S} \nabla C_{m,S} \cdot \eta_S = -\gamma_{m,S} C_{m,S} & \text{on } (\Gamma_2 \cup \Gamma_3) \times \mathbb{R}^+, \ m = 2, \ldots, 5, \\ D_{m,S} \nabla C_{m,S} \cdot \eta_S = 0 & \text{on } \Gamma_4 \times \mathbb{R}^+, \ m = 1, \ldots, 4, \\ C_{5,S} = C_V & \text{on } \Gamma_4 \times \mathbb{R}^+, \\ D_{5,S} \nabla C_{5,S} \cdot \eta_S = -D_V \nabla C_V \cdot \eta_V & \text{on } \Gamma_4 \times \mathbb{R}^+, \\ D_V \nabla C_V \cdot \eta_V = -\gamma_b C_V & \text{on } (\Gamma_5 \cup \Gamma_6) \times \mathbb{R}^+, \\ D_V \nabla C_V \cdot \eta_V = -\gamma_v C_V & \text{on } \Gamma_7 \times \mathbb{R}^+, \\ D_V \nabla C_V \cdot \eta_V = 0 & \text{on } (\Gamma_8 \cup \Gamma_9) \times \mathbb{R}^+. \end{cases} \tag{2.15}$$

2.2 *Qualitative behavior of the total mass*

In what follows we analyze the time behavior of the total mass

$$\mathcal{M}(t) = \sum_{m=1}^{5} \int_S C_{m,S}(t) dS + \int_V C_V(t) dV, \tag{2.16}$$

where the notations have been presented in Table 2.1.

Replacing (2.2) and (2.7) in

$$\mathcal{M}'(t) = \sum_{m=1}^{5} \int_S \frac{\partial C_{m,S}}{\partial t}(t) dS + \int_V \frac{\partial C_V}{\partial t}(t) dV, \tag{2.17}$$

we obtain

$$\mathcal{M}'(t) = \sum_{m=1}^{5} \int_S \Big(\nabla \cdot \big(D_{m,S}(t) \nabla C_{m,S}(t) \big) + F_{m,S}(C^*(t)) \Big) dS + \int_V \nabla \cdot \big(D_V \nabla C_V(t) \big) dV. \tag{2.18}$$

Using Gauss's theorem ([11]), taking into account the boundary conditions (2.9), (2.10), (2.12), (2.13) and (2.14), and reaction terms (2.3) and (2.4), we

deduce

$$\begin{aligned}\mathcal{M}'(t) &= \gamma_{1,S}\int_{\Gamma_2\cup\Gamma_3}(1-C_{1,S}(t))ds - \sum_{m=2}^{4}\gamma_{m,S}\int_{\Gamma_2\cup\Gamma_3}C_{m,S}(t)ds - \gamma_b\int_{\Gamma_5\cup\Gamma_6}C_V(t)ds\\ &+\int_{\Gamma_4}D_{5,S}(t)\nabla C_{5,S}(t)\cdot\eta_S ds + \int_{\Gamma_4}D_V\nabla C_V(t)\cdot\eta_V ds - \gamma_{5,S}\int_{\Gamma_2\cup\Gamma_3}C_{5,S}(t)ds\\ &-\gamma_v\int_{\Gamma_7}C_V(t)ds - \int_S\kappa_{2,S}C_{1,S}(t)C_{3,S}(t)\big(1+\beta C_{4,S}(t)\big)\,dS.\end{aligned} \tag{2.19}$$

Replacing the coupling conditions (2.11) in (2.19), we have

$$\mathcal{M}'(t) = -\Delta M_\Gamma(t) - \Delta M_H(t) + \gamma_{1,S}\Big|\Gamma_2\cup\Gamma_3\Big|, \tag{2.20}$$

where

$$\Delta M_\Gamma(t) = \sum_{m=1}^{5}\gamma_{m,S}\int_{\Gamma_2\cup\Gamma_3}C_{m,S}(t)ds + \gamma_v\int_{\Gamma_7}C_V(t)ds + \gamma_b\int_{\Gamma_5\cup\Gamma_6}C_V(t)ds, \tag{2.21}$$

and the mass of hydrolyzed oligomers is given by

$$\Delta M_H(t) = \int_S\kappa_{2,S}C_{1,S}(t)C_{3,S}(t)\big(1+\beta C_{4,S}(t)\big)dS, \tag{2.22}$$

and $\Big|\Gamma_2\cup\Gamma_3\Big|$ represents the length of the boundary segment $\Gamma_2\cup\Gamma_3$.

We note that $\Delta M_\Gamma(t)$ represents the mass of molecules that enters, per unit time, in the lumen; $\Delta M_H(t)$ stands for the mass of lactic acid produced by unit time, and resulting from the hydrolysis of oligomers.

Finally, by integrating in time we deduce

$$\mathcal{M}(t) = \mathcal{M}(0) + \gamma_{1,S}\Big|\Gamma_2\cup\Gamma_3\Big|t - \int_0^t\Delta M_H(\mu)\,d\mu - \int_0^t\Delta M_\Gamma(\mu)\,d\mu. \tag{2.23}$$

The equality (2.23) means that the total mass of the system at time t is given by the difference between the initial mass added to the mass of water that enters in the system until time t, and the mass of hydrolyzed oligomers until time t, the mass of the components that are on the boundary until time t.

2.3 *Weak formulation of the coupled problems*

In this section, we introduce a variational problem associated with the initial boundary value problem (IBVP) (2.2) − (2.7) and (2.15).

Let Ω be a bounded domain in $\mathbb{R}^2$ with boundary $\partial\Omega$. We denote by $L^2(\Omega)$ and $H^1(\Omega)$ the usual Sobolev spaces endowed with the usual inner products $(.,.)$ and $(.,.)_1$ and norms $\|.\|_{L^2(\Omega)}$ and $\|.\|_{H^1(\Omega)}$ respectively (see [3]).

The space of functions $v : (0,T) \longrightarrow H^1(\Omega)$ such that

$$\int_0^T \left\|v(t)\right\|^2_{H^1(\Omega)} dt < \infty, \tag{2.24}$$

will be denoted by $L^2(0,T;H^1(\Omega))$. By $L^\infty(0,T;L^\infty(\Omega))$ we represent the space of functions $v : (0,T) \longrightarrow L^\infty(\Omega)$ such that

$$\operatorname*{ess\,sup}_{(0,T)} \left\|v(t)\right\|_{L^\infty(\Omega)} < \infty. \tag{2.25}$$

Let $\Omega_{S,V} = S \cup V \cup \Gamma_4$ and let C, γ and D be defined by

$$C = \begin{cases} C_{5,S} & \text{in } \bar{S} \times (0,T], \\ C_V & \text{in } \bar{V} \times (0,T], \end{cases} \tag{2.26}$$

$$\gamma = \begin{cases} \gamma_{5,S} & \text{on } \Gamma_2 \cup \Gamma_3, \\ \gamma_b & \text{on } \Gamma_5 \cup \Gamma_6, \\ \gamma_v & \text{on } \Gamma_7, \end{cases} \tag{2.27}$$

and

$$D = \begin{cases} D^0_{5,S} e^{\alpha_{5,S} \frac{C^0_{2,S} - C_{2,S}}{C^0_{2,S}}} & \text{in } \bar{S} \times (0,T], \\ D_V & \text{in } \bar{V} \times (0,T]. \end{cases} \tag{2.28}$$

We remark that $C_{5,S} = C_V$ on $\bar{S} \cap \bar{V}$.

The weak solution of the IBVP (2.2)−(2.7) and (2.15) is defined by the following variational problem:

VP1: Find $(C^*, C) \in \Big(L^2(0,T;H^1(S))\Big)^4 \times L^2(0,T;H^1(\Omega_{S,V}))$ such that $\big(\frac{\partial C^*}{\partial t}, \frac{\partial C}{\partial t}\big) \in \Big(L^2(0,T;L^2(S))\Big)^4 \times L^2(0,T;L^2(\Omega_{S,V}))$ and

$$\begin{cases} \sum_{m=1}^{4}\Big(\frac{\partial C_{m,S}}{\partial t}(t), v_m\Big)_S + \Big(\frac{\partial C}{\partial t}(t), w\Big)_{\Omega_{S,V}} = -\sum_{m=1}^{4}\Big(D_{m,S}\nabla C_{m,S}(t), \nabla v_m\Big)_S \\ \qquad -\Big(D\nabla C(t), \nabla w\Big)_{\Omega_{S,V}} + \sum_{m=1}^{4}\Big(F_{m,S}(C^*(t)), v_m\Big)_S \\ \qquad +\gamma_{1,S}\Big(1 - C_{1,S}(t), v_1\Big)_{\Gamma_2\cup\Gamma_3} - \sum_{m=2}^{4}\gamma_{m,S}\Big(C_{m,S}(t), v_m\Big)_{\Gamma_2\cup\Gamma_3} \\ \qquad -\Big(\gamma C(t), w\Big)_{\Gamma}, \\ \qquad \text{a.e. in } (0,T), \text{ for all } v_m \in H^1(S),\ m = 1,\dots,4, \text{ and } w \in H^1(\Omega_{S,V}), \\ C^*(0) = (0,1,0,0), \\ C(0) = \chi_S, \end{cases} \tag{2.29}$$

where $\chi_S = \begin{cases} 1 & \text{in } S, \\ 0 & \text{in } V, \end{cases}$ and $\Gamma = \Gamma_2 \cup \Gamma_3 \cup \Gamma_5 \cup \Gamma_6 \cup \Gamma_7$.

In what follows we study the behavior of the solution of the variational problem **VP1** assuming that the diffusion coefficients $D_{m,S},\ m = 1,\dots,5$, are constants. We represent by $L^\infty(L^\infty)$ the space $L^\infty(0,T;L^\infty(\Omega))$. Let the energy functional $\mathcal{E}_\nabla(t)$ be defined by

$$\begin{aligned} \mathcal{E}_\nabla(t) &= \sum_{m=1}^{4}\Big(\Big\|C_{m,S}(t)\Big\|^2_{L^2(S)} + 2\int_0^t \Big\|\sqrt{D_{m,S}}\nabla C_{m,S}(s)\Big\|^2_{L^2(S)} ds\Big) + \Big\|C(t)\Big\|^2_{L^2(\Omega_{S,V})} \\ &\quad +2\int_0^t \Big\|\sqrt{D}\nabla C(s)\Big\|^2_{L^2(\Omega_{S,V})} ds, \quad t \in [0,T], \end{aligned} \tag{2.30}$$

where $\mathcal{E}_\nabla(0)$ is the initial energy that depends only on PLA and drug.

Theorem 2.3.1. If (C^*, C) is a solution of the variational problem **VP1** such that $C_{m,S}(t) \in H^2(S),\ m = 1,\dots,4$, then there exists a positive constant $\mathcal{K}$ depending on $\|C_*\|_{L^\infty(L^\infty)} = \max\limits_{m=1,\dots,4}\big\|C_{m,S}\big\|_{L^\infty(L^\infty)}$, such that the following holds

$$\mathcal{E}_\nabla(t) \le e^{2\mathcal{K}t}\mathcal{E}_\nabla(0) + \tfrac{\gamma_{1,S}}{2\mathcal{K}}\Big|\Gamma_2 \cup \Gamma_3\Big|\big(e^{2\mathcal{K}t} - 1\big), \quad t \in [0,T], \tag{2.31}$$

where $\Big|\Gamma_2 \cup \Gamma_3\Big|$ is the length of the boundary layer $\Gamma_2 \cup \Gamma_3$.

Proof. We take in (2.29), $v_m = C_{m,S}(t),\ m = 1, \ldots, 4$, and $w = C(t)$. It is not difficult to check that

$$\begin{aligned}\left(\tfrac{dC_{m,S}}{dt}(t), C_{m,S}(t)\right)_S &= \int_S \tfrac{dC_{m,S}}{dt}(t) C_{m,S}(t) dS \\ &= \frac{1}{2}\frac{d}{dt}\int_S C_{m,S}^2(t) dS \qquad = \frac{1}{2}\frac{d}{dt}\left\|C_{m,S}(t)\right\|^2_{L^2(S)},\end{aligned} \tag{2.32}$$

for $m = 1, \ldots, 4$.

With the same approach we have

$$\left(\frac{dC}{dt}(t), C(t)\right)_{\Omega_{S,V}} = \frac{1}{2}\frac{d}{dt}\left\|C(t)\right\|^2_{L^2(\Omega_{S,V})}. \tag{2.33}$$

We also have

$$\begin{aligned}\left(D_{m,S}\nabla C_{m,S}(t), \nabla C_{m,S}(t)\right)_S &= \frac{d}{dt}\int_0^t \left\|\sqrt{D_{m,S}}\nabla C_{m,S}(s)\right\|^2_{L^2(S)} ds,\ m = 1, \ldots, 4, \\ \left(D\nabla C(t), \nabla C(t)\right)_{\Omega_{S,V}} &= \frac{d}{dt}\int_0^t \left\|\sqrt{D}\nabla C(s)\right\|^2_{L^2(\Omega_{S,V})} ds.\end{aligned} \tag{2.34}$$

Summing up (2.32), (2.33) and (2.34) and taking into account (2.30), we obtain

$$\begin{aligned}\frac{1}{2}\frac{d}{dt}\mathcal{E}_\nabla(t) &= \sum_{m=1}^4 \left(F_{m,S}(C^*(t)), C_{m,S}(t)\right)_S + \gamma_{1,S}\left(1 - C_{1,S}(t), C_{1,S}(t)\right)_{\Gamma_2\cup\Gamma_3} \\ &\quad - \sum_{m=2}^4 \gamma_{m,S}\left\|C_{m,S}(t)\right\|^2_{L^2(\Gamma_2\cup\Gamma_3)} - \gamma\left\|C(t)\right\|^2_{L^2(\Gamma)}.\end{aligned} \tag{2.35}$$

By Cauchy inequality ([11]) with $\varepsilon = \frac{1}{2}$, we have

$$\left(1 - C_{1,S}(t), C_{1,S}(t)\right)_{\Gamma_2\cup\Gamma_3} = \int_{\Gamma_2\cup\Gamma_3}\left(C_{1,S}(t) - C_{1,S}^2(t)\right) ds \le \tfrac{1}{4}\left|\Gamma_2 \cup \Gamma_3\right| \tag{2.36}$$

Consequently the inequality (2.35) leads to

$$\frac{1}{2}\frac{d}{dt}\mathcal{E}_\nabla(t) \le \sum_{m=1}^4 \left(F_{m,S}(C^*(t)), C_{m,S}(t)\right)_S + \tfrac{\gamma_{1,S}}{4}\left|\Gamma_2 \cup \Gamma_3\right|. \tag{2.37}$$

As $H^2(S)$ is embedded in the space of continuous bounded functions in S ([3]), it can be shown that there exists a positive constant $\mathcal{K}$ that depends on

$\|C_*\|_{L^\infty(L^\infty)} = \max\limits_{m=1,\dots,4} \|C_{m,S}\|_{L^\infty(L^\infty)}$, such that

$$\sum_{m=1}^{4} \Big(F_{m,S}(C^*(t)), C_{m,S}(t) \Big)_S \leq \mathcal{K} \sum_{m=1}^{4} \Big\| C_{m,S}(t) \Big\|^2_{L^2(S)}. \tag{2.38}$$

Inequality (2.37) leads to the differential inequality

$$\frac{d}{dt}\mathcal{E}_\nabla(t) \leq 2\mathcal{K}\mathcal{E}_\nabla(t) + \tfrac{\gamma_{1,S}}{2} \Big| \Gamma_2 \cup \Gamma_3 \Big|. \tag{2.39}$$

By multiplying both sides of (2.39) by $e^{-\mathcal{K}t}$ and integrating over time, we finally deduce (2.31). □

2.4 *Stability analysis*

We consider in what follows two solutions $\mathcal{C}(t) = (C^*(t), C(t))$ and $\tilde{\mathcal{C}}(t) = (\tilde{C}^*(t), \tilde{C}(t))$ with different initial conditions $\mathcal{C}(0)$ and $\tilde{\mathcal{C}}(0)$, respectively. We recall that $C^*(t) = \big(C_{m,S}(t)\big)_{m=1,\dots,4}$, where $C_{m,S},\ m = 1, \dots, 4$, are defined in Table 2.1. To study the stability of the IBVP (2.2)-(2.7) and (2.15), we should verify that

$$\begin{aligned} \Big\| C^*(t) - \tilde{C}^*(t) \Big\|^2_{L^2(S)} \quad &+ \Big\| C(t) - \tilde{C}(t) \Big\|^2_{L^2(\Omega_{S,V})} \\ &\leq B(t) \Big(\Big\| C^*(0) - \tilde{C}^*(0) \Big\|^2_{L^2(S)} + \Big\| C(0) - \tilde{C}(0) \Big\|^2_{L^2(\Omega_{S,V})} \Big), \end{aligned} \tag{2.40}$$

for $t \in [0, T]$, where $\Big\| C^*(t) - \tilde{C}^*(t) \Big\|_{L^2(S)} = \sum\limits_{m=1}^{4} \Big\| C_{m,S}(t) - \tilde{C}_{m,S}(t) \Big\|_{L^2(S)}$ and $B(t)$ is bounded in time.

To establish the inequality (2.40) it is sufficient to assume that the reaction terms have bounded partial derivatives. As reaction terms (2.3) are nonlinear functions without bounded partial derivatives, it is not possible in this case to establish (2.40). To gain some insights on the stability behavior of the initial value problem **VP1**, we study in what follows the stability of a linearization of **VP1** in the neighborhood of a solution $\mathcal{C}(t)$.

We recall that C and D are defined by (2.26) and (2.28) respectively. Then the system of equations (2.2) and (2.7) can be rewritten in the following form

$$\begin{cases} \dfrac{d\mathcal{C}}{dt}(t) = \mathbb{F}(\mathcal{C}(t)),\ t > 0, \\ \mathcal{C}(0) \ \text{ is given,} \end{cases} \tag{2.41}$$

with $\mathcal{C}(t) = \big(C^*(t), C(t)\big)$ and $\mathbb{F}(\mathcal{C}(t)) = \Big(\mathbb{F}_m(\mathcal{C}(t))\Big)_{m=1,\dots,5}$ is represented by

$$\begin{cases} \mathbb{F}_m(\mathcal{C}(t)) = \nabla \cdot \big(D_{m,S}\nabla C_{m,S}(t)\big) + F_{m,S}(C^*(t)),\ m = 1,\dots,4, \\ \mathbb{F}_5(\mathcal{C}(t)) = \nabla \cdot \big(D\nabla C(t)\big), \end{cases} \tag{2.42}$$

and $F_{m,S}(C^*(t)),\ m = 1,\dots,4$, are defined by (2.3) and (2.4). We also assume that conditions (2.15) hold.

The linearization of the initial value problem (2.41) in $\mathcal{C}(t)$ can be written in the following form

$$\begin{cases} \dfrac{d\tilde{\mathcal{C}}}{dt}(t) = \mathbb{L}\tilde{\mathcal{C}}(t)\,, t > 0, \\ \tilde{\mathcal{C}}(0) \ \text{ is given,} \end{cases} \tag{2.43}$$

where $\mathbb{L}\tilde{\mathcal{C}}(t) = \Big(\mathbb{L}_m\tilde{\mathcal{C}}(t)\Big)_{m=1,\dots,5}$ is defined by

$$\begin{cases} \mathbb{L}_m\tilde{\mathcal{C}}(t) = \nabla \cdot \big(D_{m,S}\nabla\tilde{C}_{m,S}(t)\big) + \mathbb{F}_{J,m}(\mathcal{C}(t))\tilde{\mathcal{C}}(t),\ m = 1,\dots,4, \\ \mathbb{L}_5\tilde{\mathcal{C}}(t) = \nabla \cdot \big(D\nabla\tilde{C}(t)\big), \end{cases} \tag{2.44}$$

$\tilde{\mathcal{C}}(t) = (\tilde{C}^*(t), \tilde{C}(t))$, $\tilde{C}^*(t) = \Big(\tilde{C}_{m,S}(t)\Big)_{m=1,\dots,4}$ and

$$\mathbb{F}_{J,m}(\mathcal{C}(t))\tilde{\mathcal{C}}(t) = \begin{cases} -\sum\limits_{i=1,2} \mathcal{F}_{J,i}(\mathcal{C}(t))\tilde{\mathcal{C}}(t), & \text{m=1,} \\ -\mathcal{F}_{J,1}(\mathcal{C}(t))\tilde{\mathcal{C}}(t), & \text{m=2,} \\ \sum\limits_{i=1,2} (-1)^{i-1}\mathcal{F}_{J,i}(\mathcal{C}(t))\tilde{\mathcal{C}}(t), & \text{m=3,} \\ \sum\limits_{i=1,2} \mathcal{F}_{J,i}(\mathcal{C}(t))\tilde{\mathcal{C}}(t), & \text{m=4.} \end{cases} \tag{2.45}$$

In (2.45), $\mathcal{F}_{J,i}(\mathcal{C}(t))\tilde{\mathcal{C}}(t),\ i=1,2$, represent Fréchet derivatives given by

$$\left\{\begin{array}{ll}\mathcal{F}_{J,1}(\mathcal{C}(t))\tilde{\mathcal{C}}(t) & =\kappa_{1,S}C_{2,S}(t)(1+\alpha C_{4,S}(t))\tilde{C}_{1,S}(t)+\kappa_{1,S}C_{1,S}(t)(1+\alpha C_{4,S}(t))\tilde{C}_{2,S}(t)\\ & +\kappa_{1,S}\alpha C_{1,S}(t)C_{2,S}(t)\tilde{C}_{4,S}(t),\\ \mathcal{F}_{J,2}(\mathcal{C}(t))\tilde{\mathcal{C}}(t) & =\kappa_{2,S}C_{3,S}(t)(1+\beta C_{4,S}(t))\tilde{C}_{1,S}(t)+\kappa_{2,S}C_{1,S}(t)(1+\beta C_{4,S}(t))\tilde{C}_{3,S}(t)\\ & +\kappa_{2,S}\beta C_{1,S}(t)C_{3,S}(t)\tilde{C}_{4,S}(t).\end{array}\right. \tag{2.46}$$

Let $\tilde{\mathcal{C}}$ and $\tilde{\tilde{\mathcal{C}}}$ be solutions of the variational problem associated with the IBVP defined by (2.43) and conditions (2.15), with initial conditions $\tilde{\mathcal{C}}(0)$ and $\tilde{\tilde{\mathcal{C}}}(0)$ in which $\tilde{\mathcal{C}}(t),\tilde{\tilde{\mathcal{C}}}(t)\in\left(H^2(S)\right)^4$.

We establish in what follows an upper bound for the functional $\mathcal{E}_{\mathcal{W}}(t)$ defined by

$$\mathcal{E}_{\mathcal{W}}(t)=\sum_{m=1}^{4}\left\|W_{m,S}(t)\right\|^2_{L^2(S)}+\left\|W(t)\right\|^2_{L^2(\Omega_{S,V})},\ t\in[0,T], \tag{2.47}$$

where $W_{m,S}=\tilde{C}_{m,S}-\tilde{\tilde{C}}_{m,S},\ m=1,\ldots,4$, and

$$W=\left\{\begin{array}{ll}\tilde{C}_{5,S}-\tilde{\tilde{C}}_{5,S} & \text{in } S,\\ \tilde{C}_V-\tilde{\tilde{C}}_V & \text{in } V.\end{array}\right. \tag{2.48}$$

It can be shown that

$$\begin{array}{rl}\frac{1}{2}\frac{d}{dt}\mathcal{E}_{\mathcal{W}}(t)\leq & -\sum_{m=1}^{4}\left\|\sqrt{D_{m,S}}\nabla W_{m,S}(t)\right\|^2_{L^2(S)}-\left\|\sqrt{D}\nabla W(t)\right\|^2_{L^2(\Omega_{S,V})}\\ & +\sum_{m=1}^{4}\Big(\mathbb{F}_{J,m}(\mathcal{C}(t))W_{m,S}(t),W_{m,S}(t)\Big)_S.\end{array} \tag{2.49}$$

Consequently, there exists a positive constant $\mathcal{K}'$ depending on $\left\|C_*\right\|_{L^\infty(L^\infty)}$ such that

$$\frac{d}{dt}\mathcal{E}_{\mathcal{W}}(t)\leq 2\mathcal{K}'\mathcal{E}_{\mathcal{W}}(t),\ t>0. \tag{2.50}$$

This inequality leads to

$$\mathcal{E}_{\mathcal{W}}(t)\leq e^{2\mathcal{K}'t}\mathcal{E}_{\mathcal{W}}(0), \tag{2.51}$$

which allow us to conclude the stability of the linearization of **VP1** for short periods of time.

2.5 *Finite dimensional approximation*

To define a finite dimensional approximation for the solution of **VP1**, we fix $h > 0$ and introduce in $\Omega_{S,V}$ an admissible triangulation $\mathcal{T}_h$ such that the correspondent admissible triangulations induced in S and V, respectively $\mathcal{T}_{h_S}$ and $\mathcal{T}_{h_V}$, are compatible on Γ_4 (see Figure 2.3).

Let $C_h^* = \Big(C_{m,S,h}\Big)_{m=1,\ldots,4}$, stand for an approximation of C^* and

$$C_h = \begin{cases} C_{5,S,h} & \text{in } \bar{S} \times (0,T], \\ C_{V,h} & \text{in } \bar{V} \times (0,T], \end{cases} \tag{2.52}$$

where $C_{5,S,h} = C_{V,h}$ on Γ_4, represent an approximation of C.

To compute the semi-discrete Ritz-Galerkin approximation $\mathcal{C}_h = (C_h^*, C_h)$ for the weak solution $\mathcal{C} = (C^*, C)$ defined by **VP1**, we introduce in what follows the finite dimensional spaces

$$\mathcal{P}_\Omega^r = \Big\{ u \in C^0(\bar{\Omega}) : u\big|_\Delta = P_r,\ \Delta \in \mathcal{T}_{h_\Omega} \Big\}, \tag{2.53}$$

where $\Omega = S, \Omega_{S,V}$ and P_r denotes a polynomial in the space variables with degree at most r and $C^0(\bar{\Omega})$ denotes the space of continuous functions in $\bar{\Omega}$.

The Ritz-Galerkin approximation $\mathcal{C}_h$ is then computed by solving the following variational problem:

FEVP1: Find $(C_h^*(t), C_h(t)) \in \big(\mathcal{P}_S^r\big)^4 \times \mathcal{P}_{\Omega_{S,V}}^r$ such that

$$\begin{cases} \displaystyle\sum_{m=1}^{4} \Big(\tfrac{\partial C_{m,S,h}}{\partial t}(t), v_{m,h}\Big)_S + \Big(\tfrac{\partial C_h}{\partial t}(t), w_h\Big)_{\Omega_{S,V}} = -\sum_{m=1}^{4} \Big(D_{m,S,h}\nabla C_{m,S,h}(t), \nabla v_{m,h}\Big)_S \\ \qquad - \Big(D_h \nabla C_h(t), \nabla w_h\Big)_{\Omega_{S,V}} + \displaystyle\sum_{m=1}^{4} \Big(F_{m,S}(C_h^*(t)), v_{m,h}\Big)_S \\ \qquad + \gamma_{1,S}\Big(1 - C_{1,S,h}(t), v_{1,h}\Big)_{\Gamma_2 \cup \Gamma_3} - \Big(\gamma C_h(t), w_h\Big)_\Gamma \\ \qquad - \displaystyle\sum_{m=2}^{4} \gamma_{m,S}\Big(C_{m,S,h}(t), v_{m,h}\Big)_{\Gamma_2 \cup \Gamma_3} \\ \qquad \text{in } (0,T], \text{ for all } v_{m,h} \in \mathcal{P}_S^r,\ m = 1,\ldots,4, \text{ and } w_h \in \mathcal{P}_{\Omega_{S,V}}^r, \\ C_h^*(0) = (0,1,0,0), \\ C_h(0) = \chi_S. \end{cases} \tag{2.54}$$

In (2.54), $D_{m,S,h} = D^0_{m,S} e^{\alpha_{m,S}\frac{C^0_{2,S}-C_{2,S,h}}{C^0_{2,S}}}$ in $\bar{S}\times(0,T]$, $m=1,\dots,4$, and

$$D_h = \begin{cases} D^0_{5,S} e^{\alpha_{5,S}\frac{C^0_{2,S}-C_{2,S,h}}{C^0_{2,S}}} & \text{in } \bar{S}\times(0,T], \\ D_V & \text{in } \bar{V}\times(0,T]. \end{cases}$$

Following the proof of Theorem 2.3.1, it can be shown that a semi-discrete version of $\mathcal{E}_\nabla(t)$, defined by the Ritz-Galerkin approximation $\mathcal{C}_h$, satisfies an inequality analogous to (2.31). Moreover, for the linearization of **FEVP1** around $\mathcal{C}_h$, it can be shown an inequality analogous to (2.51).

2.6 *Full discrete IMEX problem*

We introduce in $[0,T]$ a uniform grid $\left\{t_n; n=0,\dots,N\right\}$ with $t_0=0$, $t_N=T$, $t_n - t_{n-1} = \Delta t$. By D_{-t} we denote the backward finite difference operator with respect to time variable t. The weak solution of the problem in the full discrete case is the solution of the following finite dimensional variational formulation:

Find $(C_h^{*,n+1}, C_h^{n+1}) \in \left(\mathcal{P}_S^r\right)^4 \times \mathcal{P}^r_{\Omega_{S,V}}$ such that

$$\begin{cases} \sum_{m=1}^{4}\Big(D_{-t}(C_h^{*,n+1}), v_{m,h}\Big)_S + \Big(D_{-t}(C_h^{n+1}), w_h\Big)_{\Omega_{S,V}} = -\sum_{m=1}^{4}\Big(D^n_{m,S,h}\nabla C^{n+1}_{m,S,h}, \nabla v_{m,h}\Big)_S \\ \qquad -\Big(D_h^n \nabla C_h^{n+1}, \nabla w_h\Big)_{\Omega_{S,V}} + \sum_{m=1}^{4}\Big(F_{m,S}(C_h^{n^*}), v_{m,h}\Big)_S \\ \qquad +\gamma_{1,S}\Big(1 - C^{n+1}_{1,S,h}, v_{1,h}\Big)_{\Gamma_2\cup\Gamma_3} - \Big(\gamma C_h^{n+1}, w_h\Big)_\Gamma \\ \qquad -\sum_{m=2}^{4}\gamma_{m,S}\Big(C^{n+1}_{m,S,h}, v_{m,h}\Big)_{\Gamma_2\cup\Gamma_3}, \\ \qquad \text{for all } v_{m,h}\in\mathcal{P}_S^r,\ m=1,\dots,4, \text{ and } w_h\in\mathcal{P}^r_{\Omega_{S,V}}, \\ C_h^{*,0} = (0,1,0,0), \\ C_h^0 = \chi_S, \end{cases} \tag{2.55}$$

for $n=0,\dots,N$, where

$$F_{m,S}(\mathcal{C}_h^{n^*}) = \begin{cases} -\kappa_{1,S}C^{n+1}_{1,S,h}C^n_{2,S,h}\big(1+\alpha C^n_{4,S,h}\big) - \kappa_{2,S}C^{n+1}_{1,S,h}C^n_{3,S,h}\big(1+\beta C^n_{4,S,h}\big), & \text{m=1,} \\ -\kappa_{1,S}C^{n+1}_{1,S,h}C^{n+1}_{2,S,h}\big(1+\alpha C^n_{4,S,h}\big), & \text{m=2,} \\ \kappa_{1,S}C^{n+1}_{1,S,h}C^{n+1}_{2,S,h}\big(1+\alpha C^n_{4,S,h}\big) - \kappa_{2,S}C^{n+1}_{1,S,h}C^{n+1}_{3,S,h}\big(1+\beta C^n_{4,S,h}\big), & \text{m=3,} \\ \kappa_{1,S}C^{n+1}_{1,S,h}C^{n+1}_{2,S,h}\big(1+\alpha C^{n+1}_{4,S,h}\big) + \kappa_{2,S}C^{n+1}_{1,S,h}C^{n+1}_{3,S,h}\big(1+\beta C^{n+1}_{4,S,h}\big), & \text{m=4,} \\ 0, & \text{m=5,} \end{cases} \tag{2.56}$$

are reaction functions of the problem in the implicit-explicit (IMEX) form.

2.7 *Numerical experiments*

In this section we illustrate the behaviour of the numerical solution defined by (2.55) as well as the influence of the parameters of the model in the release rate. All experiments have been done with open source partial differential equation solver freeFEM++ ([19]) with 10096 elements (5224 vertices) for $\Omega_{S,V}$ and 3250 elements (1751 vertices) for the stent S, and using IMEX backward integrator with time step size $\Delta t = 10^{-3}$.

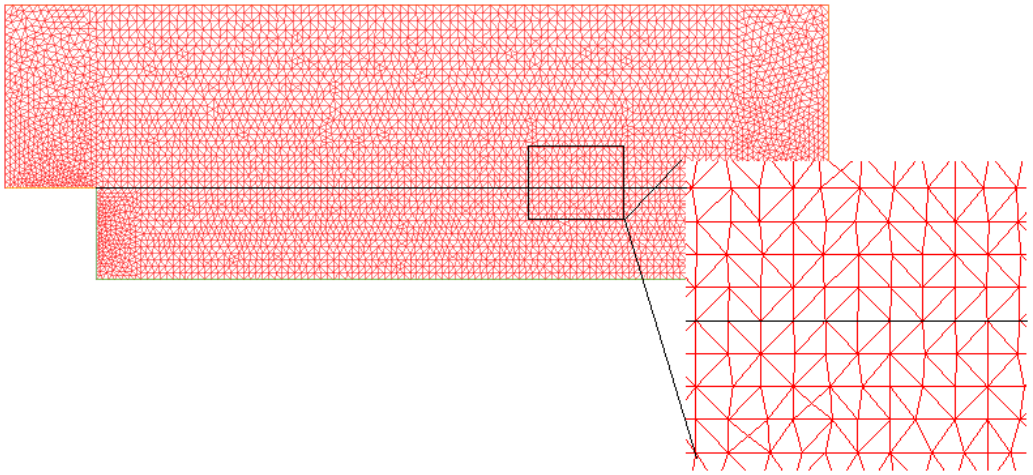

FIGURE 2.3: Triangulation in the stent and in the arterial wall.

The following parameters have been used for the modeling of the drug release from the drug eluting stent into the arterial wall:

$\gamma_{m,S} = 10^5\ cm/s,\ m = 1,\dots,5,\ \gamma_v = 10^5\ cm/s,\ \gamma_b = 10^{10}\ cm/s,\ \alpha_{m,S} = 9,\ m = 1,\dots,4,\ \alpha_{5,S} = 0.9,\ \kappa_{1,S} = 10^{-6}\ cm^2/g.s,\ \kappa_{2,S} = 10^{-8}\ cm^2/g.s,\ \alpha = 1\ s/cm^2,\ \beta = 10\ s/cm^2,\ D^0_{1,S} = 5{\times}10^{-7}\ cm^2/s,\ D^0_{2,S} = 10^{-15}\ cm^2/s,\ D^0_{3,S} = 5{\times}10^{-12}\ cm^2/s,\ D^0_{4,S} = 3 \times 10^{-12}\ cm^2/s,\ D^0_{5,S} = 2 \times 10^{-8}\ cm^2/s,\ D_V = 5 \times 10^{-8}\ cm^2/s.$

Several choices of finite element spaces can be made, but we consider here the piecewise linear finite element space P_1 ([36]).

In Figures 2.4-2.6, we plot the drug distribution in the stent and in the arterial wall after 1 day, 7 and 14 days. When the drug reaches Γ_4 (see Figure 2.1), it crosses this interface boundary to the arterial wall as mathematically described by (2.11). When the drug reaches the boundary Γ_7, it enters the *media* as described by Robin boundary condition (2.12).

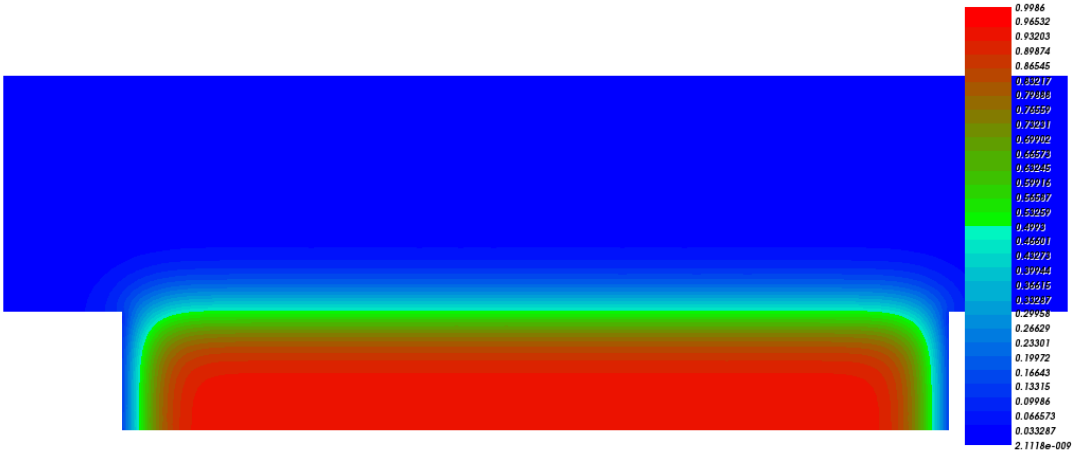

FIGURE 2.4: Drug distribution in the coating and the arterial wall after 1 day.

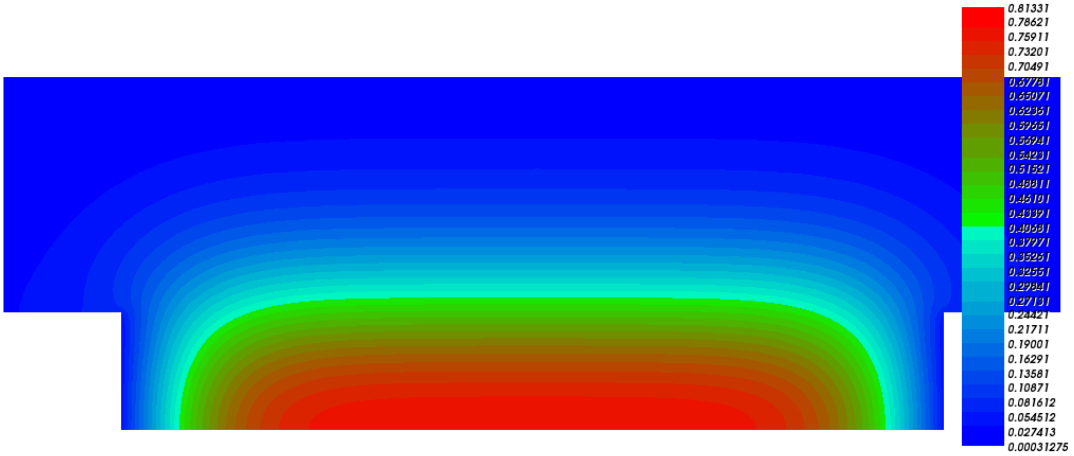

FIGURE 2.5: Drug distribution in the coating and the arterial wall after 7 days.

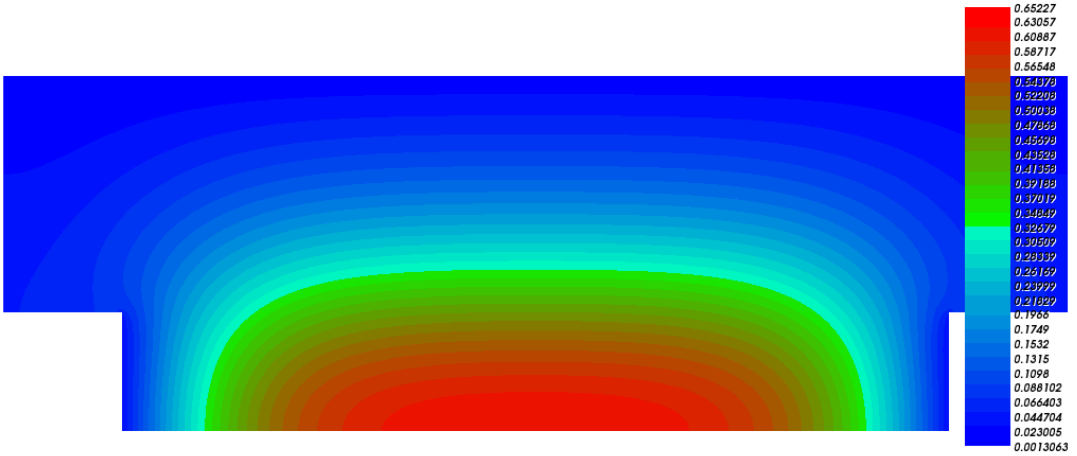

FIGURE 2.6: Drug distribution in the coating and the arterial wall after 14 days.

In Figures 2.7-2.9, we exhibit the penetration of the water into the coated stent. We observe that the water penetrates into the PLA until it reaches a steady state level.

FIGURE 2.7: Concentration of water in the coating after 1 day.

FIGURE 2.8: Concentration of water in the coating after 7 days.

FIGURE 2.9: Concentration of water in the coating after 14 days.

FIGURE 2.10: Concentration of PLA in the coating after 1 day.

FIGURE 2.11: Concentration of PLA in the coating after 7 days.

FIGURE 2.12: Concentration of PLA in the coating after 14 days.

In Figures 2.10-2.12, the degradation of PLA into smaller molecules which are released into the lumen is shown. It is assumed that the penetration of the PLA and also its products, oligomers and lactic acid, into the arterial wall are negligible. The evolution of PLA concentration is compatible with erosion during degradation.

In Figure 2.13, we see that the hydrolysis rate $\kappa_{1,S}$ of PLA has an effect on the diffusion coefficient of the drug in the stent ($D_{5,S}$). It is observed that if the reaction rate $\kappa_{1,S}$ increases, the diffusion coefficient of the drug from the stent will increase.

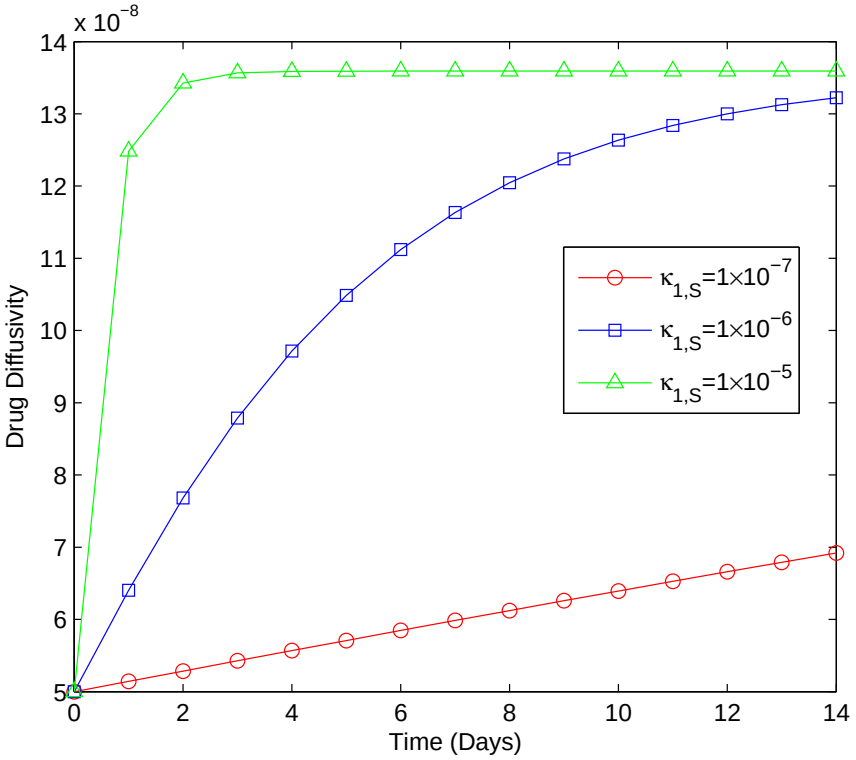

FIGURE 2.13: Diffusion coefficient of the drug in the stent for different reaction rates $\kappa_{1,S}$.

Increasing the parameter α will also increases the diffusion of the drug from the stent in an exponential manner (see Figure 2.14).

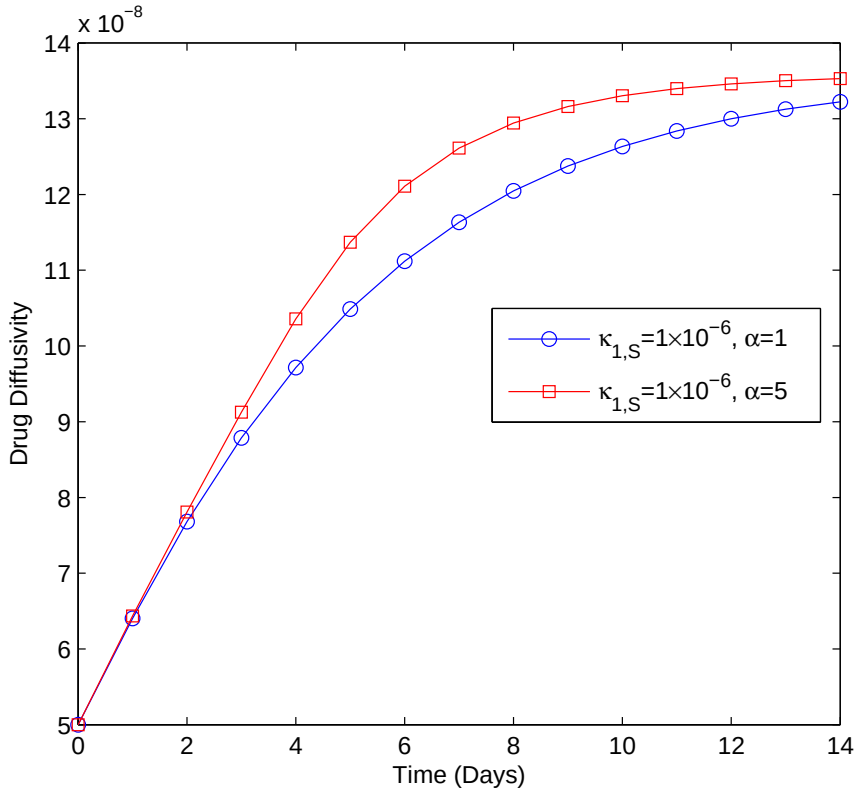

FIGURE 2.14: Diffusion coefficient of the drug in the stent for different values of α.

We define the mass of species in the coated stent and the mass of drug in the arterial wall by

$$M_{m,S,h}(t_n) = \int_S C_{m,S,h}(t_n)dS, \ m = 1, \ldots, 5, \quad M_{V,h}(t_n) = \int_V C_{V,h}(t_n)dV, \quad (2.57)$$

respectively, where $M_{m,S,h}(t_n)$ and $M_{V,h}(t_n)$ are the numerical approximations for masses at time level t_n.

In Figures 2.15-2.18, we exhibit the mass of drug as well as the mass of the water, PLA and lactic acid in the coated stent during the first 2 weeks after stent implantation using different diffusion coefficients of drug in the stent.

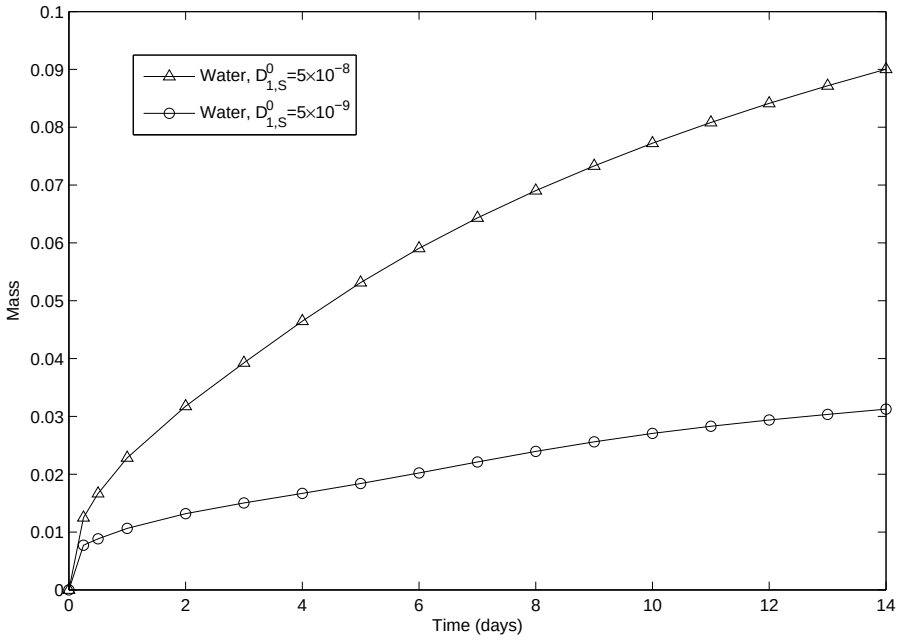

FIGURE 2.15: Mass of water in the stent for different values of $D^0_{1,S}$.

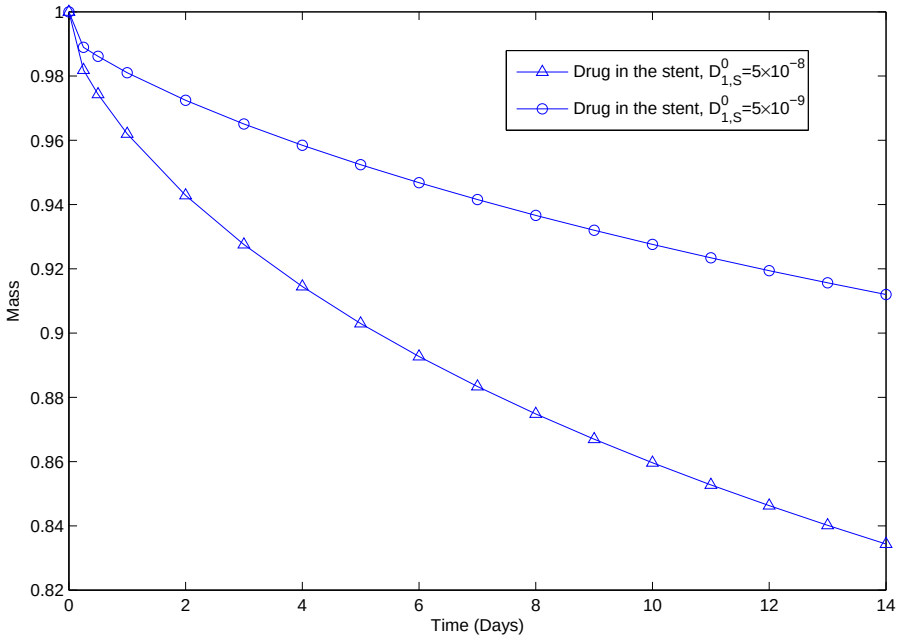

FIGURE 2.16: Mass of drug in the stent for different values of $D^0_{1,S}$.

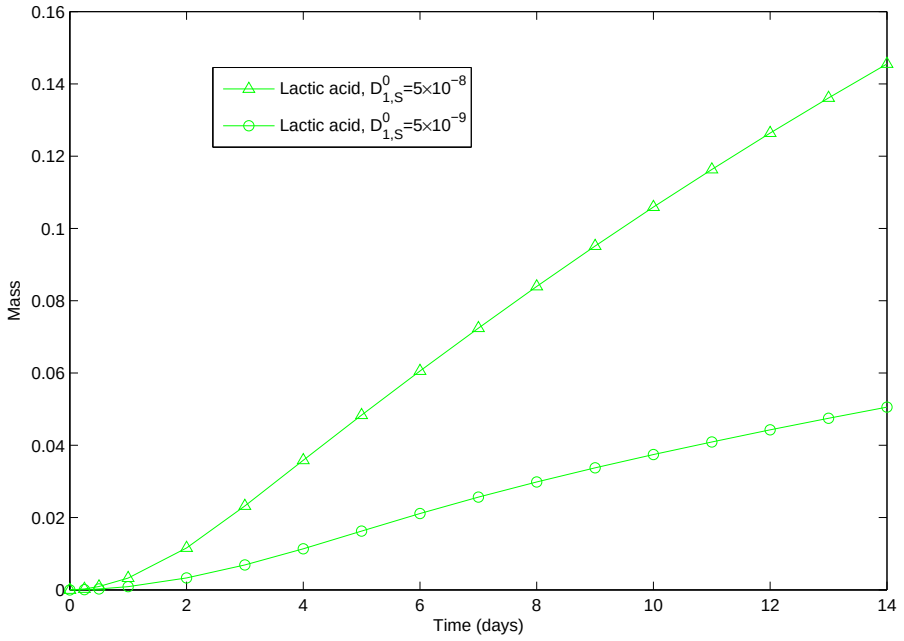

FIGURE 2.17: Mass of lactic acid in the stent for different values of $D^0_{1,S}$.

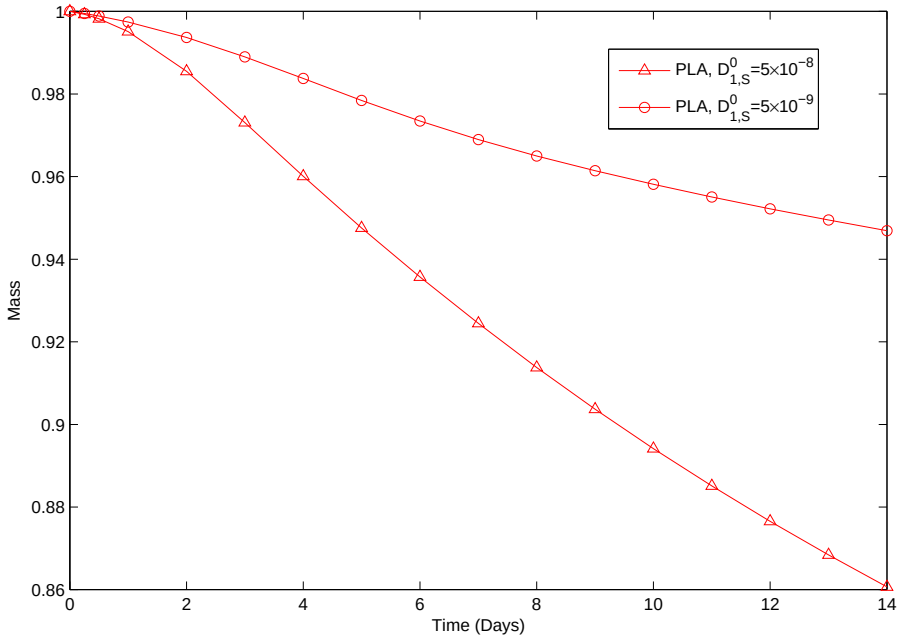

FIGURE 2.18: Mass of PLA in the stent for different values of $D^0_{1,S}$.

In Figures 2.15-2.18, we observe that small diffusion coefficients will decrease the accumulation of drug and PLA degradation in the stent. It will also decrease the mass of water and lactic acid in the stent.

Figures 2.19-2.22 illustrate the influence of reaction rates on the release process. In Figure 2.19 we observe that when the reaction rate $\kappa_{1,S}$ decreases, more water enters to the stent. A little increment will also occur when $\kappa_{2,S}$ decreases.

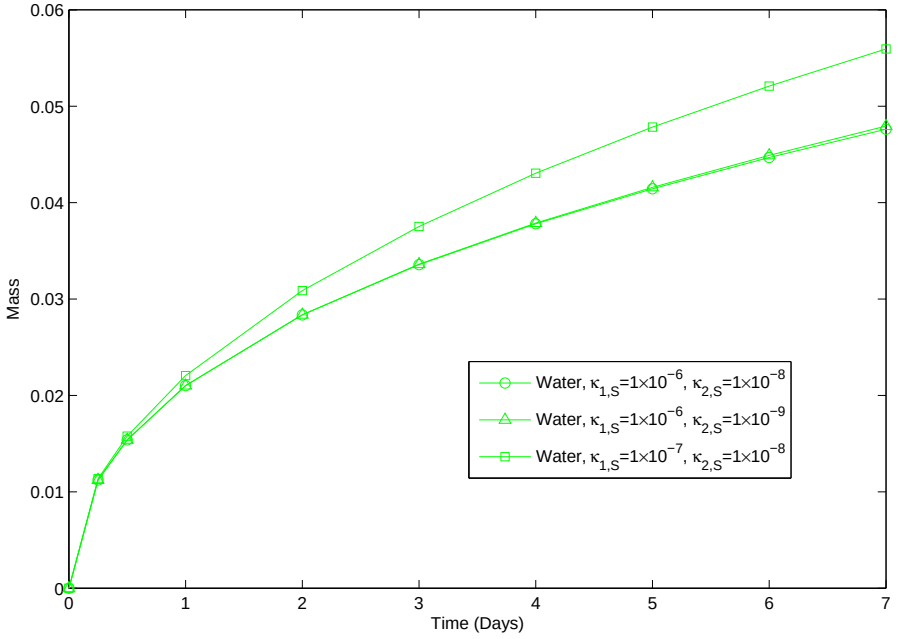

FIGURE 2.19: Mass of water in the stent for different reaction rates.

We see in Figure 2.20 that if both values of the reaction rates $\kappa_{1,S}$ and $\kappa_{2,S}$ are decreasing, some reduction in lactic acid production is observed. However we observe that $\kappa_{1,S}$, the PLA hydrolysis rate (2.1), has a primary role. The rate $\kappa_{2,S}$ of the subsequent reactions plays a minor role.

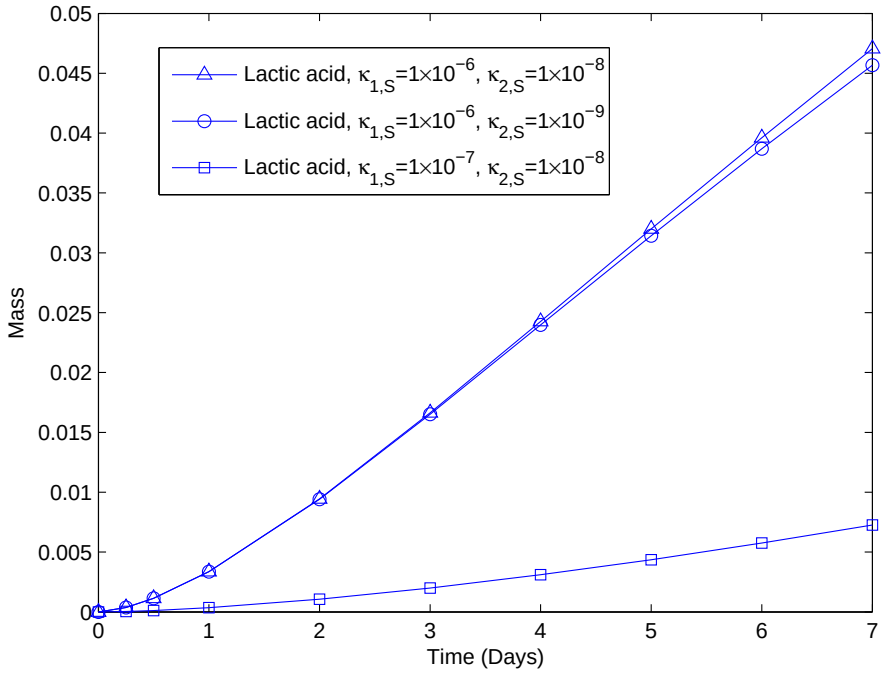

FIGURE 2.20: Mass of lactic acid in the stent for different reaction rates.

Figures 2.21 and 2.22 indicate that a decrement in $\kappa_{1,S}$ will decelerate the speed of drug release and PLA degradation in the stent.

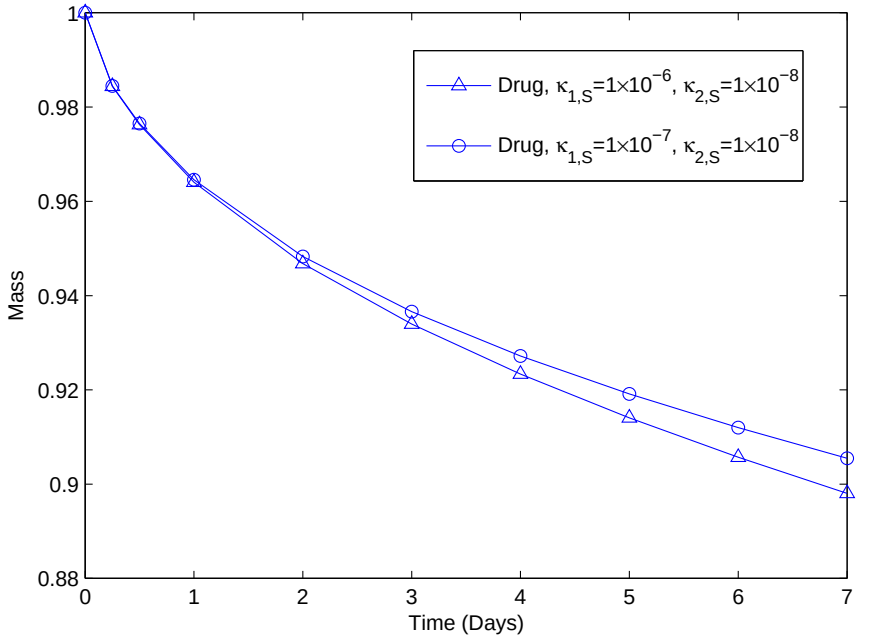

FIGURE 2.21: Mass of drug in the stent for different reaction rates.

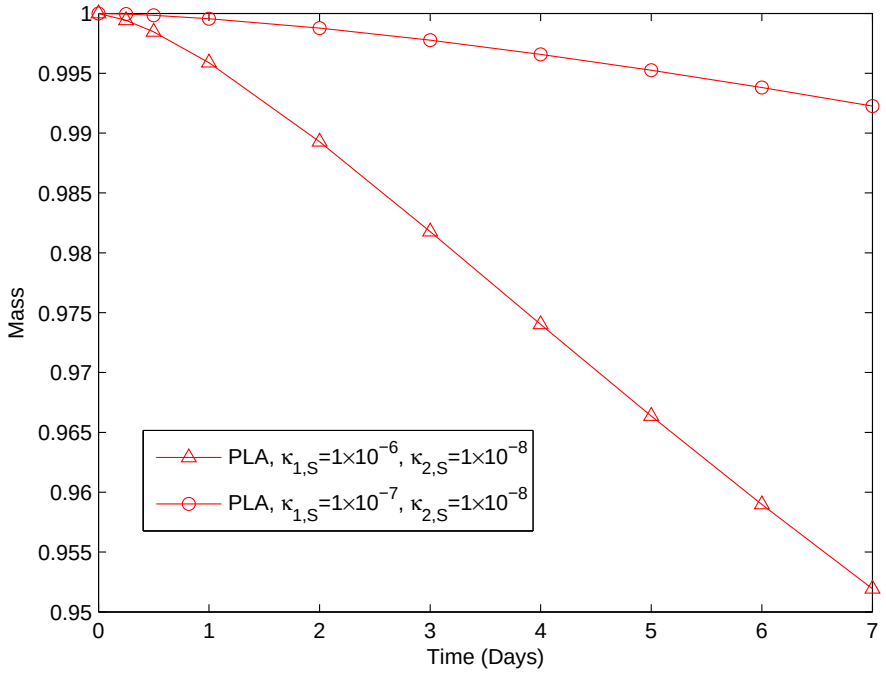

FIGURE 2.22: Mass of PLA in the stent for different reaction rates.

In this chapter we focused on the influence of polymer degradation parameters on the drug release from a DES into an arterial wall. The numerical results obtained are physically sound. The clarification of degradation mechanisms and the quantification of that influence can provide useful guidelines to manufacturers. The model proposed in this chapter simulates "*in vivo*" drug release. However the viscoelastic properties of the vessel walls were not taken into account. A detailed description of their rheological properties will be introduced in Chapter 3.

Chapter 3

A Non-Fickian Coupled Model

In this chapter, we will address to a more complex coupled model than the one introduced in Chapter 2. We evolve from the model introduced in Section 2.1, where the transport of drug in the stent coating and in the arterial wall is dominated by diffusion, to a model where convective transport of the drug is considered and the viscoelastic properties of the arterial wall are taken into account.

Experiments like *creep test* ([16, 29, 41]) have clearly demonstrated that the vascular tissue is viscoelastic. Thus when a constant force is exerted on an artery over an extended period of time, it will first deform like an elastic body and then continue to deform or flow for a finite period of time.

Arterial stiffness is considered as an excellent indicator of cardiovascular morbidity and mortality in a large percentage of the population as referenced in [20]. Taking into consideration the arterial stiffness in the mathematical modeling of drug release from the stent into the arterial wall can help to understand the pharmacokinetic effects of the drug in atherosclerosis.

During the last years, a number of studies have proposed mathematical models for coupled drug delivery in the cardiovascular tissues. We refer without being exhaustive to [2, 5, 18, 25, 28, 34, 46] and also [35] as a review paper. Most of these studies address the release of drug and its numerical behavior while the viscoelasticity of the arterial wall is disregarded.

In this chapter, we propose a non-Fickian coupled model for predicting the biodegradation of PLA, as a drug carrier in the coated stent, and the simultaneous release of the drug from the stent coating into the arterial wall. The effect of

viscoelasticity of the arterial wall in the drug release is investigated using *Maxwell-Wiechert* model ([6]) and Fung's quasilinear viscoelastic model ([16]).

The chapter is organized as follows. Section 3.1 is devoted to the description of the model and its initial, boundary and interface conditions. In Section 3.2, we explain the mass behavior of molecules from the viewpoint of a phenomenological approach. In Section 3.3, we present a variational formulation and establish an energy estimate for the continuous model. The stability of a linearized problem is also studied. Using an implicit-explicit finite element method, we establish a semi-discrete variational form in Section 3.4 and a full discrete variational form in Section 3.5. Numerical simulations as well as a sensitivity analysis of the viscoelastic parameters are discussed in Section 3.6.

3.1 *Description of the model*

Let us consider a two dimensional domain obtained as a section of a three dimensional realistic geometry. Due to the symmetry of the geometry, we consider only a part of the section. We introduce the two dimensional domain $S \subset \mathbb{R}^2$ which represents the polymeric coating of the stent and $V \subset \mathbb{R}^2$ which represents the arterial wall. A schematic representation of the two dimensional domain used in this model is shown in Figure 3.1.

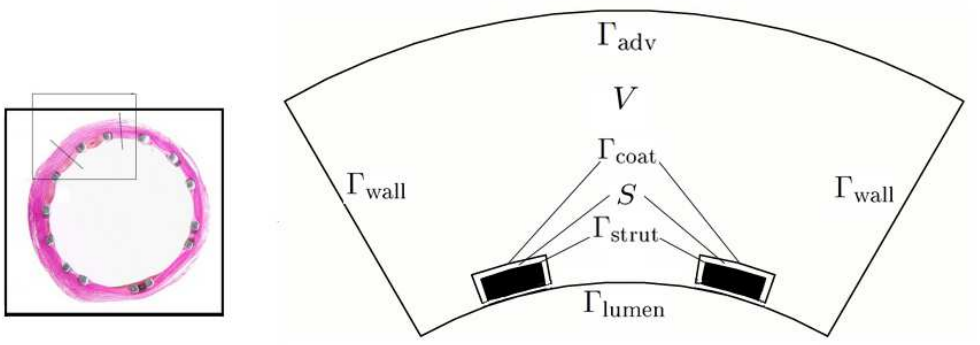

FIGURE 3.1: DES inside of the arterial wall (left: http://www.ibmt.med.uni-rostock.de/nachwuchsgruppe.html).

In Figure 3.1, for the sake of simplicity we have assumed that the DES is completely embedded in the arterial wall. This is a reasonable assumption because

of the complex dynamics of tissue healing and regrowth which takes place immediately after DES implantation in the arterial wall. The evolution of neo-intima around the stent is considered negligible ([26, 46]).

In addition to assumptions 2 and 4 in Section 2.1, the following assumptions are also taken into consideration in the mathematical model:

1. Viscoelastic properties of the polymeric part of the stent is considered negligible;
2. The arterial wall is considered as an homogeneous porous medium with the main properties of *media*;
3. Permeability and viscosity of the stent and arterial wall are considered constants.

Chemical reactions, convection and non-Fickian diffusion are three main phenomena which explain the kinetics of the drug and the biodegradable polymer.

3.1.1 *Chemical reactions*

The chemical reactions responsible for the degradation of PLA into oligomers and lactic acid in the stent coating were presented in Section 2.1. We introduce now the degradation of oligomers into lactic acid that occurs in the arterial wall.

Let $C_{1,V}$ denotes the concentration of water in the arterial wall. The concentration of oligomers in the arterial wall is denoted by $C_{3,V}$. By $C_{4,V}$ we denote the concentration of lactic acid in the arterial wall. Finally, by $C_{5,V}$ we represent the concentration of drug in the arterial wall (see Table 3.1).

Molecule	Coated stent (S)	Vessel wall (V)
Water	$C_{1,S}$	$C_{1,V}$
PLA	$C_{2,S}$	-
Oligomers	$C_{3,S}$	$C_{3,V}$
Lactic acid	$C_{4,S}$	$C_{4,V}$
Drug	$C_{5,S}$	$C_{5,V}$

TABLE 3.1: Notation for the concentrations.

Reactions for the degradation of PLA in the stent are defined by (2.1). The only reaction in the arterial wall is the hydrolysis of the oligomers resulting in

lactic acid. This reaction is schematically represented by

$$C_{1,V} + C_{3,V} \xrightarrow{\kappa_{1,V}} C_{4,V}, \tag{3.1}$$

where $\kappa_{1,V}$ denotes the reaction rate of the hydrolysis of oligomers in the arterial wall.

The evolution in time and space of each concentration depends on the type of chemical reaction involved: production or consumption reaction. To simplify the presentation of the reaction terms that affect the behavior of each concentration, we introduce the notations:

$$\mathcal{C}_S = \Big(C_{m,S}\Big)_{m=1,\dots,5}, \quad \mathcal{C}_V = \Big(C_{m,V}\Big)_{\substack{m=1,\dots,5,\\ m\neq 2}}, \quad \text{and} \quad \mathcal{C} = \big(\mathcal{C}_S, \mathcal{C}_V\big). \tag{3.2}$$

Let $F_{m,S}(\mathcal{C}_S),\ m = 1, \dots, 5$, be defined by (2.3) and (2.4). In the arterial wall we define the following reaction terms

$$F_{m,V}(\mathcal{C}_V) = \begin{cases} -\mathcal{F}_{1,V}(\mathcal{C}_V), & \text{m=1,} \\ -\mathcal{F}_{1,V}(\mathcal{C}_V), & \text{m=3,} \\ \mathcal{F}_{1,V}(\mathcal{C}_V), & \text{m=4,} \\ 0, & \text{m=5,} \end{cases} \tag{3.3}$$

where $\mathcal{F}_{1,V}(\mathcal{C}_V)$ is given by

$$\mathcal{F}_{1,V}(\mathcal{C}_V) = \kappa_{1,V} C_{1,V} C_{3,V}\big(1 + \gamma C_{4,V}\big). \tag{3.4}$$

In (3.4) γ is a positive dimensional constant.

3.1.2 *Convection*

The transport of oligomers, lactic acid and drug in the coated stent and in the arterial wall occurs by diffusion and convection. The same phenomena occur in the transport of PLA in the coated stent. The convection is caused by a pressure gradient in the fluid. Let u_V and p_V represent the velocity and the pressure of the plasma in the arterial wall. We assume that the plasma is incompressible, which mathematically implies that the divergence of its velocity is zero, $\nabla \cdot u_V = 0$. The behavior of the plasma is described by Darcy's law.

To prescribe suitable boundary conditions in the arterial wall, we require that $u_V \cdot \eta_V = 0$ on Γ_{wall} for symmetry, where η_V represents the exterior unit normal. Moreover, we observe that the filtration of the plasma inside the arterial wall is driven by a decreasing pressure gradient from the inner layer of the artery (Γ_{lumen}) to the outer layer of the artery (Γ_{adv}). By consequence we require that $p_V = p_{\text{lumen}}$ on Γ_{lumen} and $p_V = p_{\text{adv}}$ on Γ_{adv}. We notice that p_{lumen} is assumed to be uniform and independent of space and time variables on Γ_{lumen}. The velocity and the pressure in the arterial wall satisfy the following equations:

$$\begin{cases} u_V = -\frac{k_V}{\mu_V}\nabla p_V & \text{in } V, \\ \nabla \cdot u_V = 0 & \text{in } V, \\ p_V = p_{lumen} & \text{on } \Gamma_{\text{lumen}}, \\ p_V = p_{adv} & \text{on } \Gamma_{\text{adv}}, \\ u_V \cdot \eta_V = 0 & \text{on } \Gamma_{\text{wall}}. \end{cases} \tag{3.5}$$

We assume in what follows that the incompressible plasma can penetrate inside the coated stent. Let u_S and p_S represent the velocity and the pressure of fluid in the stent. As the metallic part of the stent is rigid we consider no flux of plasma in Γ_{strut}. So the velocity and the pressure in the coated stent are described by

$$\begin{cases} u_S = -\frac{k_S}{\mu_S}\nabla p_S & \text{in } S, \\ \nabla \cdot u_S = 0 & \text{in } S, \\ u_S \cdot \eta_S = 0 & \text{on } \Gamma_{\text{strut}}, \end{cases} \tag{3.6}$$

where η_S represents the exterior unit normal.

Systems of equations (3.5) and (3.6) are completed with the matching conditions

$$\begin{cases} p_S = p_V & \text{on } \Gamma_{\text{coat}}, \\ u_S \cdot \eta_S = -u_V \cdot \eta_V & \text{on } \Gamma_{\text{coat}}. \end{cases} \tag{3.7}$$

The boundaries Γ_{lumen}, Γ_{adv}, Γ_{wall}, Γ_{strut} and Γ_{coat} introduced in (3.5), (3.6) and (3.7) are defined in Figure 3.1. In (3.5) and (3.6), k_S and k_V are permeability coefficients which characterize the capacity of the stent and arterial wall to allow the flow of small molecules across them. These coefficients depend on the properties of the medium and also on the concentrations of PLA, oligomers, lactic acid and drug in the stent and oligomers, lactic acid and drug in the arterial wall. To simplify the model, we assume that $k_j,\ j = S, V$, are constants.

In (3.5) and (3.6), $\mu_j, j = S, V$, are the viscosities of the fluid in the stent and the arterial wall respectively, which represents the resistance of the fluid to gradual deformation. These coefficients depend on the chemical compounds presented in the stent and in the arterial wall. To simplify, we assume in what follows that the viscosities $\mu_j, j = S, V$, are also constants.

3.1.3 *Viscoelastic effects*

Viscoelasticity is the ability of a material to exhibit both solid-like and fluid-like behavior. Viscoelastic models have been widely used to characterize mechanistic properties of the vascular tissues due to their ability to tailor both the viscoelastic relaxation function and the nonlinear elastic stress-strain relation. Numerous viscoelastic models, derived under different experimental conditions, have been proposed in the literature. We refer without being exhaustive to [6, 27, 29, 39, 40].

A constitutive equation typically determines the relationship between the stress (internal force) that a material is subjected and the strain (deformation) response. A reliable constitutive model for arterial walls is an essential prerequisite for studying mechanical factors of atherosclerosis.

Analogical models are currently used to describe viscoelasticity. The simplest linear viscoelastic models are attributed to *Maxwell*, *Voigt*, and *Kelvin* ([6]). The Maxwell fluid model is represented by a dashpot in series with an elastic spring. The Voigt solid model is represented by a dashpot in parallel with an elastic spring. The Kelvin model, also called the standard linear solid combines a Maxwell element in parallel with an elastic spring.

In what follows, we present a linear viscoelastic model (*Maxwell-Wiechert* model, [6]). The multiple relaxation times used in this model are well adapted to predict viscoelastic behavior in living tissues ([29]). We postpone for a later section for some considerations on the use of a nonlinear viscoelastic model (Fung's quasilinear viscoelastic model, [16]).

In the *Maxwell-Wiechert* model (Figure 3.2), the relation between the stress and the strain is given by the following convolution integral:

$$\sigma_V(t) = -\left(k_r \varepsilon_V(t) + \int_0^t K(t-s)\frac{\partial \varepsilon_V}{\partial s}(s)ds\right), \tag{3.8}$$

where σ_V stands for the stress which is an internal force that represents the response to the strain caused by an incoming drug. In (3.8), κ_r is the Young's modulus of the spring arm.

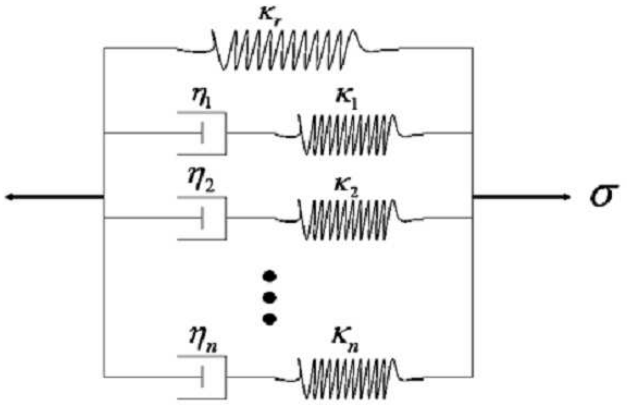

FIGURE 3.2: Generalized Maxwell-Wiechert linear model ([6]).

It should be noted that the negative sign in (3.8) indicates that σ and ε are of opposite sign. This represents the fact that the arterial wall acts like a barrier to the entry of the drug ([13, 14, 23]).

The convolution memory kernel in (3.8) is defined by

$$K(t-s) = \sum_{i=1}^{n} \kappa_i e^{-\frac{t-s}{\tau_i}}, \tag{3.9}$$

where $\tau_i = \frac{\eta_i}{\kappa_i},\ i = 1, \ldots, n$. The constants $\kappa_i,\ i = 1, \ldots, n$, represent the Young modulus of the Maxwell arms while $\eta_i,\ i = 1, \ldots, n$, are their viscosities. For $t = 0$ the total Young's modulus of Maxwell-Wiechert model is $\kappa_r + \sum_{i=1}^{n} \kappa_i$ while, for $t \to \infty$, its value is κ_r.

Replacing (3.9) in (3.8), we have

$$\sigma_V(t) = -\left(k_r \varepsilon_V(t) + \sum_{i=1}^{n} \int_0^t \kappa_i e^{-\frac{t-s}{\tau_i}} \frac{\partial \varepsilon_V}{\partial s}(s) ds \right). \tag{3.10}$$

By integrating by parts, assuming $\varepsilon_V(0) = 0$, and considering a linear relationship between strain and concentrations in the arterial wall ([10, 12–15, 22, 23]), $\varepsilon_V(t) =$

$\alpha_m C_{m,V}(t),\ m = 1, \ldots, 5,\ m \neq 2$, we will finally have

$$\sigma_{m,V}(t) = -\alpha_m \left((\kappa_r + \sum_{i=1}^{n} \kappa_i) C_{m,V}(t) - \sum_{i=1}^{n} \frac{\kappa_i}{\tau_i} \int_0^t e^{-\frac{t-s}{\tau_i}} C_{m,V}(s) ds \right), \quad (3.11)$$

for $m = 1, \ldots, 5,\ m \neq 2$.

Particular attention will be devoted to the case $n = 1$, that is a mechanical analog composed by an elastic arm and a Maxwell arm.

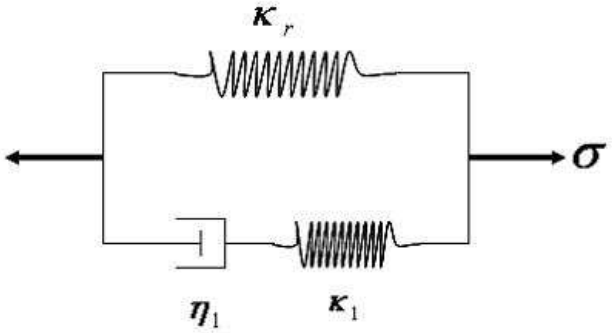

FIGURE 3.3: Maxwell-Wiechert model with $n = 1$ ([6]).

The following formulation

$$\sigma_{m,V}(t) = -\alpha_m \left((\kappa_r + \kappa_1) C_{m,V}(t) - \frac{\kappa_1}{\tau_1} \int_0^t e^{-\frac{t-s}{\tau_1}} C_{m,V}(s) ds \right), \quad (3.12)$$

for $m = 1, \ldots, 5,\ m \neq 2$, is a particular case of (3.11) when $n = 1$.

3.1.4 *A reaction-diffusion-convection problem*

The reaction-convection-diffusion processes which take place in the stent are described by the following system of equations

$$\frac{\partial C_{m,S}}{\partial t} = \nabla \cdot \left(D_{m,S} \nabla C_{m,S} - u_S C_{m,S} \right) + F_{m,S}(\mathcal{C}_S), \quad (3.13)$$

in $S \times \mathbb{R}^+$, for $m = 1, \ldots, 5$. The diffusion coefficients $D_{m,S},\ m = 1, \ldots, 5$, are defined by (2.6), being of the variables summarized in Table 3.1.

The transport process that occurs in the arterial wall is due to convective transport and non-Fickian diffusion driven by the stress. It is described by the

following set of equations

$$\frac{\partial C_{m,V}}{\partial t} = \nabla \cdot \left(\bar{D}_{m,V}\nabla C_{m,V} - u_V C_{m,V}\right) + \nabla \cdot \left(\bar{D}_\sigma \nabla \sigma_{m,V}\right) + F_{m,V}(\mathcal{C}_V), \qquad (3.14)$$

in $V \times \mathbb{R}^+$, for $m = 1, \ldots, 5,\ m \neq 2$.

We recall that the subscript $m = 2$ refers to PLA. As PLA has a large molecular weight ($M_W \geq 1.2 \times 10^5\ g/mol$) compared to the other species present in the process, it will not cross the interface boundary Γ_{coat} to enter the arterial wall. So (3.14) is not applied for PLA.

It should be noted that the velocities u_S and u_V in (3.13) and (3.14) are computed by solving the coupled problem (3.5)-(3.7). The reaction functions $F_{m,j}(\mathcal{C}_j),\ j = S, V$, in (3.13) and (3.14), are defined by (2.3), (2.4), (3.3) and (3.4). In (3.14), the stress $\sigma_{m,V},\ m = 1, \ldots, 5,\ m \neq 2$, is given by (3.11) and $\bar{D}_\sigma$ represents the "weight" of the non-Fickian diffusion whose physical meaning can be found in [13, 14].

In what follows, particular attention will be devoted to system (3.13) and (3.14) when the viscoelastic behavior of the arterial wall is described by Maxwell-Wiechert model with $n = 1$. The coupled problem (3.13) and (3.14) in this case takes the form

$$\begin{cases} \frac{\partial C_{m,S}}{\partial t} = \nabla \cdot \left(D_{m,S}\nabla C_{m,S} - u_S C_{m,S}\right) + F_{m,S}(\mathcal{C}_S) & \text{in } S \times \mathbb{R}^+,\ m = 1, \ldots, 5, \\ \frac{\partial C_{m,V}}{\partial t} = \nabla \cdot \left(D_{m,V}\nabla C_{m,V} - u_V C_{m,V}\right) + F_{m,V}(\mathcal{C}_V) & \\ \quad + \int_0^t e^{-\frac{t-s}{\tau_1}} \nabla \cdot \left(D_{m,\sigma}\nabla C_{m,V}(s)\right) ds & \text{in } V \times \mathbb{R}^+,\ m = 1, \ldots, 5, m \neq 2, \end{cases} \qquad (3.15)$$

where $D_{m,V} = \bar{D}_{m,V} - \alpha_m(\kappa_r + \kappa_1)\bar{D}_\sigma$ and $D_{m,\sigma} = \alpha_m \frac{\kappa_1}{\tau_1}\bar{D}_\sigma$ for $m = 1, \ldots, 5,\ m \neq 2$.

To ensure the positivity of the effective Fickian diffusion coefficient $D_{m,V}$, the diffusion coefficients $\bar{D}_{m,V}$, the Young modulus κ_r and κ_1, the parameter α_m and the non-Fickian weight coefficient $\bar{D}_\sigma$ should satisfy the relation $\bar{D}_\sigma < \frac{\bar{D}_{m,V}}{\alpha_m(\kappa_r+\kappa_1)}$. This assumption guarantees that Fickian diffusion dominates the viscoelastic opposition, which is a physical condition for the effective penetration of drug in the arterial wall.

For a sake of simplicity, we assume that the diffusion coefficients in the arterial wall $D_{m,V},\ m = 1, \ldots, 5,\ m \neq 2$, are constants.

To complete the coupled problem (3.15), we define in what follows the initial, the boundary and the interface conditions. At the initial time, we assume that the PLA and drug are distributed uniformly in the stent. We also assume that at the initial time no degradation has occurred and consequently neither oligomers nor lactic acid are present in the coating. The initial concentrations in the coating and in the arterial wall are then given by

$$\begin{cases} C_{m,S}(0) = 0, \ m = 1, 3, 4, \\ C_{m,S}(0) = 1, \ m = 2, 5, \end{cases} \tag{3.16}$$

and

$$\begin{cases} C_{1,V}(0) = 1, \\ C_{m,V}(0) = 0, \quad m = 3, 4, 5, \end{cases} \tag{3.17}$$

respectively.

We represent by $J_{m,S}$ and $J_{m,V}$, the mass fluxes of species in the stent and in the arterial wall defined respectively by

$$\begin{aligned} J_{m,S} &= -\Big(D_{m,S}\nabla C_{m,S} - u_S C_{m,S} \Big), \ m = 1, \ldots, 5, \\ J_{m,V} &= -\left(D_{m,V}\nabla C_{m,V} - u_V C_{m,V} + D_{m,\sigma}\int_0^t e^{-\frac{t-s}{\tau_1}} \nabla C_{m,V}(s) ds \right), \ {}^{m=1,\ldots,5,}_{m\neq 2}. \end{aligned} \tag{3.18}$$

As the metallic stent strut is impermeable to the drug, fluid and PLA degradation products, which diffuse from the stent coating, no mass flux passes through the boundary Γ_{strut}. So

$$J_{m,S} \cdot \eta_S = 0 \quad \text{ on } \Gamma_{\text{strut}} \times \mathbb{R}^+, \ m = 1, \ldots, 5. \tag{3.19}$$

Equations in S and V are coupled by appropriate conditions at the interface boundary Γ_{coat}. Its formulation depends on the structure of the stent coating. A possible choice could be the continuity of the concentrations and the continuity of local fluxes, that is

$$\begin{cases} C_{m,S} = C_{m,V} & \text{on } \Gamma_{\text{coat}} \times \mathbb{R}^+, m = 1, \ \ldots, 5, \ m \neq 2, \\ J_{m,S} \cdot \eta_S = -J_{m,V} \cdot \eta_V & \text{on } \Gamma_{\text{coat}} \times \mathbb{R}^+, \ m = 1, \ldots, 5, \ m \neq 2. \end{cases} \tag{3.20}$$

A more realistic interface condition considers that the coated stent, loaded with the drug is covered by a second thin layer, called *topcoat*. This layer acts like a

membrane between the transport domains to slow down the release rate from the stent into the arterial wall. We postpone its mathematical description to a later section.

We stress that Γ_{coat} is impermeable to PLA due to its large molecular weight, so $J_{2,S} \cdot \eta_S = 0$ on Γ_{coat}. The symmetric boundaries Γ_{wall} of the arterial wall implies no-flux, that is

$$J_{m,V} \cdot \eta_V = 0 \quad \text{on } \Gamma_{\text{wall}} \times \mathbb{R}^+,\ m = 1, \ldots, 5,\ m \neq 2. \tag{3.21}$$

We also assume that adventitia is impermeable to all species present in the arterial wall. So the boundary condition (3.21) also holds for Γ_{adv}.

Since the drug, the oligomers and the lactic acid flow directly from the arterial wall into the blood and are transported fast away from the region of interest, we consider

$$J_{m,V} \cdot \eta_V = -\gamma_{m,V} C_{m,V} \quad \text{on } \Gamma_{\text{lumen}} \times \mathbb{R}^+,\ m = 3, 4, 5, \tag{3.22}$$

with a high transference rate $\gamma_{m,V}$.

As the water penetrates from the blood artery into the arterial wall, we consider the natural boundary condition

$$J_{1,V} \cdot \eta_V = \gamma_{1,V}(1 - C_{1,V}) \quad \text{on } \Gamma_{\text{lumen}} \times \mathbb{R}^+, \tag{3.23}$$

for the water concentration.

Summarizing boundary and interface conditions, we have:

$$\begin{cases} J_{m,S} \cdot \eta_S = 0 & \text{on } \Gamma_{\text{strut}} \times \mathbb{R}^+,\ m = 1, \ldots, 5, \\ J_{2,S} \cdot \eta_S = 0 & \text{on } \Gamma_{\text{coat}} \times \mathbb{R}^+, \\ C_{m,S} = C_{m,V} & \text{on } \Gamma_{\text{coat}} \times \mathbb{R}^+,\ m = 1, \ldots, 5,\ m \neq 2, \\ J_{m,S} \cdot \eta_S = -J_{m,V} \cdot \eta_V & \text{on } \Gamma_{\text{coat}} \times \mathbb{R}^+,\ m = 1, \ldots, 5,\ m \neq 2, \\ J_{1,V} \cdot \eta_V = \gamma_{1,V}(1 - C_{1,V}) & \text{on } \Gamma_{\text{lumen}} \times \mathbb{R}^+, \\ J_{m,V} \cdot \eta_V = -\gamma_{m,V} C_{m,V} & \text{on } \Gamma_{\text{lumen}} \times \mathbb{R}^+,\ m = 3, 4, 5, \\ J_{m,V} \cdot \eta_V = 0 & \text{on } (\Gamma_{\text{wall}} \cup \Gamma_{\text{adv}}) \times \mathbb{R}^+,\ m = 1, \ldots, 5,\ m \neq 2. \end{cases} \tag{3.24}$$

3.2 *Qualitative behavior of the total mass*

In what follows we analyze the behavior of the total mass of species in the model. We consider

$$\mathcal{M}(t) = \int_S \mathcal{C}_S(t)dS + \int_V \mathcal{C}_V(t)dV, \tag{3.25}$$

where $\int_S \mathcal{C}_S(t)dS = \sum_{m=1}^{5}\int_S C_{m,S}(t)dS$, $\int_V \mathcal{C}_V(t)dV = \sum_{\substack{m=1\\m\neq 2}}^{5}\int_V C_{m,V}(t)dV$, where the concentration variables are defined in Table 3.1.

Replacing (3.15) in

$$\mathcal{M}'(t) = \sum_{m=1}^{5}\int_S \frac{\partial C_{m,S}}{\partial t}(t)dS + \sum_{\substack{m=1\\m\neq 2}}^{5}\int_V \frac{\partial C_{m,V}}{\partial t}(t)dV, \tag{3.26}$$

we obtain

$$\begin{aligned}\mathcal{M}'(t) &= \sum_{m=1}^{5}\int_S \nabla\cdot\big(D_{m,S}(t)\nabla C_{m,S}(t) - u_S C_{m,S}(t)\big)dS + \sum_{m=1}^{5}\int_S F_{m,S}(\mathcal{C}_S(t))dS\\ &+\sum_{\substack{m=1\\m\neq 2}}^{5}\int_V \nabla\cdot\big(D_{m,V}\nabla C_{m,V}(t) - u_V C_{m,V}(t)\big)dV + \sum_{\substack{m=1\\m\neq 2}}^{5}\int_V F_{m,V}(\mathcal{C}_V(t))dV\\ &+\sum_{\substack{m=1\\m\neq 2}}^{5}\int_V\int_0^t e^{-\frac{t-s}{\tau_1}}\nabla\cdot\big(D_{m,\sigma}\nabla C_{m,V}(s)\big)dsdV.\end{aligned}$$

Using Gauss's theorem ([11]) and applying the boundary conditions, we have

$$\begin{aligned}\mathcal{M}'(t) &= \sum_{\substack{m=1\\m\neq 2}}^{5}\int_{\Gamma_{\text{coat}}} J_{m,S}(t)\cdot\eta_S ds + \sum_{\substack{m=1\\m\neq 2}}^{5}\int_{\Gamma_{\text{coat}}} J_{m,V}(t)\cdot\eta_V ds + \int_S\sum_{m=1}^{5}F_{m,S}(\mathcal{C}_S(t))dS\\ &+\int_V\sum_{\substack{m=1\\m\neq 2}}^{5}F_{m,V}(\mathcal{C}_V(t))dV + \gamma_{1,V}\int_{\Gamma_{\text{lumen}}}(1-C_{1,V}(t))ds - \sum_{m=3}^{5}\gamma_{m,V}\int_{\Gamma_{\text{lumen}}}C_{m,V}(t)ds,\end{aligned} \tag{3.27}$$

where $J_{m,j}(t),\ j=S,V,\ m=1,\dots,5,\ m\neq 2$, are defined by (3.18).

Let

$$\Delta M_{\Gamma_{\text{lumen}}}(t) = \sum_{\substack{m=1 \\ m\neq 2}}^{5} \gamma_{m,V} \int_{\Gamma_{\text{lumen}}} C_{m,V}(t) ds,$$
$$\Delta M_H(t) = \int_S \kappa_{2,S} C_{1,S}(t) C_{3,S}(t)(1+\beta C_{4,S}(t)) dS + \int_V \kappa_{1,V} C_{1,V}(t) C_{3,V}(t)\big(1+\gamma C_{4,V}(t)\big) dV. \tag{3.28}$$

We note that $\Delta M_{\Gamma_{\text{lumen}}}(t)$ represents the mass per unit time of species (except PLA) that enters in Γ_{lumen} at the instant t, while $\Delta M_H(t)$ stands for the total mass of hydrolyzed oligomers that enter per unit time in the stent and the arterial wall at the same instant.

Using (3.28) and replacing the interface condition (3.20) in (3.27), we easily establish

$$\mathcal{M}'(t) = \gamma_{1,V} \left|\Gamma_{\text{lumen}}\right| - \Delta M_H(t) - \Delta M_{\Gamma_{\text{lumen}}}(t). \tag{3.29}$$

By integration over time, (3.29) leads to

$$\mathcal{M}(t) \quad = \mathcal{M}(0) + \gamma_{1,V} \left|\Gamma_{\text{lumen}}\right| t - \int_0^t \Delta M_H(\mu) d\mu - \int_0^t \Delta M_{\Gamma_{\text{lumen}}}(\mu)\, d\mu. \tag{3.30}$$

The equation (3.30) means that the total mass in the system at a certain time t, $t \in [0, T]$, is given by the difference between the initial mass added with the mass of plasma that enters in the system until time t and the cumulative masses of molecules on Γ_{lumen} and in the stent and the arterial wall.

3.3 *Weak formulation*

In this section, we introduce a variational form of the IBVP (3.15) – (3.17) and (3.24).

3.3.1 *Porous media problem*

In order to find the pressure drop in the stented arterial wall, as k_j and μ_j, $j = S, V$, are constants, it is convenient to rewrite equations (3.5) – (3.7) in terms of pressure drop

in the following coupled form:

$$\begin{cases} -\nabla \cdot (\frac{k_V}{\mu_V} \nabla p_V) = 0 & \text{in } V, \\ -\nabla \cdot (\frac{k_S}{\mu_S} \nabla p_S) = 0 & \text{in } S, \\ p_V = p_{\text{lumen}} & \text{on } \Gamma_{\text{lumen}}, \\ p_V = p_{\text{adv}} & \text{on } \Gamma_{\text{adv}}, \\ \nabla p_V \cdot \eta_V = 0 & \text{on } \Gamma_{\text{wall}}, \\ p_V = p_S & \text{on } \Gamma_{\text{coat}}, \\ \frac{k_V}{\mu_V} \nabla p_V \cdot \eta_V = -\frac{k_S}{\mu_S} \nabla p_S \cdot \eta_S & \text{on } \Gamma_{\text{coat}}, \\ \nabla p_S \cdot \eta_S = 0 & \text{on } \Gamma_{\text{strut}}. \end{cases} \tag{3.31}$$

For a sake of simplicity, we assume $p_{\text{adv}} = 0$ and a nonzero pressure $p_{\text{lumen}} = p_0$ independent of time and space variables (see Section 3.1.2).

In what follows we use the notations

$$\mathcal{A}_j(p_j, q_j) = \left(\tfrac{\kappa_j}{\mu_j} \nabla p_j, \nabla q_j\right)_j, \ j = S, V. \tag{3.32}$$

As the pressure is nonzero on Γ_{lumen} and null on Γ_{adv}, we introduce the space

$$H^1_{\text{lumen,adv}}(V) = \left\{ \vartheta \in H^1(V) \text{ such that } \vartheta = 0 \text{ on } \Gamma_{\text{lumen}} \cup \Gamma_{\text{adv}} \right\}, \tag{3.33}$$

and the space

$$\mathcal{V} = \left\{ (\vartheta_S, \vartheta_V) \in H^1(S) \times H^1_{\text{lumen,adv}}(V) \text{ such that } \vartheta_S = \vartheta_V \text{ on } \Gamma_{\text{coat}} \right\}, \tag{3.34}$$

to couple the pressures in the stent coating and in the arterial wall over Γ_{coat}.

Let $w \in H^1(V)$ be such that $w = p_0$ on Γ_{lumen} and $p^*_V = p_V - w \in H^1_{\text{lumen,adv}}(V)$. The weak formulation of problem (3.31) is as follows: Find $(p_S, p^*_V) \in \mathcal{V}$ such that

$$\mathcal{A}_S(p_S, q_S) + \mathcal{A}_V(p^*_V, q_V) = -\mathcal{A}_V(w, q_V), \quad \forall\ (q_S, q_V) \in \mathcal{V}. \tag{3.35}$$

It is obvious that p_V can be recovered by $p_V = p^*_V + w$. Velocities u_S and u_V can be then obtained by Darcy's law $u_j = -\frac{k_j}{\mu_j} \nabla p_j, \ j = S, V$.

In the case that k_j and μ_j, $j = S, V$, depend on the concentration of species, problem (3.31) needs to be solved simultaneously for each time level coupled with problem for concentrations. Another approach that can be used to define the variational problem for the velocities $u_j, \ j = S, V$, is the so called mixed variational formulation where the velocities $u_j, \ j = S, V$, and the pressures $p_j, \ j = S, V$, are simultaneously computed.

In this case the numerical approximations for the velocities and the pressures are then obtained using the mixed finite element methods ([4, 7]).

3.3.2 *Convection-diffusion-reaction problem*

We assume in what follows that the diffusion coefficients $D_{m,S},\ m = 1, \ldots, 5$, are constants. We adopt the following notations:

$$\begin{aligned}
a_S\big(v_S(t), w_S\big) &= \sum_{m=1}^{5} \Big(D_{m,S} \nabla v_{m,S}(t) - u_S v_{m,S}(t), \nabla w_{m,S} \Big)_S, \\
a_V\big(v_V(t), w_V\big) &= \sum_{\substack{m=1 \\ m\neq 2}}^{5} \Big(D_{m,V} \nabla v_{m,V}(t) - u_V v_{m,V}(t), \nabla w_{m,V} \Big)_V \\
&\quad + \sum_{\substack{m=1 \\ m\neq 2}}^{5} \int_0^t e^{-\frac{t-s}{\tau_1}} \Big(D_{m,\sigma} \nabla v_{m,V}(s), \nabla w_{m,V} \Big)_V ds, \\
a_{\text{lumen}}(v_V(t), w_V) &= \gamma_{1,V} \Big(1 - v_{1,V}(t), w_{1,V} \Big)_{\Gamma_{\text{lumen}}} - \sum_{m=3}^{5} \gamma_{m,V} \Big(v_{m,V}(t), w_{m,V} \Big)_{\Gamma_{\text{lumen}}}.
\end{aligned} \tag{3.36}$$

To take into account the interface boundary conditions over Γ_{coat} in the variational problem, we consider the Sobolev spaces

$$\mathcal{W} = \Big\{ (v_S, v_V) \in \Big(H^1(S) \Big)^5 \times \Big(H^1(V) \Big)^4 \text{ such that } v_{m,S} = v_{m,V} \text{ on } \Gamma_{\text{coat}},\ m = 1, 3, 4, 5 \Big\}, \tag{3.37}$$

where $\big(v_S, v_V\big) = \Big(\big(v_{m,S}\big)_{m=1,\ldots,5}, \big(v_{m,V}\big)_{\substack{m=1,\ldots,5 \\ m\neq 2}} \Big)$ and

$$L^2(0, T; \mathcal{W}) = \Big\{ w : (0, T) \longrightarrow \mathcal{W} \text{ such that } \int_0^T \Big\| w(t) \Big\|_{\mathcal{W}}^2 dt < \infty \Big\}. \tag{3.38}$$

The weak solution of the problem (3.15) – (3.17) and (3.24) is the solution of the following variational problem:

VP2: Find $\big(\mathcal{C}_S, \mathcal{C}_V\big) \in L^2(0, T; \mathcal{W})$ such that $\big(\frac{\partial \mathcal{C}_S}{\partial t}, \frac{\partial \mathcal{C}_V}{\partial t}\big) \in \Big(L^2(0, T; L^2(S)) \Big)^5 \times \Big(L^2(0, T; L^2(V)) \Big)^4$ and

$$\begin{cases}
\displaystyle\sum_{j=S,V} \Big(\big(\frac{\partial \mathcal{C}_j}{\partial t}(t), v_j\big)_j + a_j\big(\mathcal{C}_j(t), v_j\big) \Big) = \sum_{j=S,V} \big(\mathcal{F}_j(\mathcal{C}_j(t)), v_j \big)_j + a_{\text{lumen}}(\mathcal{C}_V(t), v_V), \\
\qquad \text{a.e in } (0, T), \text{ for all } (v_S, v_V) \in \mathcal{W}, \\
\mathcal{C}_S(0) = (0, 1, 0, 0, 1),\ \mathcal{C}_V(0) = (1, 0, 0, 0),
\end{cases} \tag{3.39}$$

where $\mathcal{C}_j,\ j = S, V$, are defined in (3.2) and

$$\big(\mathcal{F}_S(\mathcal{C}_S), \mathcal{F}_V(\mathcal{C}_V)\big) = \bigg(\big(F_{m,S}(\mathcal{C}_S)\big)_{m=1,\dots,5}, \big(F_{m,V}(\mathcal{C}_V)\big)_{\substack{m=1,\dots,5,\\ m\neq 2}}\bigg), \tag{3.40}$$

is defined by (2.3), (2.4), (3.3) and (3.4).

We introduce the energy functional

$$\mathcal{E}_1(t) = \sum_{j=S,V}\bigg(\Big\|\mathcal{C}_j(t)\Big\|^2_{L^2(j)} + \int_0^t \Big\|\nabla\mathcal{C}_j(s)\Big\|^2_{L^2(j)} ds\bigg) + \bigg\|\int_0^t e^{-\frac{t-s}{\tau_1}}\nabla\mathcal{C}_V(s)ds\bigg\|^2_{L^2(V)}, \tag{3.41}$$

for $t \in [0, T]$, where

$$\Big\|\mathcal{C}_S(t)\Big\|_{L^2(S)} = \sum_{m=1}^{5}\Big\|C_{m,S}(t)\Big\|_{L^2(S)} \text{ and } \Big\|\mathcal{C}_V(t)\Big\|_{L^2(V)} = \sum_{\substack{m=1\\ m\neq 2}}^{5}\Big\|C_{m,V}(t)\Big\|_{L^2(V)}. \tag{3.42}$$

An upper bound for the energy functional (3.41) is established in the following theorem.

Theorem 3.3.1. If $(\mathcal{C}_S, \mathcal{C}_V)$ is a solution of the variational problem **VP2**, then assuming $\big(\mathcal{C}_S(t), \mathcal{C}_V(t)\big) \in \big(H^2(S)\big)^5 \times \big(H^2(V)\big)^4$ we have

$$\mathcal{E}_1(t) \ \leq \frac{1}{\min\big\{1,\phi,D_\sigma\big\}} e^{2(\mathcal{K}+\varphi)t}\mathcal{E}_1(0) + \frac{\gamma_{1,V}}{2(\mathcal{K}+\varphi)}|\Gamma_{\text{lumen}}|\bigg(e^{2(\mathcal{K}+\varphi)t} - 1\bigg), \tag{3.43}$$

where $\mathcal{K}, \phi, \varphi$ and D_σ are concentration-independent constants while $|\Gamma_{\text{lumen}}|$ is the length of the transition boundary Γ_{lumen}.

Proof. Taking in (3.39), $v_j = \mathcal{C}_j(t),\ j = S, V$, in the left side of (3.39) we will have

$$\bigg(\frac{\partial\mathcal{C}_j}{\partial t}(t), \mathcal{C}_j(t)\bigg)_j = \frac{1}{2}\frac{d}{dt}\Big\|\mathcal{C}_j(t)\Big\|^2_{L^2(j)},\ j = S, V. \tag{3.44}$$

It is obvious that

$$\frac{d}{dt}\bigg\|\int_0^t e^{-\frac{t-s}{\tau_1}}\nabla\mathcal{C}_V(s)ds\bigg\|^2_{L^2(V)} = 2\bigg(\frac{\partial}{\partial t}\int_0^t e^{-\frac{t-s}{\tau_1}}\nabla\mathcal{C}_V(s)ds, \int_0^t e^{-\frac{t-s}{\tau_1}}\nabla\mathcal{C}_V(s)ds\bigg)_V. \tag{3.45}$$

Applying Leibnitz integral theorem to the right hand side of (3.45), we will obtain

$$\begin{aligned}\frac{d}{dt}\bigg\|\int_0^t e^{-\frac{t-s}{\tau_1}}\nabla\mathcal{C}_V(s)ds\bigg\|^2_{L^2(V)} &= 2\int_0^t e^{-\frac{t-s}{\tau_1}}\bigg(\nabla\mathcal{C}_V(s), \nabla\mathcal{C}_V(t)\bigg)_V ds\\ &\quad -\frac{2}{\tau_1}\bigg\|\int_0^t e^{-\frac{t-s}{\tau_1}}\nabla\mathcal{C}_V(s)ds\bigg\|^2_{L^2(V)}.\end{aligned} \tag{3.46}$$

The inequality

$$\Big(u_j\mathcal{C}_j(t),\nabla\mathcal{C}_j(t)\Big)_j \leq \big\|u_j\big\|_\infty\Big(\varepsilon_j^2\Big\|\mathcal{C}_j(t)\Big\|^2_{L^2(j)}+\tfrac{1}{4\varepsilon_j^2}\Big\|\nabla\mathcal{C}_j(t)\Big\|^2_{L^2(j)}\Big), \tag{3.47}$$

holds for arbitrary non-zero ε_j, for $j=S,V$.

Replacing (3.44), (3.46) and (3.47) in (3.39), we establish the following differential inequality

$$\begin{aligned}\frac{1}{2}\frac{d}{dt}\sum_{j=S,V}\Big(\Big\|\mathcal{C}_j(t)\Big\|^2_{L^2(j)} &+\phi\int_0^t\Big\|\nabla\mathcal{C}_j(s)\Big\|^2_{L^2(j)}ds+D_\sigma\Big\|\int_0^t e^{-\frac{t-s}{\tau_1}}\nabla\mathcal{C}_V(s)ds\Big\|^2_{L^2(V)}\Big)\\ &\leq\sum_{j=S,V}\big\|u_j\big\|_\infty\varepsilon_j^2\Big\|\mathcal{C}_j(t)\Big\|^2_{L^2(j)}-\tfrac{D_\sigma}{\tau_1}\Big\|\int_0^t e^{-\frac{t-s}{\tau_1}}\nabla\mathcal{C}_V(s)ds\Big\|^2_{L^2(V)}\\ &+\sum_{j=S,V}\Big(\mathcal{F}_j(\mathcal{C}_j(t),\mathcal{C}_j(t)\Big)_j+\lambda_{\text{lumen}}.\end{aligned} \tag{3.48}$$

In (3.48), λ_{lumen} is given by

$$\begin{aligned}\lambda_{\text{lumen}} &=\gamma_{1,V}\Big(1-C_{1,V}(t),C_{1,V}(t)\Big)_{\Gamma_{\text{lumen}}}-\sum_{m=3}^{5}\gamma_{m,V}\Big(C_{m,V}(t),C_{m,V}(t)\Big)_{\Gamma_{\text{lumen}}}\\ &\leq\tfrac{\gamma_{1,V}}{4}\Big|\Gamma_{\text{lumen}}\Big|-\sum_{m=3}^{5}\gamma_{m,V}\Big\|C_{m,V}(t)\Big\|^2_{\Gamma_{\text{lumen}}},\end{aligned} \tag{3.49}$$

and

$$\begin{cases}\phi=\min\limits_{j=S,V}\big\{2D_j-\frac{\big\|u_j\big\|_\infty}{2\varepsilon_j^2}\big\},\\ D_S=\min\limits_{m=1,\dots,5}\big\{D_{m,S}\big\},\\ D_V=\min\limits_{\substack{m=1,\dots,5,\\ m\neq2}}\big\{D_{m,V}\big\},\\ D_\sigma=\min\limits_{\substack{m=1,\dots,5,\\ m\neq2}}\big\{D_{m,\sigma}\big\}.\end{cases} \tag{3.50}$$

It should be noted that ε_j in (3.48) should be such that $\varepsilon_j>\sqrt{\frac{\big\|u_j\big\|_\infty}{4D_j}},\ j=S,V$.

As $H^2(j),\ j=S,V$, are embedded in the space of continuous bounded functions, ([3]), it can be shown that there exist positive constants $\mathcal{K}_j,\ j=S,V$, depending on $\|\mathcal{C}_j\|_{L^\infty(L^\infty)}$ such that

$$\Big(\mathcal{F}_j(\mathcal{C}_j(t),\mathcal{C}_j(t)\Big)_j\leq\mathcal{K}_j\Big\|\mathcal{C}_j(t)\Big\|^2_{L^2(j)}\leq\mathcal{K}\Big\|\mathcal{C}_j(t)\Big\|^2_{L^2(j)},\ j=S,V, \tag{3.51}$$

where $\mathcal{K} = \max\limits_{j=S,V} \{\mathcal{K}_j\}$.

Replacing (3.51) in (3.48) and taking

$$\varphi = \max_{j=S,V} \left\{ \varepsilon_j^2 \left\| u_j \right\|_\infty \right\}, \tag{3.52}$$

in the differential inequality (3.48), we will have

$$\begin{aligned} \frac{1}{2}\frac{d}{dt} \sum_{j=S,V} \Bigg(\left\| \mathcal{C}_j(t) \right\|^2_{L^2(j)} \quad & + \phi \int_0^t \left\| \nabla \mathcal{C}_j(s) \right\|^2_{L^2(j)} ds + D_\sigma \left\| \int_0^t e^{-\frac{t-s}{\tau_1}} \nabla \mathcal{C}_V(s) ds \right\|^2_{L^2(V)} \Bigg) \\ & \leq \sum_{j=S,V} \left(\varphi + \mathcal{K} \right) \left\| \mathcal{C}_j(t) \right\|^2_{L^2(j)} + \tfrac{\gamma_{1,V}}{4} \left| \Gamma_{\text{lumen}} \right|. \end{aligned} \tag{3.53}$$

Multiplying differential inequality (3.53) by $e^{-(\mathcal{K}+\varphi)t}$ and then integrating over time we deduce

$$\mathcal{E}_1(t) \quad \leq \tfrac{1}{\min\left\{1,\phi,D_\sigma\right\}} e^{2(\mathcal{K}+\varphi)t} \mathcal{E}_1(0) + \tfrac{\gamma_{1,V}}{2(\mathcal{K}+\varphi)} \left| \Gamma_{\text{lumen}} \right| \left(e^{2(\mathcal{K}+\varphi)t} - 1 \right). \tag{3.54}$$

□

Estimate (3.54) proves a boundness property of the solution of the model for finite intervals of time.

Corollary 3.3.2. If $(\mathcal{C}_S, \mathcal{C}_V)$ is a solution of the variational problem **VP2** and

$$\mathcal{E}_2(t) = \sum_{j=S,V} \left(\left\| \mathcal{C}_j(t) \right\|^2_{L^2(j)} \quad + \int_0^t \left\| \nabla \mathcal{C}_j(s) \right\|^2_{L^2(j)} ds \right) \tag{3.55}$$

for $t \in [0,T]$, assuming $\left(\mathcal{C}_S(t), \mathcal{C}_V(t)\right) \in \left(H^2(S)\right)^5 \times \left(H^2(V)\right)^4$ then

$$\mathcal{E}_2(t) \leq \frac{1}{\min\left\{1,\phi\right\}} e^{2\max\left\{\mathcal{K}+\varphi_1,\varphi_2\right\}t} \mathcal{E}_2(0) + \frac{\gamma_{1,V}}{2\max\left\{\mathcal{K}+\varphi_1,\varphi_2\right\}} \left| \Gamma_{\text{lumen}} \right| \left(e^{2\max\left\{\mathcal{K}+\varphi_1,\varphi_2\right\}t} - 1 \right), \tag{3.56}$$

where φ_1 and φ_2 are concentration-independent constants, $\varepsilon_j \neq 0,\ j = S,V$, and $\phi = \min\limits_{j=S,V} \left\{ 2D_j - \frac{\left\| u_j \right\|_\infty}{2\varepsilon_j^2} \right\} > 0$.

Proof. We take into account the inequality

$$\int_0^t e^{-\frac{t-s}{\tau_1}} \left(\nabla \mathcal{C}_V(s), \nabla \mathcal{C}_V(t) \right)_V ds \quad \leq \tfrac{\tau_1}{8\xi_V^2} \int_0^t \left\| \nabla \mathcal{C}_V(s) \right\|^2_{L^2(V)} ds + \xi_V^2 \left\| \mathcal{C}_V(t) \right\|^2_{L^2(V)}, \tag{3.57}$$

for $\xi_V \neq 0$.

Defining

$$\begin{aligned}\varphi_1 &= \max\left\{\varepsilon_S^2\|u_S\|_\infty, \varepsilon_V^2\|u_V\|_\infty + \xi_V^2\right\},\\ \varphi_2 &= \max_{\substack{m=1,\dots,5,\\ m\neq 2}}\left\{\frac{D_{m,\sigma}^2\tau_1}{16\xi_V^2}\right\},\end{aligned} \tag{3.58}$$

where $\varepsilon_j \neq 0,\ j = S, V$, the result is easily obtained following the proof of Theorem 3.3.1. □

Let

$$\begin{aligned}\mathcal{C}(t) &= \left(\big(C_{m,S}(t)\big)_{m=1,\dots,5}, \big(C_{m,V}(t)\big)_{\substack{m=1,\dots,5,\\ m\neq 2}}\right),\\ \hat{\mathcal{C}}(t) &= \left(\big(\hat{C}_{m,S}(t)\big)_{m=1,\dots,5}, \big(\hat{C}_{m,V}(t)\big)_{\substack{m=1,\dots,5,\\ m\neq 2}}\right),\end{aligned} \tag{3.59}$$

be two solutions of the problem (3.15) with different initial conditions

$$\begin{aligned}\mathcal{C}(0) &= \left(\big(C_{m,S}(0)\big)_{m=1,\dots,5}, \big(C_{m,V}(0)\big)_{\substack{m=1,\dots,5,\\ m\neq 2}}\right),\\ \hat{\mathcal{C}}(0) &= \left(\big(\hat{C}_{m,S}(0)\big)_{m=1,\dots,5}, \big(\hat{C}_{m,V}(0)\big)_{\substack{m=1,\dots,5,\\ m\neq 2}}\right).\end{aligned} \tag{3.60}$$

To analyze the stability of the model, we need to establish

$$\sum_{j=S,V}\left\|\mathcal{C}_j(t) - \hat{\mathcal{C}}_j(t)\right\|^2_{L^2(j)} \leq \mathcal{B}(t)\sum_{j=S,V}\left\|\mathcal{C}_j(0) - \hat{\mathcal{C}}_j(0)\right\|^2_{L^2(j)}, \tag{3.61}$$

for $t \in [0, T]$, where $\mathcal{B}(t)$ is bounded in time. To prove the last inequality for a system of quasi-linear diffusion-convection-reaction equations (3.15), it is sufficient to assume that the reaction terms have bounded partial derivatives. But we can not use this argument in our case. To gain some insight on the stability behavior of **VP2**, we study in what follows the stability of the linearization of **VP2** in a solution $\mathcal{C}(t)$.

Let $\mathcal{C} = \big(\mathcal{C}_S, \mathcal{C}_V\big)$. System (3.15) can be rewritten in the following form

$$\begin{cases}\dfrac{d\mathcal{C}}{dt}(t) = \mathbb{F}(\mathcal{C}(t)),\ t > 0,\\ \mathcal{C}(0)\ \text{ is given,}\end{cases} \tag{3.62}$$

where $\mathbb{F}(\mathcal{C}(t)) = \left(\left(\mathbb{F}_{m,S}(\mathcal{C}_S(t))\right)_{m=1,\dots,5}, \left(\mathbb{F}_{m,V}(\mathcal{C}_V(t))\right)_{\substack{m=1,\dots,5,\\ m\neq 2}} \right)$ is defined by

$$\begin{cases} \mathbb{F}_{m,S}(\mathcal{C}_S(t)) & = \nabla \cdot \left(D_{m,S}\nabla C_{m,S}(t) - u_S C_{m,S}(t) \right) + F_{m,S}(\mathcal{C}_S(t)), \quad m = 1,\dots,5, \\ \mathbb{F}_{m,V}(\mathcal{C}_V(t)) & = \nabla \cdot \left(D_{m,V}\nabla C_{m,V}(t) - u_V C_{m,V}(t) \right) + F_{m,V}(\mathcal{C}_V(t)) \\ & \quad + \int_0^t e^{-\frac{t-s}{\tau_1}} \nabla \cdot \left(D_{m,\sigma}\nabla C_{m,V}(s) \right) ds, \qquad \substack{m=1,\dots,5,\\ m\neq 2}, \end{cases} \tag{3.63}$$

and $F_{m,S},\ m = 1,\dots,5$, and $F_{m,V},\ m = 1,\dots,5,\ m \neq 2$, are given by (2.3), (2.4), (3.3) and (3.4). We also assume that conditions (3.24) hold.

The linearization of the initial value problem (3.62) can be written in the following form

$$\begin{cases} \dfrac{d\tilde{\mathcal{C}}}{dt}(t) = \mathbb{L}\tilde{\mathcal{C}}(t)\,, t > 0, \\ \tilde{\mathcal{C}}(0) \ \text{ is given,} \end{cases} \tag{3.64}$$

where $\mathbb{L}\tilde{\mathcal{C}}(t) = \left(\left(\mathbb{L}_{m,S}(\tilde{\mathcal{C}}_S(t))\right)_{m=1,\dots,5}, \left(\mathbb{L}_{m,V}(\tilde{\mathcal{C}}_V(t))\right)_{\substack{m=1,\dots,5,\\ m\neq 2}} \right)$ is defined by

$$\begin{cases} \mathbb{L}_{m,S}(\tilde{\mathcal{C}}_S(t)) & = \nabla \cdot \left(D_{m,S}\nabla \tilde{C}_{m,S}(t) - u_S \tilde{C}_{m,S}(t) \right) + \mathbb{F}_{J_{m,S}}(\mathcal{C}_S(t))\tilde{\mathcal{C}}_S(t), \quad m = 1,\dots,5, \\ \mathbb{L}_{m,V}(\tilde{\mathcal{C}}_V(t)) & = \nabla \cdot \left(D_{m,V}\nabla \tilde{C}_{m,V}(t) - u_V \tilde{C}_{m,V}(t) \right) + \mathbb{F}_{J_{m,V}}(\mathcal{C}_V(t))\tilde{\mathcal{C}}_V(t) \\ & \quad + \int_0^t e^{-\frac{t-s}{\tau_1}} \nabla \cdot \left(D_{m,\sigma}\nabla \tilde{C}_{m,V}(s) \right) ds, \qquad \substack{m=1,\dots,5,\\ m\neq 2}, \end{cases} \tag{3.65}$$

with

$$\mathbb{F}_{J_{m,S}}(\mathcal{C}_S(t))\tilde{\mathcal{C}}_S(t) = \begin{cases} -\sum\limits_{i=1,2} \mathcal{F}_{J,i}(\mathcal{C}_S(t))\tilde{\mathcal{C}}_S(t), & \text{m=1,} \\ -\mathcal{F}_{J,1}(\mathcal{C}_S(t))\tilde{\mathcal{C}}_S(t), & \text{m=2,} \\ \sum\limits_{i=1,2} (-1)^{i-1}\mathcal{F}_{J,i}(\mathcal{C}_S(t))\tilde{\mathcal{C}}_S(t), & \text{m=3,} \\ \sum\limits_{i=1,2} \mathcal{F}_{J,i}(\mathcal{C}_S(t))\tilde{\mathcal{C}}_S(t), & \text{m=4,} \\ 0, & \text{m=5,} \end{cases} \tag{3.66}$$

and

$$\mathbb{F}_{J_{m,V}}(\mathcal{C}_V(t))\tilde{\mathcal{C}}_V(t) = \begin{cases} -\mathcal{F}_{J,3}(\mathcal{C}_V(t))\tilde{\mathcal{C}}_V(t), & \text{m=1,} \\ -\mathcal{F}_{J,3}(\mathcal{C}_V(t))\tilde{\mathcal{C}}_V(t), & \text{m=3,} \\ \mathcal{F}_{J,3}(\mathcal{C}_V(t))\tilde{\mathcal{C}}_V(t), & \text{m=4,} \\ 0, & \text{m=5.} \end{cases} \tag{3.67}$$

In (3.66) and (3.67), $\mathcal{F}_{J,1}(\mathcal{C}_S(t))\tilde{\mathcal{C}}_S(t)$, $\mathcal{F}_{J,2}(\mathcal{C}_S(t))\tilde{\mathcal{C}}_S(t)$ and $\mathcal{F}_{J,3}(\mathcal{C}_V(t))\tilde{\mathcal{C}}_V(t)$ represent Fréchet derivatives and are defined by

$$\begin{cases} \mathcal{F}_{J,1}(\mathcal{C}_S(t))\tilde{\mathcal{C}}_S(t) & = \kappa_{1,S}C_{2,S}(t)(1+\alpha C_{4,S}(t))\tilde{C}_{1,S}(t) + \kappa_{1,S}C_{1,S}(t)(1+\alpha C_{4,S}(t))\tilde{C}_{2,S}(t) \\ & \quad +\kappa_{1,S}\alpha C_{1,S}(t)C_{2,S}(t)\tilde{C}_{4,S}(t), \\ \mathcal{F}_{J,2}(\mathcal{C}_S(t))\tilde{\mathcal{C}}_S(t) & = \kappa_{2,S}C_{3,S}(t)(1+\beta C_{4,S}(t))\tilde{C}_{1,S}(t) + \kappa_{2,S}C_{1,S}(t)(1+\beta C_{4,S}(t))\tilde{C}_{3,S}(t) \\ & \quad +\kappa_{2,S}\beta C_{1,S}(t)C_{3,S}(t)\tilde{C}_{4,S}(t), \\ \mathcal{F}_{J,3}(\mathcal{C}_V(t))\tilde{\mathcal{C}}_V(t) & = \kappa_{1,V}C_{3,V}(t)(1+\alpha C_{4,V}(t))\tilde{C}_{1,V}(t) + \kappa_{1,V}C_{1,V}(t)(1+\gamma C_{4,V}(t))\tilde{C}_{3,V}(t) \\ & \quad +\kappa_{1,V}\gamma C_{1,S}(t)C_{3,V}(t)\tilde{C}_{4,V}(t). \end{cases} \tag{3.68}$$

Let $\mathcal{C}(t)$ and $\tilde{\mathcal{C}}(t)$ be solutions of (3.64) satisfying the same boundary conditions (3.24) with initial conditions $\mathcal{C}(0)$ and $\tilde{\mathcal{C}}(0)$. We define $\mathcal{W}_j(t) = \mathcal{C}_j(t) - \tilde{\mathcal{C}}_j(t),\ j = S, V$. The influence of the initial perturbation on the solution of the problem (3.64) is estimated in the following result.

Theorem 3.3.3. Let

$$\mathcal{E}_{\mathcal{W}}(t) = \sum_{j=S,V}\left(\left\|\mathcal{W}_j(t)\right\|^2_{L^2(j)} + \int_0^t \left\|\nabla\mathcal{W}_j(s)\right\|^2_{L^2(j)} ds\right) + \left\|\int_0^t e^{-\frac{t-s}{\tau_1}}\nabla\mathcal{W}_V(s)ds\right\|^2_{L^2(V)}, \tag{3.69}$$

for $t \in [0,T]$, be the energy functional associated with the perturbation $\mathcal{W}$. Then

$$\mathcal{E}_W(t) \leq \frac{1}{\min\left\{1,\phi,D_\sigma\right\}} e^{2(\mathcal{K}'+\varphi)t}\mathcal{E}_W(0), \tag{3.70}$$

where $\mathcal{K}', \phi$ and φ are concentration-independent constants.

Proof. It is readily proved that the following equality holds:

$$\begin{aligned} \int_0^t e^{-\frac{t-s}{\tau_1}}\Big(\nabla\mathcal{W}_V(s), \nabla\mathcal{W}_V(t)\Big)_V ds &= \frac{1}{2}\frac{d}{dt}\left\|\int_0^t e^{-\frac{t-s}{\tau_1}}\nabla\mathcal{W}_V(s)ds\right\|^2_{L^2(V)} \\ &\quad + \frac{1}{\tau_1}\left\|\int_0^t e^{-\frac{t-s}{\tau_1}}\nabla\mathcal{W}_V(s)ds\right\|^2_{L^2(V)}. \end{aligned} \tag{3.71}$$

From (3.64), taking ϕ, φ and D_σ as in (3.50) and (3.52), we can easily obtain

$$\begin{aligned} \frac{1}{2}\frac{d}{dt}\sum_{j=S,V}\left(\left\|\mathcal{W}_j(t)\right\|^2_{L^2(j)} + \phi\int_0^t \left\|\nabla\mathcal{W}_j(s)\right\|^2_{L^2(j)} ds\right) + \mathcal{D}_\sigma\left\|\int_0^t e^{-\frac{t-s}{\tau_1}}\nabla\mathcal{W}_V(s)ds\right\|^2_{L^2(V)} \\ \leq \sum_{j=S,V}\varphi\left\|\mathcal{W}_j(t)\right\|^2_{L^2(j)} - \frac{\mathcal{D}_\sigma}{\tau_1}\left\|\int_0^t e^{-\frac{t-s}{\tau_1}}\nabla\mathcal{W}_V(s)ds\right\|^2_{L^2(V)} \\ + \sum_{j=S,V}\Big(\mathbb{F}_{J_j}(\mathcal{C}_j(t))\mathcal{W}_j(t), \mathcal{W}_j(t)\Big)_j, \end{aligned} \tag{3.72}$$

where $\mathbb{F}_{J_j}(\mathcal{C}_j(t))\mathcal{W}_j(t),\ j = S, V$, are defined in (3.66) − (3.68).

As

$$\sum_{j=S,V}\Big(\mathbb{F}_{J_j}(\mathcal{C}_j(t))\mathcal{W}_j(t),\mathcal{W}_j(t)\Big)_j \leq \mathcal{K}'\sum_{j=S,V}\Big\|\mathcal{W}_j(t)\Big\|^2_{L^2(j)}, \tag{3.73}$$

we can establish

$$\mathcal{E}_W(t) \leq \frac{1}{\min\Big\{1,\phi,D_\sigma\Big\}}e^{2(\mathcal{K}'+\varphi)t}\mathcal{E}_W(0). \tag{3.74}$$

□

3.4 *Finite dimensional approximation*

To define a finite dimensional approximation for the solution of (3.15) – (3.17) and (3.24), we fix $h>0$ and define in $\Omega = S\cup V\cup\Gamma_{\text{coat}}$ (Figure 3.1) an admissible triangulation $\mathcal{T}_h$, depending on $h>0$, such that the corresponding admissible triangulations in S and V, respectively $\mathcal{T}_{h_S}$ and $\mathcal{T}_{h_V}$, are compatible in Γ_{coat} (see the zoomed part of Figure 3.4). We represent by Δ_1 a typical element of $\mathcal{T}_{h_S}$ and by Δ_2 a typical element of $\mathcal{T}_{h_V}$.

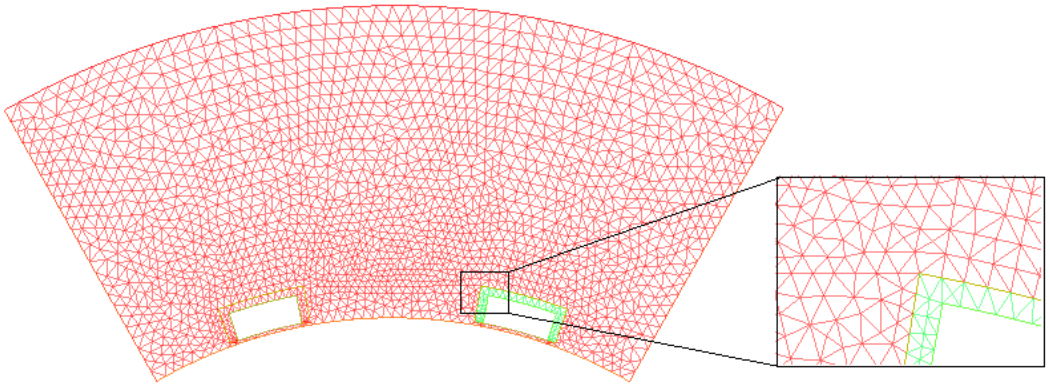

FIGURE 3.4: Triangulations in the stent and in the vessel wall.

Let $S_h = \bigcup_{\Delta_1\in\mathcal{T}_{h_S}}\Delta_1$, $V_h = \bigcup_{\Delta_2\in\mathcal{T}_{h_V}}\Delta_2$ and let $\mathcal{A}_{S,h}(.,.)$ and $\mathcal{A}_{V,h}(.,.)$ be defined as $\mathcal{A}_S(.,.)$ and $\mathcal{A}_V(.,.)$ (see (3.32)) but with the L^2 inner product defined on S_h and V_h, respectively. To define the bilinear form corresponding to $a_{\text{lumen}}(.,.)$ (see (3.36)), we represent by $\Gamma_{\text{lumen},h}$ and $\Gamma_{\text{adv},h}$ the boundaries of V_h that replace Γ_{lumen} and Γ_{adv} respectively.

3.4.1 *Discrete porous media problem*

We assume that $p_{\text{adv}} = 0$ and $p_{\text{lumen}} = p_{h_0}$. Let $w_h \in H^1(V_h)$ is such that $w_h = p_{0,h}$ on $\Gamma_{\text{lumen},h}$. We define in what follows the space of globally continuous functions on S_h and V_h whose restrictions to each element Δ_1 and Δ_2 respectively, are polynomials of degree at most r, i.e.

$$\mathcal{V}_h = \Big\{ (\vartheta_{S,h}, \vartheta_{V,h}) \quad \in C^0(\bar{S_h}) \times C^0(\bar{V_h}) \text{ such that } \vartheta_{S,h} = \vartheta_{V,h} \text{ on } \Gamma_{\text{coat}}, \\ \vartheta_{V,h} = 0 \text{ on } \Gamma_{\text{lumen,h}} \cup \Gamma_{\text{adv,h}}, (\vartheta_{S,h}, \vartheta_{V,h})\big|_{\Delta_1 \times \Delta_2} \in P_r \times P_r, \\ \text{for all } \Delta_1 \in \mathcal{T}_{h_S}, \Delta_2 \in \mathcal{T}_{h_V} \Big\} \subset H^1(S_h) \times H^1_{\text{lumen,adv}}(V_h), \tag{3.75}$$

where $H^1_{\text{lumen,adv}}(V_h)$ is defined by (3.33) with $\Gamma_{\text{lumen}} \cup \Gamma_{\text{adv}}$ replaced by $\Gamma_{\text{lumen,h}} \cup \Gamma_{\text{adv,h}}$. In (3.75), P_r denotes the space of polynomials of degree at most r. The finite dimensional formulation for system (3.31) is as follows:

Find $(p_{S,h}, p^*_{V,h}) \in \mathcal{V}_h$ such that

$$\mathcal{A}_{S,h}(p_{S,h}, q_{S,h}) + \mathcal{A}_{V,h}(p^*_{V,h}, q_{V,h}) = -\mathcal{A}_{V,h}(w_h, q_{V,h}), \quad \forall\ (q_{S,h}, q_{V,h}) \in \mathcal{V}_h, \tag{3.76}$$

where $p^*_{V,h} = p_{V,h} - w_h \in H^1_{\text{lumen,adv}}(V_h)$.

Velocities $u_{S,h}$ and $u_{V,h}$ can be then obtained by Darcy's law $u_{j,h} = -\frac{k_j}{\mu_j}\nabla p_{j,h}$, for $j = S, V$.

3.4.2 *Discrete convection-diffusion-reaction problem*

We use in what follows the following notations

$$\big(v_{S,h}, v_{V,h}\big) = \Big(\big(v_{m,S,h}\big)_{m=1,\dots,5}, \big(v_{m,V,h}\big)_{\substack{m=1,\dots,5,\\ m\neq 2}} \Big). \tag{3.77}$$

To compute the semi-discrete Ritz-Galerkin approximation $\mathcal{C}_h$ for the weak solution of $\mathcal{C}$ defined by **VP2**, we consider the space

$$\mathcal{W}_h = \Big\{ \big(v_{S,h}, v_{V,h}\big) \quad \in \big(C^0(\bar{S_h})\big)^5 \times \big(C^0(\bar{V_h})\big)^4 \text{ such that } v_{m,S,h} = v_{m,V,h} \text{ on } \Gamma_{\text{coat}}, \\ \text{for } m = 1,3,4,5, (v_{S,h}, v_{V,h})\big|_{\Delta_1 \times \Delta_2} \in (P_q)^5 \times (P_q)^4, \\ \Delta_1 \in \mathcal{T}_{h_S}, \Delta_2 \in \mathcal{T}_{h_V} \Big\} \subset \big(H^1(S_h)\big)^5 \times \big(H^1(V_h)\big)^4, \tag{3.78}$$

where P_q denotes the space of polynomials of degree at most q (not necessarily equal to r).

By $a_{j,h}(.,.)$ we represent the bilinear form defined as $a_j(.,.)$ ((3.36)) with the L^2 inner products defined on S_h for $j = S$ and V_h for $j = V$. By $a_{\text{lumen},h}(.,.)$ we denote the bilinear form defined as $a_{\text{lumen}}(.,.)$ ((3.36)), considering the boundary integrals on $\Gamma_{\text{lumen},h}$.

The weak solution of the problem **VP2**, in the semi discrete case, is the solution of the following finite dimensional variational formulation:

FEVP2: Find $\left(\mathcal{C}_{S,h}, \mathcal{C}_{V,h}\right) \in L^2(0,T;\mathcal{W}_h)$ such that $(\frac{\partial \mathcal{C}_{S,h}}{\partial t}, \frac{\partial \mathcal{C}_{V,h}}{\partial t}) \in \left(L^2(0,T;L^2(S_h))\right)^5 \times \left(L^2(0,T;L^2(V_h))\right)^4$ and

$$\begin{cases} \displaystyle\sum_{j=S,V}\left(\left(\tfrac{\partial \mathcal{C}_{j,h}}{\partial t}(t), v_{j,h}\right)_{j,h} + a_{j,h}\left(\mathcal{C}_{j,h}(t), v_{j,h}\right)\right) & = \displaystyle\sum_{j=S,V}\left(\mathcal{F}_j(\mathcal{C}_{j,h}(t)), v_{j,h}\right)_{j,h} \\ & \quad + a_{\text{lumen},h}(\mathcal{C}_{V,h}(t), v_{V,h}), \qquad (3.79) \\ \text{a.e in } (0,T), \text{ for all } (v_{S,h}, v_{V,h}) \in \mathcal{W}_h, & \\ \mathcal{C}_{S,h}(0) = (0,1,0,0,1),\ \mathcal{C}_{V,h}(0) = (1,0,0,0). & \end{cases}$$

To conclude this section, we introduce the semi-discrete energy functional

$$\mathcal{E}_h(t) = \sum_{j=S,V}\left(\left\|\mathcal{C}_{j,h}(t)\right\|^2_{L^2(j_h)} + \int_0^t \left\|\nabla \mathcal{C}_{j,h}(s)\right\|^2_{L^2(j_h)} ds\right) + \left\|\int_0^t e^{-\frac{t-s}{\tau_1}} \nabla \mathcal{C}_{V,h}(s) ds\right\|^2_{L^2(V_h)} \quad (3.80)$$

for $t \in [0,T]$, where $\left(\mathcal{C}_{S,h}(t), \mathcal{C}_{V,h}(t)\right)$ is the solution of **FEVP2**. This functional is the semi-discrete version of the energy functional (3.41). Following a procedure analogous to the one in Theorem 3.3.1, a discrete version of inequality (3.43) can be established.

3.5 *Full discrete IMEX problem*

We introduce in $[0,T]$ a uniform grid $\left\{t_n; n = 0, \ldots, N\right\}$ with $t_0 = 0$, $t_N = T$, and $t_n - t_{n-1} = \Delta t$. Let $\left(\mathcal{C}^n_{S,h}, \mathcal{C}^n_{V,h}\right)$ be a fully discrete approximations of the

solution of the problem. We adopt in what follows the following notations:

$$
\begin{aligned}
a_{S,h}\big(v_{S,h}^{n+1}, w_{S,h}\big) &= \sum_{m=1}^{5}\left(D_{m,S,h}^{n}\nabla v_{m,S,h}^{n+1} - u_{S,h}v_{m,S,h}^{n+1}, \nabla w_{m,S,h}\right)_{S_h},\\
a_{V,h}\big(v_{V,h}^{n+1}, w_{V,h}\big) &= \sum_{\substack{m=1\\ m\neq 2}}^{5}\left(D_{m,V}\nabla v_{m,V,h}^{n+1} - u_{V,h}v_{m,V,h}^{n+1}, \nabla w_{m,V,h}\right)_{V_h}\\
&\quad + \Delta t\sum_{\substack{m=1\\ m\neq 2}}^{5} D_{m,\sigma}\left(\sum_{i=0}^{n\Delta t} e^{-\frac{(n-i)\Delta t}{\tau_1}}\nabla v_{m,V,h}^{n+1}(i\Delta t), \nabla w_{m,V,h}\right)_{V_h},\\
a_{\text{lumen},h}(v_{V,h}^{n+1}, w_{V,h}) &= \gamma_{1,V}\left(1 - v_{1,V,h}^{n+1}, w_{1,V,h}\right)_{\Gamma_{\text{lumen,h}}} - \sum_{m=3}^{5}\gamma_{m,V}\left(v_{m,V,h}^{n+1}, w_{m,V,h}\right)_{\Gamma_{\text{lumen,h}}}.
\end{aligned}
\tag{3.81}
$$

The weak solution of the problem **VP2** in the fully discrete case is the solution of the following finite dimensional variational formulation:

Find $\big(\mathcal{C}_{S,h}^{n+1}, \mathcal{C}_{V,h}^{n+1}\big) \in \mathcal{W}_h$ such that

$$
\begin{cases}
\displaystyle\sum_{j=S,V}\Big(\big(D_{-t}(\mathcal{C}_{j,h}^{n+1}), w_{j,h}\big)_j + a_{j,h}\big(\mathcal{C}_{j,h}^{n+1}, w_{j,h}\big)\Big) = \sum_{j=S,V}\left(F_j(\mathcal{C}_{j,h}^{n*}), w_{j,h}\right)_j \\
\qquad\qquad\qquad\qquad + a_{\text{lumen},h}(\mathcal{C}_{V,h}^{n+1}, w_{V,h}), \\
\qquad \text{for all } (w_{S,h}, w_{V,h}) \in \mathcal{W}_h, \\
\mathcal{C}_{S,h}^{0} = (0,1,0,0,1),\ \mathcal{C}_{V,h}^{0} = (1,0,0,0),
\end{cases}
\tag{3.82}
$$

for $n = 0, \ldots, N$, where

$$
\left(F_S(\mathcal{C}_{S,h}^{n*}), F_V(\mathcal{C}_{V,h}^{n*})\right) = \left(\big(F_{m,S}(\mathcal{C}_{S,h}^{n*})\big)_{m=1,\ldots,5}, \big(F_{m,V}(\mathcal{C}_{V,h}^{n*})\big)_{\substack{m=1,\ldots,5,\\ m\neq 2}}\right), \tag{3.83}
$$

and

$$
F_{m,S}(\mathcal{C}_{S,h}^{n*}) = \begin{cases}
-\kappa_{1,S}C_{1,S,h}^{n+1}C_{2,S,h}^{n}\big(1+\alpha C_{4,S,h}^{n}\big) - \kappa_{2,S}C_{1,S,h}^{n+1}C_{3,S,h}^{n}\big(1+\beta C_{4,S,h}^{n}\big), & \text{m=1},\\
-\kappa_{1,S}C_{1,S,h}^{n+1}C_{2,S,h}^{n+1}\big(1+\alpha C_{4,S,h}^{n}\big), & \text{m=2},\\
\kappa_{1,S}C_{1,S,h}^{n+1}C_{2,S,h}^{n+1}\big(1+\alpha C_{4,S,h}^{n}\big) - \kappa_{2,S}C_{1,S,h}^{n+1}C_{3,S,h}^{n+1}\big(1+\beta C_{4,S,h}^{n}\big), & \text{m=3},\\
\kappa_{1,S}C_{1,S,h}^{n+1}C_{2,S,h}^{n+1}\big(1+\alpha C_{4,S,h}^{n+1}\big) + \kappa_{2,S}C_{1,S,h}^{n+1}C_{3,S,h}^{n+1}\big(1+\beta C_{4,S,h}^{n+1}\big), & \text{m=4},\\
0, & \text{m=5},
\end{cases}
\tag{3.84}
$$

and

$$
F_{m,V}(\mathcal{C}_{V,h}^{n*}) = \begin{cases}
-\kappa_{2,V}C_{1,V,h}^{n+1}C_{3,V,h}^{n}\big(1+\beta C_{4,V,h}^{n}\big), & \text{m=1},\\
-\kappa_{2,V}C_{1,V,h}^{n+1}C_{3,V,h}^{n+1}\big(1+\beta C_{4,V,h}^{n}\big), & \text{m=3},\\
\kappa_{2,V}C_{1,V,h}^{n+1}C_{3,V,h}^{n+1}\big(1+\beta C_{4,V,h}^{n+1}\big), & \text{m=4},\\
0, & \text{m=5},
\end{cases}
\tag{3.85}
$$

are IMEX discretizations of the reaction functions.

3.6 *Numerical simulations*

All numerical experiments have been done with the open source PDE solver freeFEM++ ([19]) considering the triangulation plotted in Figure 3.4 with 3688 elements (1968 vertices) for the arterial wall and 100 elements (83 vertices) for each stent the IMEX method (3.82) with time step size $\Delta t = 10^{-3}$.

Several choices of finite element spaces can be made, but we use here the piecewise linear finite element space P_1 for concentrations and quadratic finite element space P_2 for the pressure ([36]).

We define the mass in the coated stent and in the arterial wall by

$$\begin{aligned} \mathcal{M}_{m,S,h}(t_n) &= \int_{S_h} C_{m,S,h}(t_n) dS,\ m = 1, \ldots, 5, \\ \mathcal{M}_{m,V,h}(t_n) &= \int_{V_h} C_{m,V,h}(t_n) dV,\ m = 1, \ldots, 5,\ m \neq 2, \end{aligned} \tag{3.86}$$

respectively, where $\mathcal{M}_{m,j,h}(t_n),\ j = S, V$, are the numerical approximations for masses at time level t_n.

The thickness of media ($2 \times 10^{-2} cm$) and stent coating ($5 \times 10^{-4} cm$) have been extracted from literature. The following values for the parameters have been considered in the numerical experiments ([33, 34, 46]):

$\kappa_{1,S} = \kappa_{2,V} = 10^{-6}\ cm^2/g.s,\ \kappa_{2,S} = 10^{-7}\ cm^2/g.s,\ \gamma_{m,V} = 10^{10}\ cm/s,\ D^0_{1,S} = 10^{-8}\ cm^2/s,\ D^0_{2,S} = 10^{-15}\ cm^2/s,\ D^0_{3,S} = 10^{-10}\ cm^2/s,\ D^0_{4,S} = 2{\times}10^{-10}\ cm^2/s,\ D^0_{5,S} = 10^{-8}\ cm^2/s, k_S = 2 \times 10^{-14}\ cm^2,\ k_V = 10^{-15}\ cm^2,\ \mu_S = 0.72 \times 10^{-2}\ g/cm.s,\ \mu_V = 0.5{\times}10^{-2}\ g/cm.s, D_{1,V} = 10^{-8}\ cm^2/s,\ D^0_{3,V} = 10^{-10}\ cm^2/s,\ D^0_{4,V} = 2{\times}10^{-10}\ cm^2/s,\ D^0_{5,V} = 5 \times 10^{-9}\ cm^2/s, \alpha = 1\ s/cm^2,\ \beta = \gamma = 10\ s/cm^2.$

We set $p_{\text{lumen}} = 100$ mmHg and $p_{\text{adv}} = 0$ mmHg, so we impose a pressure difference between the inner boundary (Γ_{lumen}) and the outer boundary (Γ_{adv}) of the arterial wall. A velocity field in the coupled stent-wall system is caused by this pressure jump.
An approximation for the pressure drop defined by system (3.31) is shown in Figure 3.5. While pressure on Γ_{coat} is around 76.88 mmHg, it is observed that the average pressure in the arterial wall and in the stent are 35.93 mmHg and 75.34 mmHg respectively.

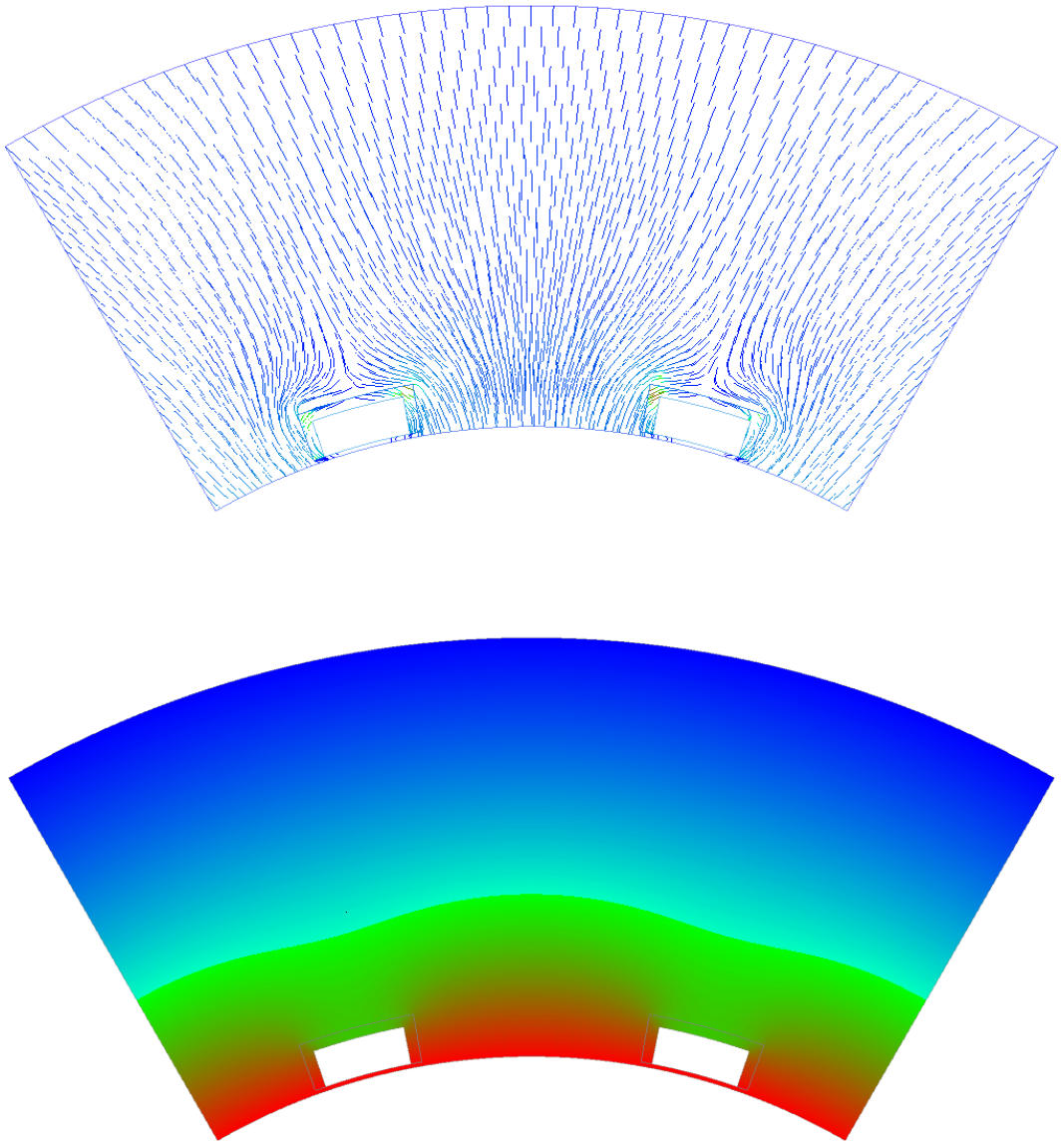

FIGURE 3.5: Velocity field (top) and pressure drop (bottom) in the stented arterial wall.

The release of the drug from the stent into the arterial wall is shown in Figure 3.6. As time evolves the concentration of the drug increases in the arterial wall.

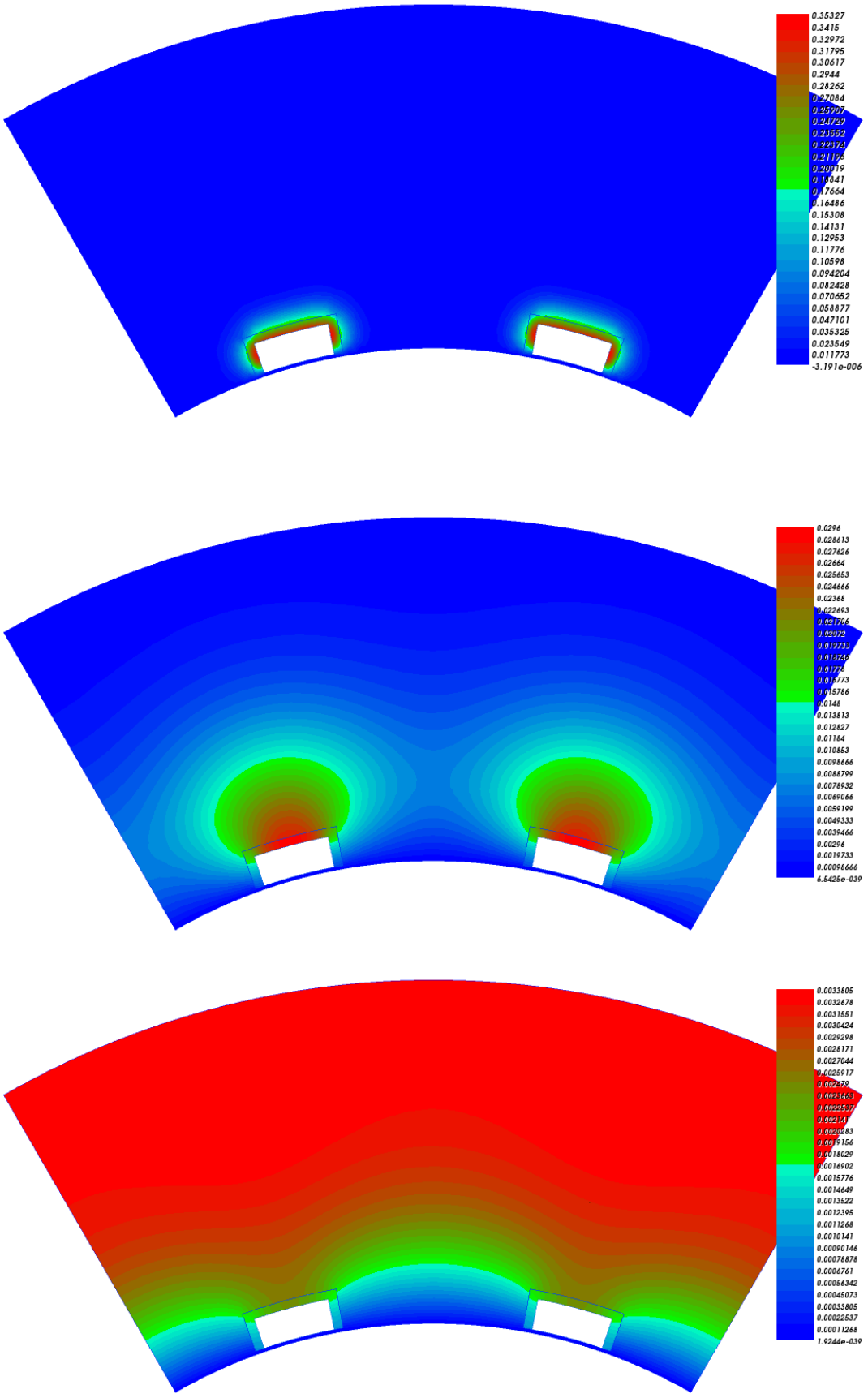

FIGURE 3.6: Drug distribution in the stented arterial wall during 6 months (top to bottom: 1 day, 1 month and 6 months).

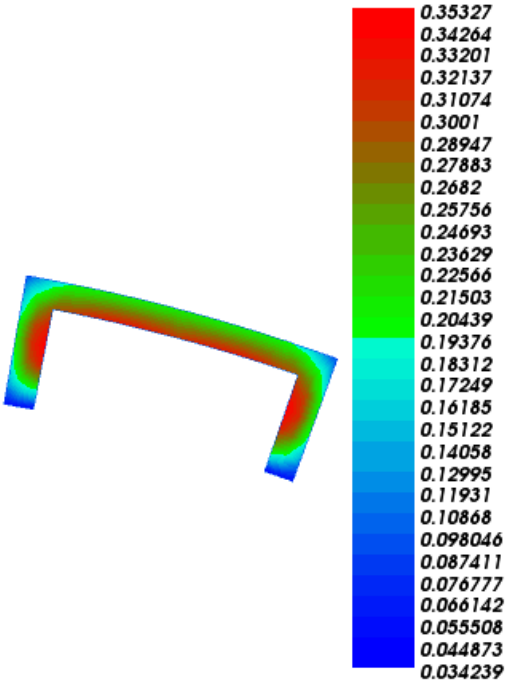

FIGURE 3.7: Drug distribution in the stent after 1 day.

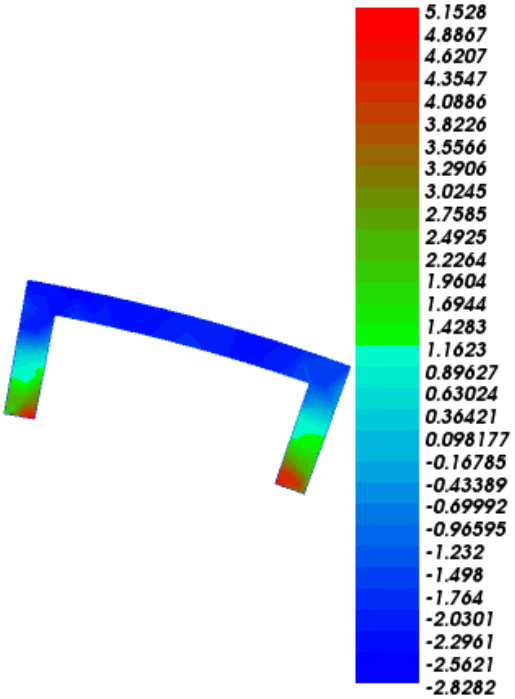

FIGURE 3.8: The flux of drug in the stent after 1 day.

The pattern of the drug diffusion and drug flux in the stent is shown in Figures 3.7 and 3.8. We can see that drug starts to be released from the corners and underneath of the stent. As it is seen in Figure 3.8, due to the washout of the drug close to the lumen, the flux of drug underneath the stent, is much higher than other parts of the stent.

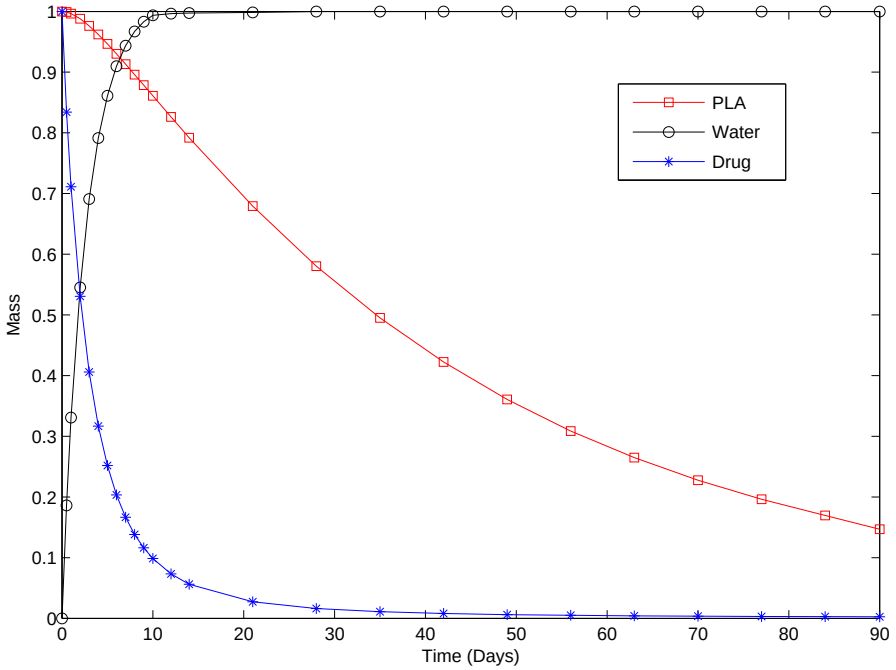

FIGURE 3.9: Evolution of masses of water, PLA and drug in the stent during 90 days.

The behavior of the mass of drug, the mass of PLA and the amount of water in the biodegradable stent is shown in Figure 3.9. The drug presents a steep initial gradient and gradually vanishes after three months. The penetration of water in the stent presents a steep initial slope and after around 20 days achieves a steady state. We can also observe in Figure 3.9 that as PLA degrades, the release rate of drug decreases.

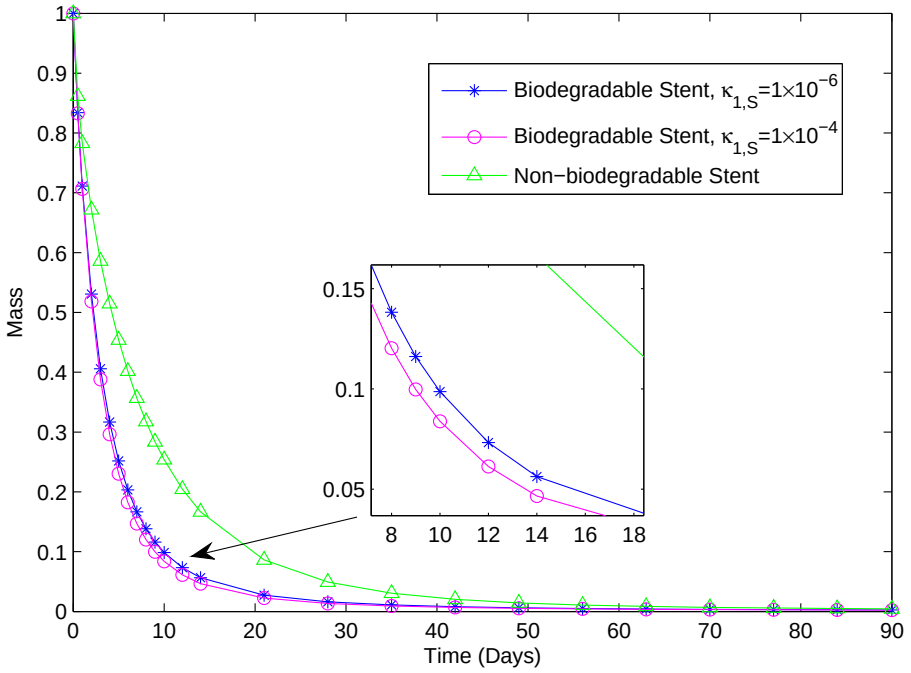

FIGURE 3.10: Evolution of the mass of drug in biodegradable stent versus non-biodegradable stent.

The release of drug from a biodegradable stent and a non-biodegradable stent is compared in Figure 3.10. We observe that due to the degradation of the polymer, the drug release from a biodegradable stent is faster than the drug release from a non-biodegradable stent. The drug release rate directly depends on the reaction rate $\kappa_{1,S}$.

The influence of the stiffness of the vessel wall in the diffusion process of the drug is shown in Figures 3.11 and 3.12. A healthy coronary artery with Young modulus $\kappa_r = 1.2$ MPa ([17]) is compared with a highly diseased coronary artery with Young modulus $\kappa_r = 4.1$ MPa ([30]).

As κ_r increases due to age or atherosclerosis, the vessel wall is less elastic, that is more stiff, and less drug penetrates into the coronary wall. We believe this is an interesting finding from the medical viewpoint, because cardiovascular morbidity is related with arterial stiffness ([20]). It means that the concentration of drug in the DES should be tailored to the severity of the arterial disease.

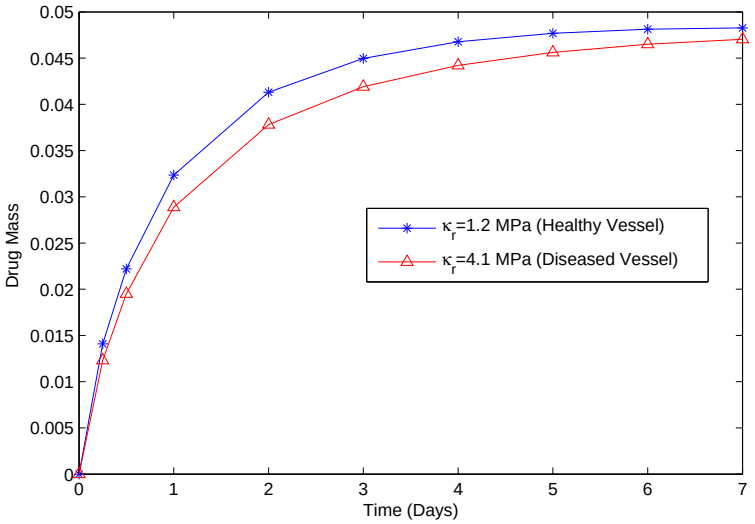

FIGURE 3.11: Evolution of the drug mass in the arterial wall for short time, $\tau_1 = 0.5$, $\kappa_1 = 1$.

The long term influence of stiffness of the coronary wall in the diffusion process of the drug is shown in Figure 3.12. In the beginning of the treatment, a diseased coronary wall receives less drug due to its large κ_r, when compared with a healthy coronary wall. We observe that a crossing occurs around day 15. This finding is justified by the fact that the stiffness of the vessel wall imposes a resistance to the penetration of the drug in the beginning of the process, leading to a drug accumulation in a long period of time.

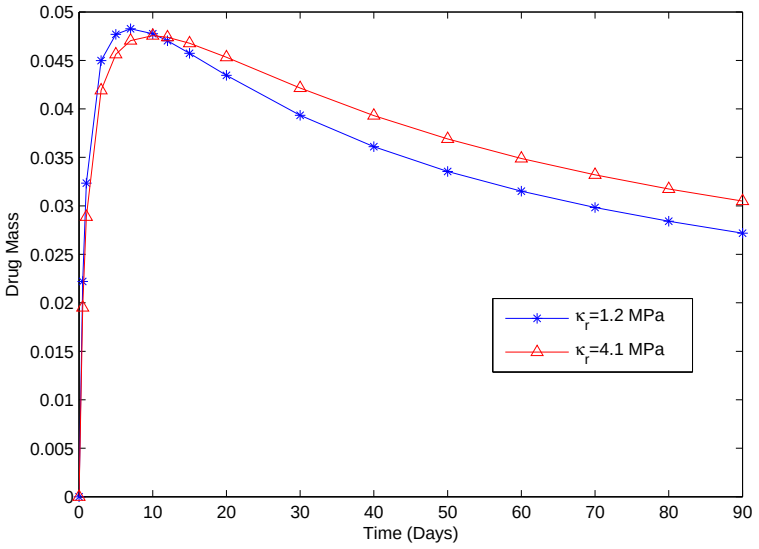

FIGURE 3.12: Evolution of the drug mass in the arterial wall for long time, $\tau_1 = 0.5$, $\kappa_1 = 1$.

The effect of the viscoelastic diffusion coefficient D_σ on the drug release is shown in Figure 3.13. When D_σ increases, we can expect less accumulation of drug in the vessel wall in the beginning of the process. This is due to an increasing of the resistance of the arterial wall to the drug penetration.

When an additional thin layer named *topcoat* is applied to the PLA matrix, instead of the interface conditions (3.20), we consider the following interface conditions:

$$\begin{cases} J_{m,S} \cdot \eta_S = P_c(C_{m,S} - C_{m,V}) & \text{on } \Gamma_{\text{coat}} \times \mathbb{R}^+, \ m = 1, \ldots, 5, \ m \neq 2, \\ J_{m,S} \cdot \eta_S = -J_{m,V} \cdot \eta_V & \text{on } \Gamma_{\text{coat}} \times \mathbb{R}^+, \ m = 1, \ldots, 5, \ m \neq 2, \end{cases} \tag{3.87}$$

where P_c is the permeability of the interface layer Γ_{coat}.

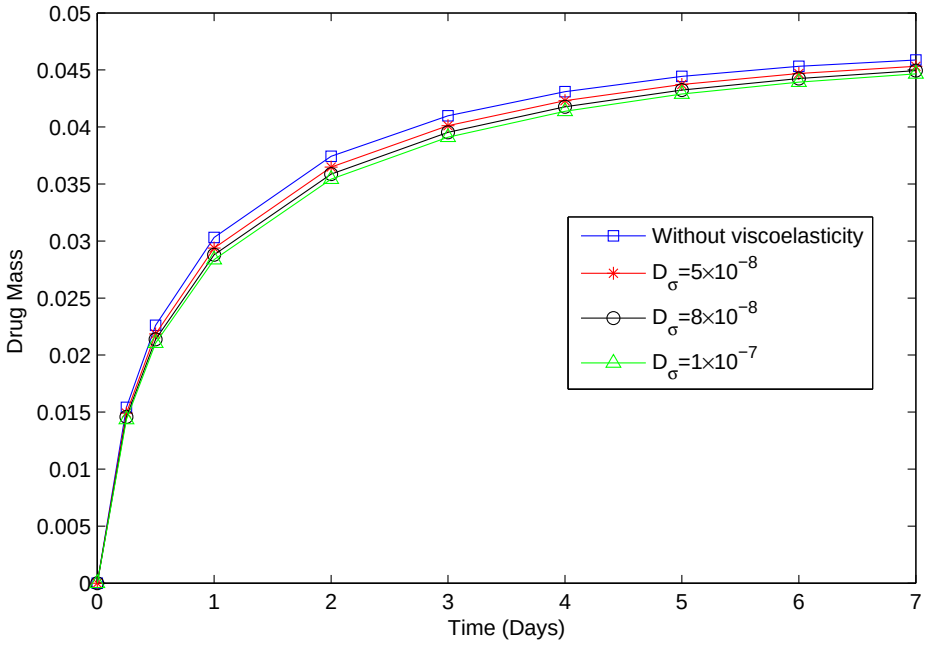

FIGURE 3.13: Evolution of the drug mass in the arterial wall for different values of D_σ.

The first condition in (3.87) is the second Kedem-Katchalsky equation ([33] and the reference [19] therein). We remark that the topcoat is used to slow down the release rate of the drug and it gives more controllability of the drug delivery process.

Figure 3.14 presents the effect of permeability of the interface layer Γ_{coat} on the drug release when a topcoat is applied to the PLA. The accumulation of drug will decrease, when a topcoat with smaller permeability is applied to the coated stent.

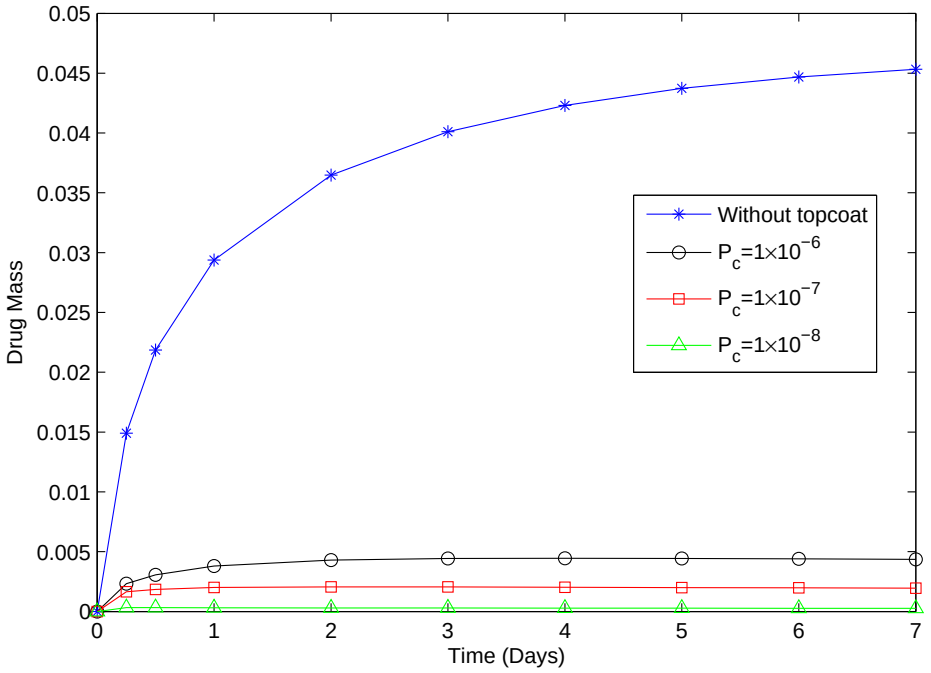

FIGURE 3.14: Evolution of the drug mass in the arterial wall for different values of P_c.

This means that the release of drug from the stent into an arterial wall can be controlled by applying topcoats with different permeabilities.

An alternative model to Maxwell-Wiechert model

Fung's quasilinear viscoelastic model ([16]) is commonly used to describe the viscoelastic properties of the living tissues. Several authors consider that Fung's quasilinear viscoleastic model is a simple method to incorporate nonlinearity and viscoelasticity and is a good model for living tissues with moderate deformation ([1, 16, 29, 42]). Fung's quasilinear model assumes that a viscoelastic kernel can be separated into time-dependent and strain-dependent components.

In what follows we show that the effect of the rheological properties of the vessel wall, on drug permeation, are described analogously by Maxwell-Wiechert model and Fung's model.

In the framework of Fung's model, the relation between stress and strain is given by the following convolution integral

$$\sigma_V(t) = -\int_0^t \tilde{K}(t-s)\frac{\partial}{\partial s}\sigma^e(\epsilon_V(s))ds, \tag{3.88}$$

where

$$\tilde{K}(t-s) = \frac{1 + c\int_{\tau_1}^{\tau_2} \frac{1}{\tau} e^{-\frac{t-s}{\tau}} d\tau}{1 + c\ln(\frac{\tau_2}{\tau_1})} \tag{3.89}$$

and

$$\sigma^e(\varepsilon_V(t)) = \lambda_1\big(e^{\lambda_2\varepsilon_V(t)} - 1\big) \simeq \lambda_1\lambda_2\varepsilon_V(t). \tag{3.90}$$

In (3.89), $\tilde{K}(t-s)$ is a special case of the more general convolution kernel proposed by Fung ([16]),

$$\tilde{K}(t-s) = \frac{1 + \int_0^\infty S(\zeta)e^{-\frac{t-s}{\zeta}} d\zeta}{1 + \int_0^\infty S(\zeta)d\zeta}. \tag{3.91}$$

Fung's model is quasi-linear because the dependence of the response on the loading history can be obtained from a linear convolution integral which preserves the benefits of the linearity in the study of the model and simplify the model predictions. Nonlinearity appears in the viscoelastic constitutive law where the strain ε_V is replaced by a nonlinear function of the strain $\sigma^e(\varepsilon_V)$. The main feature of the model is that the stress and the strain are related by an intermediate variable, the so called elastic stress $\sigma^e(\varepsilon_V)$, that separates the nonlinearity from the viscoelasticity.

In (3.89), $c > 0$ represents the degree of viscous effects, τ_1 and τ_2 represent the short-term and long-term time constants respectively. In (3.90), $\sigma^e(\varepsilon_V)$ represents the instantaneous nonlinear elastic strain, $\lambda_1 > 0$ is the elastic stress constant and λ_2 is a non-dimensional parameter representing the nonlinearity of instantaneous elastic response.

Replacing (3.89) and (3.90) into (3.88), we obtain

$$\sigma_V(t) = -\frac{\lambda_1\lambda_2}{1+c\ln(\frac{\tau_2}{\tau_1})}\left(\varepsilon_V(t) + c\int_0^t\int_{\tau_1}^{\tau_2}\frac{1}{\tau}e^{-\frac{t-s}{\tau}}d\tau\frac{\partial\varepsilon_V}{\partial s}(s)ds\right). \tag{3.92}$$

In this section we consider equation (3.92) as an alternative to equation (3.11) to compute the stress in the arterial wall.

The quasilinear viscoelastic model has five material parameters (three for the reduced relaxation function (3.89) and two for the elastic response (3.90)) which must be determined experimentally. Although some estimations are available in the literature for ligaments ([21]), femur-MCL-tibia complexes ([1]) and spinal tissue ([42]), to the best knowledge of the authors, physiological values of these five parameters are not available in the case of coronary walls.

Due to the lack of appropriate information, we fix four parameters $\lambda_1 = 0.2$ Mpa, $\lambda_2 = 25$, $\tau_1 = 0.5$ s and $\tau_2 = 1800$ s and choose $c = 0.37$ to have $\tilde{\kappa}_r = 1.2$ Mpa for healthy arterial wall ([17]) and $c = 0.02$ to have $\tilde{\kappa}_r = 4.1$ Mpa for highly diseased arterial wall ([30]).

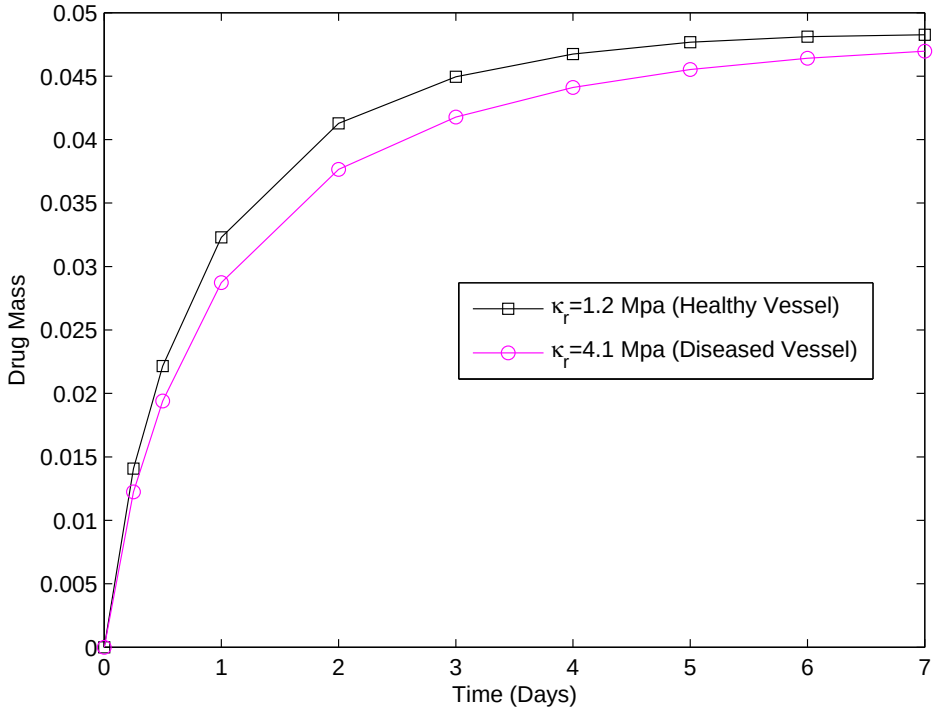

FIGURE 3.15: Evolution of the drug mass in the arterial wall for different values of $\tilde{\kappa}_r$ for short time (Fung's model).

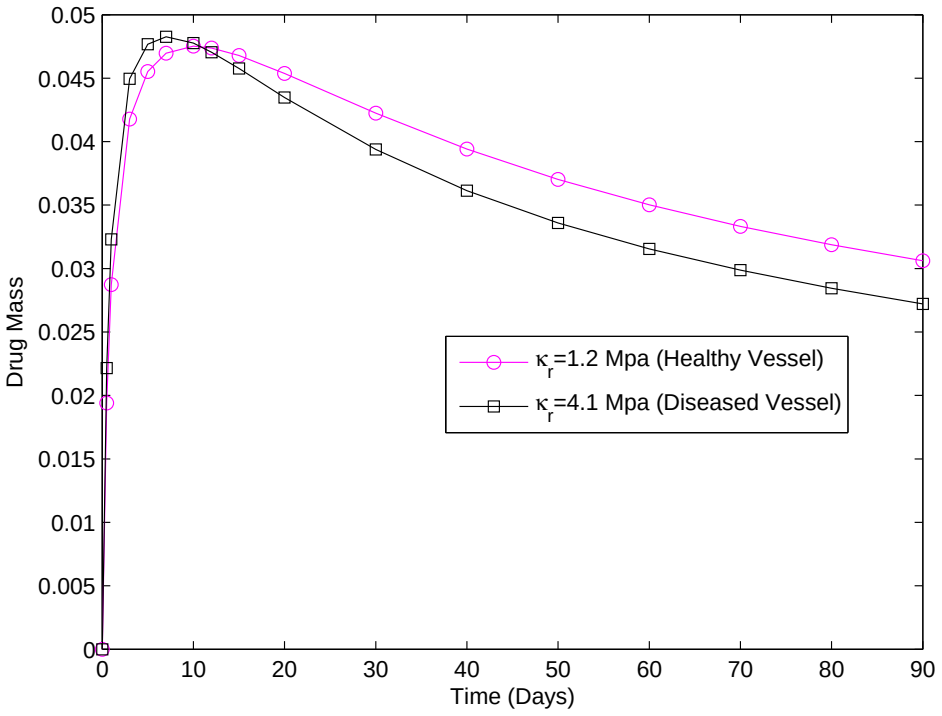

FIGURE 3.16: Evolution of the drug mass in the arterial wall for different values of $\tilde{\kappa}_r$ for long time (Fung's model).

The plots in Figures 3.15 and 3.16 show that the profile of drug release exhibits the same qualitative behavior as before. We conclude that the barrier to drug permeation in stiff vessel walls, in the first period of drug delivery, is a clinical finding suggested by Fung's and Maxwell-Wiechert mechanistic models.

In these last years a great emphasis has been placed on the importance of arterial stiffness in cardiovascular diseases. As a consequence the evaluation of vessels stiffness is being used in the clinical assessment of patients. For this reason our primary focus in this chapter was the study of the influence of the rheological properties of arterial walls on the drug release from a DES. These drug delivery devices are used in the case of patients with severe diseased arteries, characterized by large Young modules. Our numerical results show the difference between drug distribution in healthy and diseased arterial walls. We believe these results have clinical importance and provide manufacturers with useful information to produce tailored DES tuned to specific needs of patients.

Chapter 4

The Effect of Reversible Binding

Hydrophilic drugs, like heparin, are known to be ineffective because they are rapidly cleared. Nowadays they have been practically discarded from clinical use in favour of the more persistent hydrophobic drugs such as paclitaxel, sirolimus and everolimus. Comparing heparin and paclitaxel illustrates the role of reversible binding process between drug and binding sites, in maintaining the drug in the arterial wall for a longer period of time. This comparison could help to construct much effective drug eluting stents in the future.

In this chapter, we extend the model proposed in Chapter 3 to take into account the reversible nature of the bindings between the hydrophilic and the hydrophobic drugs and specific sites inside the arterial wall ([26, 43]).

The chapter is organized as follows. Section 4.1 is devoted to the description of reversible binding reactions. In Section 4.2 we set up the model and its initial, boundary and interface conditions. The effect of reversible binding sites in the presence of drug in the arterial wall as well as numerical simulations of different drugs, with different reversible binding properties, in the healthy and diseased arterial wall are discussed in Section 4.3.

4.1 *Reversible binding reactions*

Receptors are gateways where physiological responses of cells are produced and are often the target of drugs. Drug, as a natural ligand in the arterial wall, binds to target binding sites to which it has high affinity. The concentration of drug in

the arterial wall depends on the rate at which it diffuses through the tissue and their propensity to bind with immobilized binding sites in the arterial wall.

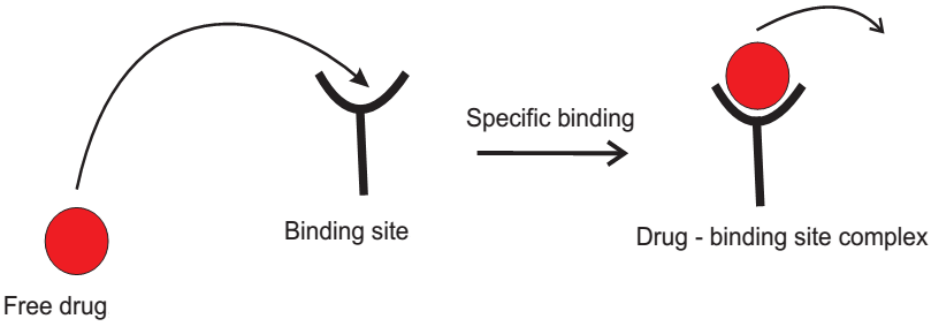

FIGURE 4.1: Schematic representation of a free drug molecule, binding to a specific binding site and a specific drug-binding site complex ([43]).

Bindings occur when a ligand (drug) and a receptor (binding site) collide due to diffusion forces and when the collision has the correct orientation and enough energy. When binding has occurred, drug and binding site remain bound together for an amount of time, depending on the degree of affinity between them ([26]). After dissociation, the drug and the binding site keep the same properties as before binding. The drug-binding site reaction is schematically represented by

$$\text{Drug} + \text{Binding sites} \underset{\text{dissociation}}{\overset{\text{association}}{\rightleftharpoons}} \text{Drug-binding complex.} \tag{4.1}$$

To define the mathematical kinetic model associated to (4.1), the following assumptions are made:

- All the binding sites are equally accessible to drug;
- All the binding sites are either free or bound to drug, this means that there are not states of partial binding;
- Neither drug nor binding sites are altered by binding.

The concentration of free drug in the arterial wall is represented by $C_{5,V}$ with initial concentration $C^0_{5,V} = 0$, while $C_{6,V}$ represents the density of free binding sites in the arterial wall with initial density $C^0_{6,V} \neq 0$. The concentration of activated drug-binding sites is represented by $C_{7,V}$, and we assume that its initial concentration is null. The drug-binding reaction is schematically represented by

$$C_{5,V} + C_{6,V} \underset{\kappa_{u,V}}{\overset{\kappa_{b,V}}{\rightleftharpoons}} C_{7,V}, \tag{4.2}$$

where $\kappa_{b,V}$ is the association rate between the drug and the binding sites and $\kappa_{u,V}$ is the dissociation rate. It should be noted that $K_b = \frac{C^0_{6,V}\kappa_{b,V}}{\kappa_{u,V}} \gg 1$ corresponds to drugs that have high affinity for their target binding sites.

The drug assumes two different states: the dissolved state where drug moves by convection and non-Fickian diffusion and the bound state where drug attaches reversibly to specific sites inside the arterial wall and no longer diffuses or is transported by water.

4.2 *Non-Fickian reaction-diffusion-convection system*

Under the previous assumptions the coupled non-Fickian nonlinear reaction-diffusion-convection model used in Chapter 3 is modified. The following system of non-linear equations is obtained:

$$\begin{cases} \frac{\partial C_{m,S}}{\partial t} &= -\nabla \cdot J_{m,S}(\mathcal{C}_S) + F_{m,S}(\mathcal{C}_S) \quad \text{in } S \times \mathbb{R}^+,\ m = 1, \dots, 5, \\ \frac{\partial C_{m,V}}{\partial t} &= -\nabla \cdot J_{m,V}(\mathcal{C}_V) + F_{m,V}(\mathcal{C}_V) \quad \text{in } V \times \mathbb{R}^+,\ m = 1, \dots, 5,\ m \neq 2, \\ \frac{\partial C_{6,V}}{\partial t} &= F_{6,V}(\mathcal{C}_V) \quad \text{in } V \times \mathbb{R}^+, \\ \frac{\partial C_{7,V}}{\partial t} &= F_{7,V}(\mathcal{C}_V) \quad \text{in } V \times \mathbb{R}^+, \end{cases} \tag{4.3}$$

where $\mathcal{C}_S$ is defined by (3.2) and $\mathcal{C}_V = \left(C_{m,V}\right)_{\substack{m=1,\dots,7,\\ m\neq 2}}$ and the mass fluxes in the stent, $J_{m,S}(\mathcal{C}_S)$, and in the arterial wall, $J_{m,V}(\mathcal{C}_V)$, are defined by (3.18).

The equation (2.6) is used for the diffusion coefficients of species in the stent. For a sake of simplicity, we assume that the diffusion coefficients in the vessel wall $D_{m,V},\ m = 1, \dots, 5,\ m \neq 2$, are constants.

In (4.3), $F_{m,S},\ m = 1, \dots, 5$, are reaction terms that are defined by (2.3) and (2.4). In the arterial wall we assume that the degradation of oligomers and also the binding and unbinding of the drug take place. The reaction functions are defined by (3.3) for $m = 1, 3, 4$, and

$$F_{m,V}(\mathcal{C}_V) = \begin{cases} -\mathcal{F}_{2,V}(\mathcal{C}_V), & \text{m=5}, \\ -\mathcal{F}_{2,V}(\mathcal{C}_V), & \text{m=6}, \\ \mathcal{F}_{2,V}(\mathcal{C}_V), & \text{m=7}, \end{cases} \tag{4.4}$$

. In (4.4), $\mathcal{F}_{2,V}(\mathcal{C}_V)$ is defined by

$$\mathcal{F}_{2,V}(\mathcal{C}_V) = \kappa_{b,V} C_{5,V} C_{6,V} - \kappa_{u,V} C_{7,V}. \tag{4.5}$$

To complete the coupled problem (4.3), we specify in what follows the initial, the boundary and the interface conditions. The initial conditions in the coating and in the arterial wall are given by

$$\begin{cases} C_{m,S}(0) = 0,\ m = 1,3,4,\ C_{m,S}(0) = C^0_{m_S},\ m = 2,5, \\ C_{m,V}(0) = C^0_{m_V},\ m = 1,6,\ C_{m,V}(0) = 0,\ m = 3,4,5,7. \end{cases} \tag{4.6}$$

The boundary and interface conditions are defined by (3.24).

4.3 *Numerical experiments*

To simulate numerically the IBVP (4.3), (4.6) and (3.24), we consider a finite element method analogous to the one presented in Chapter 3. The method is defined considering the variational formulations of the last IBVP which can easily be stated following Section 3.3 in Chapter 3. The fully discrete finite element method for the IBVP is analogous to the method presented in Section 3.5 with the convenient modifications, that are induced by the presence of the two last equations in (4.3) and by the new reaction terms in the equation for the drug concentration in the arterial wall (see (4.3)).

The finite element approximations that we present were obtained considering the data used in the numerical simulations of Chapter 3. We also consider in our experiments $C^0_{6,V} = 10^{-5}\ cm^2/s$ and the parameters in Table 4.1 for a hydrophilic drug (heparin) and a hydrophobic drug (paclitaxel) ([5, 43, 45])

Drug	$D^0_{5,S}[cm^2/s]$	$D_{5,V}[cm^2/s]$	$k_{b,V}[g/cm^2 s]$	$k_{u,V}[1/s]$	K_b
Heparin	10^{-10}	7.7×10^{-8}	9.2×10^4	15×10^{-3}	60
Paclitaxel	5.7×10^{-9}	2.6×10^{-8}	3.6×10^6	9×10^{-2}	400

TABLE 4.1: Properties of heparin and paclitaxel.

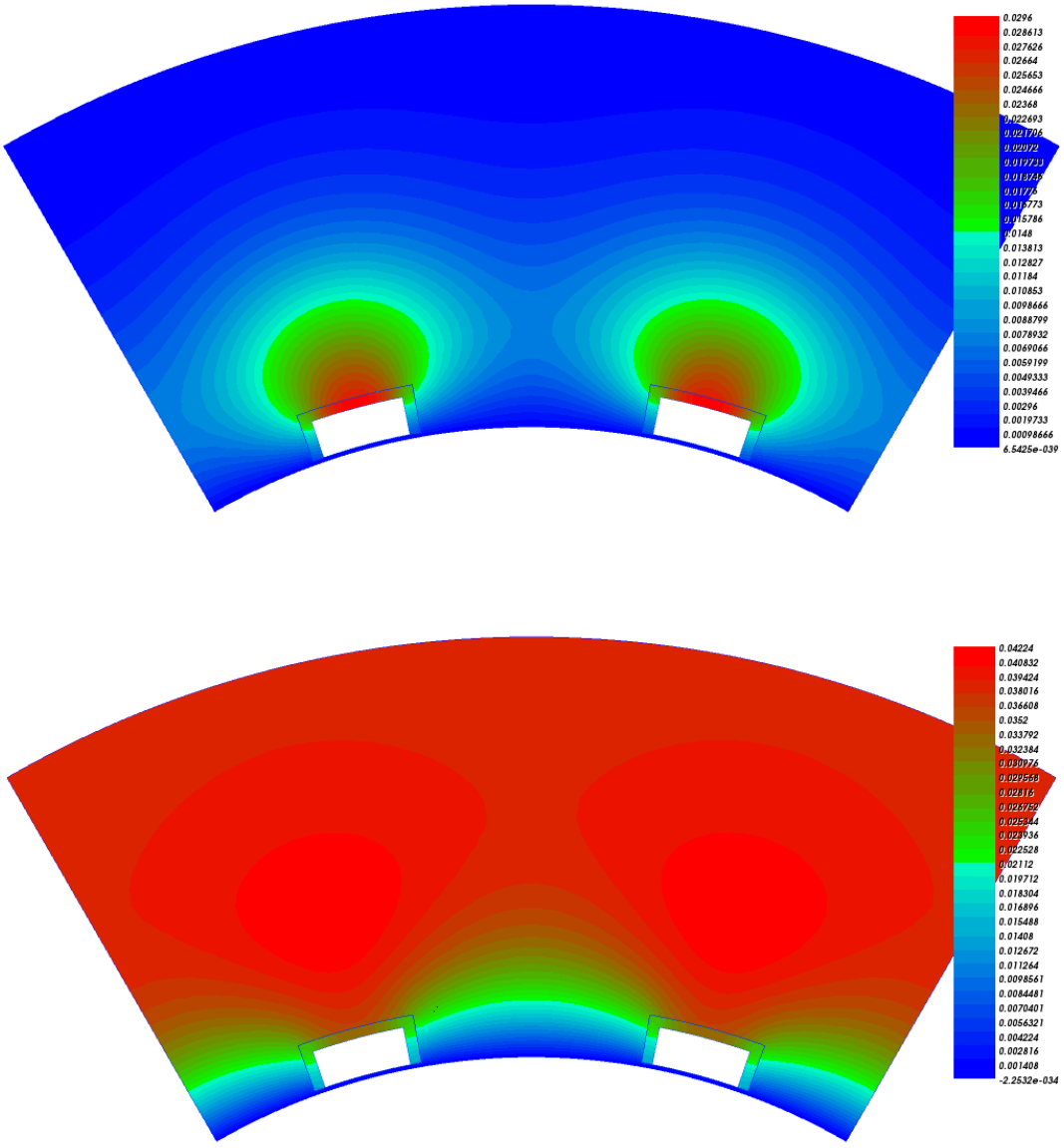

FIGURE 4.2: Distribution of heparin in the arterial wall in the models without binding sites (top) and with binding sites (bottom) after 30 days.

Distribution of heparin in the arterial wall, with and without binding, after 30 days is plotted in Figure 4.2. Figure 4.3 illustrates the evolution of the mass of heparin mass with and without binding. We remark that when binding occurs the drug has a longer residence time in the arterial wall. We observe that the concentration of drug in the arterial wall, when affinity between drug and living tissue occurs, is higher than in the case of non affinity.

Taxus^{TM} paclitaxel eluting stent from Boston Scientific, Natick, MA, USA, applies paclitaxel, a fairly hyrophobic drug ($K_b = 400$), as a therapeutic agent

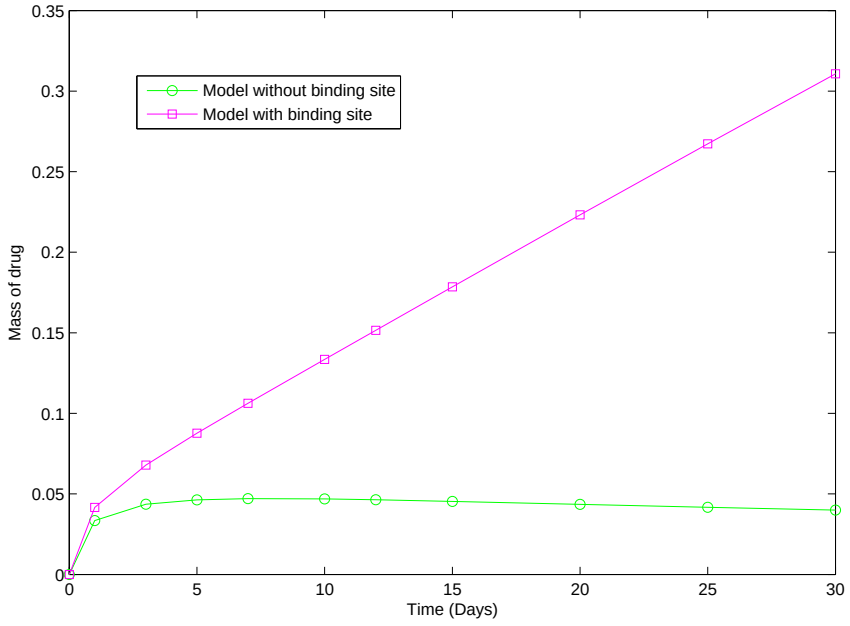

FIGURE 4.3: Evolution of the mass of heparin in the arterial wall with and without binding sites during 30 days.

to control migration of smooth muscle cells from endothelium caused by in-stent restenosis. Heparin, a hydrophobic drug ($K_b = 60$), is used in Carmeda BioActive Surface (CBAS) heparin coating made by Carmeda, Upplands Vasby, Stockholm, Sweden.

It should be noted that drugs like sirolimus ($K_b = 1700$), known also as rapamycin, which is loaded in sirolimus eluting stent from Cordis, Johnson & Johnson, Miami Lake, FL, USA, and also everolimus ($K_b = 1700$) loaded in XIENCE V^{TM} everolimus eluting stent manufactured by Abbott Vascular, Santa Clara, CA, USA, are more hydrophobic than paclitaxel and are used to remain in the arterial wall for a longer period.

Distribution of heparin and paclitaxel in the arterial wall after 30 days are illustrated in Figure 4.4, while the evolution of the masses of heparin and paclitaxel, released from drug eluting stents in the arterial wall are compared in Figure 4.5. We observe that resident time of paclitaxel is higher than of the heparin. This means that heparin leaves the arterial wall faster than the paclitaxel.

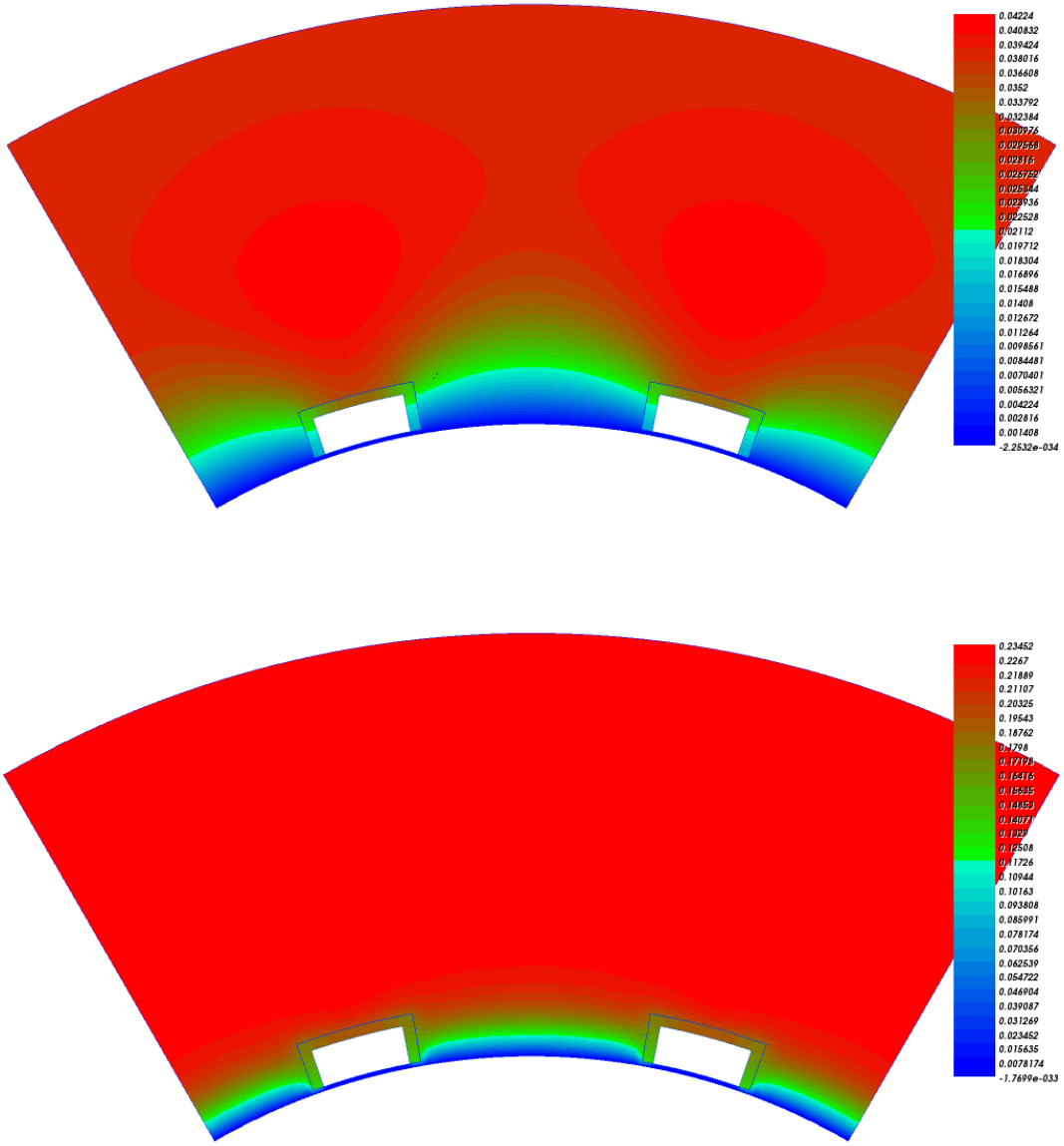

FIGURE 4.4: Distribution of heparin (top) and paclitaxel (bottom) in the arterial wall after 30 days.

Evolution of paclitaxel in a healthy coronary artery with Young modulus $\kappa_r = 1.2$ MPa ([17]) is compared with a highly diseased coronary artery with Young modulus $\kappa_r = 4.1$ MPa ([30]) in Figure 4.6. When κ_r increases due to age or atherosclerosis, less drug penetrates to the coronary wall in the beginning of the process. A crossing occurs around day 7. This result is justified by the fact that the stiffness of the arterial wall imposes a resistance to the penetration of the drug in the beginning of the process and leads to a drug accumulation in the long time.

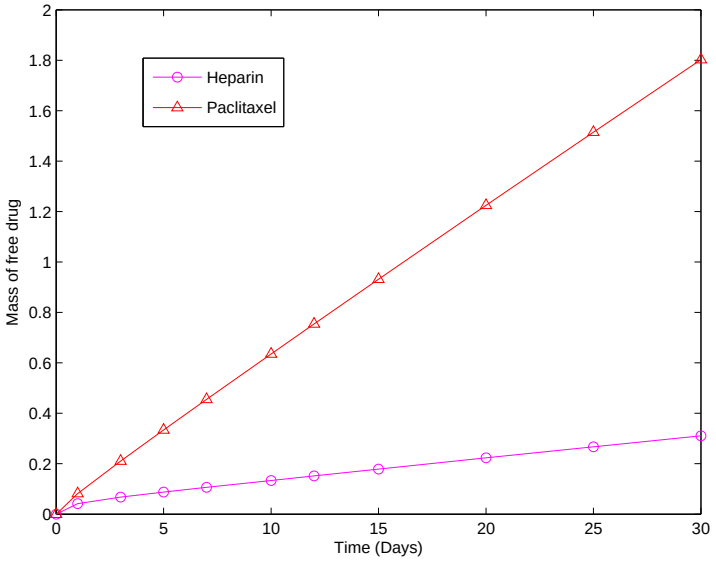

FIGURE 4.5: Evolution of masses of heparin and paclitaxel in the arterial wall during 30 days.

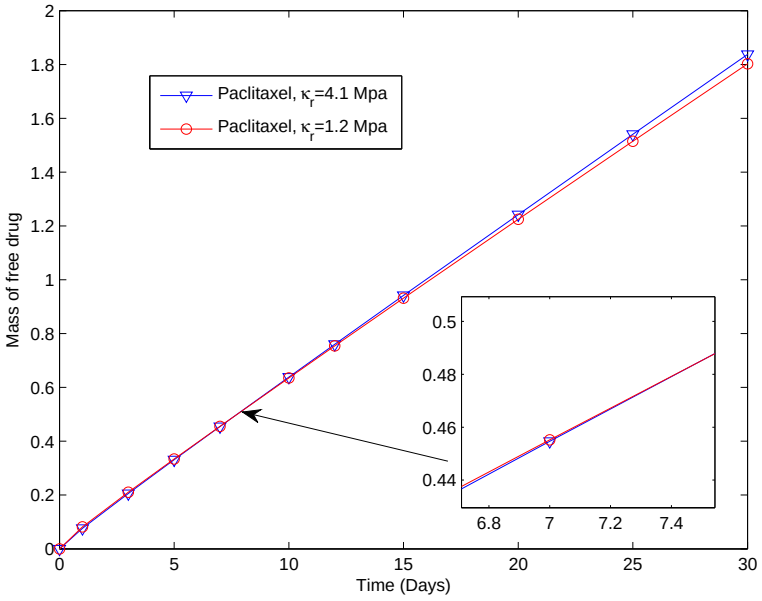

FIGURE 4.6: Evolution of the mass of free paclitaxel in the healthy and diseased arterial wall during 30 days.

Figure 4.7 shows that the amount of bounded paclitaxel in the healthy artery is larger than in the diseased artery.

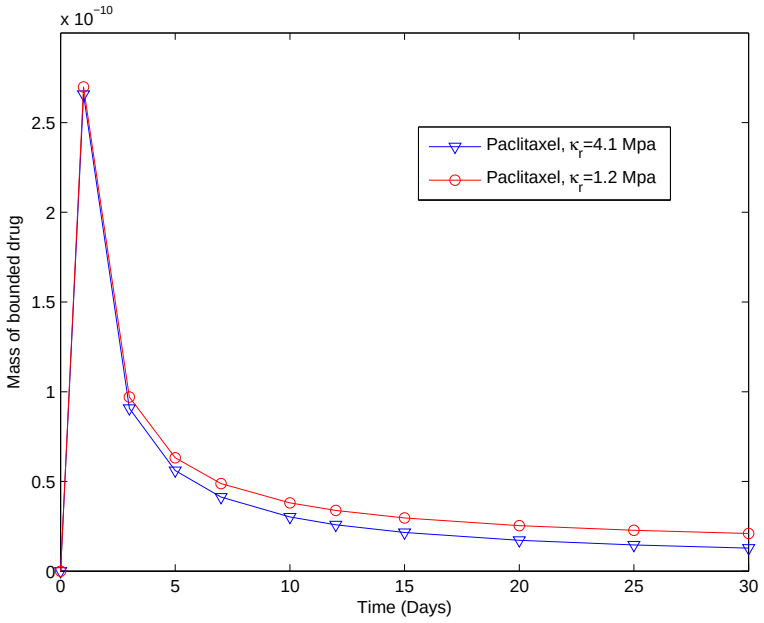

FIGURE 4.7: Evolution of the mass of bound paclitaxel in the healthy and diseased arterial wall during 30 days.

In this chapter we studied the influence of reversible binding sites on the drug release from a DES to an arterial wall. The mathematical model and the time discrete finite element method used in the numerical simulations were obtained modifying the mathematical model and the method of Chapter 3 to include binding and unbinding effects. The numerical results highlight the difference between the behaviour of a hydrophilic drug like heparin and a hydrophobic drug like paclitaxel.

Chapter 5

Conclusions and Future Work

5.1 *Conclusions*

In this thesis we presented some coupled models to simulate the release of a therapeutic agent from a drug eluting stent into the arterial wall. Different types of interface and natural boundary conditions are taken into consideration based on the physiological assumptions of the problem. The coating of the stent is assumed to be biodegradable, viscoelastic properties of the arterial wall and affinity between drug and vessel walls are considered in the complete model studied in Chapters 3 and 4 . From a theoretical viewpoint, appropriate variational formulations for mathematical models have been introduced and energy estimates for the continuous and fully discrete models have been established. We have introduced IMEX finite element methods to solve the initial boundary value problems associated to the system of equations of the models.

From the numerical viewpoint some particular aspects of clinical importance such as sensitivity to the effective parameters that characterize the biodegradable polymeric stent, the influence of the viscoelasticity of the arterial wall, the effect of permeability of the stent coating and the effect of reversible binding reaction in the release of different drugs are addressed in the thesis.

Regarding the biodegradable polymer, it is illustrated that the drug release from a biodegradable stent is faster than the release of drug from a non-biodegradable stent. This finding, which was obviously expected, has been quantified. We believe that this quantification should be taken into consideration in the design of stents, that is in the selection of the polymer and the initial concentration of drug.

Concerning the second clinical aspect, we showed that during an initial period of time the permeation of the drug in the arterial wall is affected by its stiffness i.e. the total mass of drug that enters into the arterial wall is a decreasing function of the Young modulus. Patients who need a cardiovascular stent generally have atherosclerosis and consequently stiffer arterial walls, that is they have higher Young modulus. To prevent an inflammatory response and the smooth muscle cell growth, a correct concentration of the drug must penetrate into the arterial wall from the moment that the stent is implanted. Our findings suggest that the initial concentration of the drug in the stent should be tailored to the rheological properties of the arterial wall.

The third clinical aspect that we want to stress is the control of the release profile according to the permeability of the coating: release can be speeded up or delayed as different polymers are used. Application of different topcoats may alter the penetration rate of the drug from the stent into the arterial wall.

Our last clinical finding is the effect of reversible binding reaction in the release of different drugs. We observed that a hydrophobic drug such as paclitaxel stays longer than a hydrophilic drug like heparin in the arterial wall. This result can help to construct more effective drug eluting stents in the future.

Although our numerical results have been validated from a qualitative viewpoint using data extracted from scientific works, by leading experts in the cardiovascular drug delivery field, a comparison of the model with experimental results would open new routes of research.

5.2 *Future work*

Viscoelastic properties of the polymeric stent

It is known that polymers like PLA exhibit viscoelastic properties influenced by the degradation of the polymer into smaller molecules. In recent years several models have been proposed to describe non-Fickian diffusion in polymers by introducing viscoelastic properties ([6]). Much less attention has been devoted to the mathematical modeling of viscoelasticity of the polymeric coating of the stent in drug release.

We plan to address this problem in the near future by using appropriate linear viscoelastic model such as *Maxwell-Viechert* Model. We believe this will open a new research line to develop optimal design for drug eluting stents.

Bioabsorbable drug eluting stents

Recently some leading companies in the design of cardiovascular stents, such as Abbott Vascular, Santa Clara, CA, USA, and Boston Scientific, Natick, MA, USA, have started to design a new generation of drug eluting stents named bioabsorbable stents. This type of stent is mostly made by completely bioabsorbable polymers with stent strut made by biocompatible metals like magnesium, iron or other alloys. These metals are resorbed from the body after around three months, which corresponds to the most critical period after stent implantation. In current biodegradable DES, manufacturers use metals like titanium or chromium which are not metabolized by the body. This fact have several drawbacks as for example causing a late stent thrombosis.

ABSORB which has been recently launched by Abbott Vascular is a bioresorbable vascular scaffold system that elutes everolimus in a similar way to the drug eluting stent XIENCE V^{TM} and then is naturally resorbed leaving no permanent scaffold. ABSORB is composed of four key design elements: a bioresorbable scaffold (Poly (L-lactide)), a bioresorbable coating (poly (D,L lactide)), everolimus and the XIENCE V^{TM} delivery system.

To model this next generation of stents, new reaction equations and modified interface and boundary conditions are needed. To the best of our knowledge, mathematical modeling, numerical and theoretical studies of this kind of stents have not been yet in the literature. We plan to model, in the time coming, drug delivery from ABSORB into a viscoelastic vessel.

Bibliography

[1] S. D. Abramowitch and S. L.-Y. Woo, *A new analytical approach to evaluate the viscoelastic properties of the goat medial collateral ligament using the quasilinear viscoelastic theory*, Proceedings of the Summer Bioengineering Conference, ASME, Key Biscayne, Florida, (2003), pp. 47–92.

[2] G. Acharya and K. Park, *Mechanisms of controlled drug release from drug-eluting stents*, Advanced Drug Delivery Reviews, 58 (2006), pp. 387–401.

[3] R. Adams and J. Fournier, *Sobolev Spaces*, Elsevier 2nd edition, 2003.

[4] D. Boffi, F. Brezzi, and M. Fortin, *Mixed Finite Element Methods and Applications*, Springer Series in Computational Mathematics, Vol 44, 2013.

[5] A. Borghi, E. Foa, R. Balossino, F. Migliavacca, and G. Dubini, *Modelling drug elution from stents: effects of reversible binding in the vascular wall and degradable polymeric matrix*, Computer Methods in Biomechanics and Biomedical Engineering, 11 (2008), pp. 367–377.

[6] H. F. Brinson and L. C. Brinson, *Polymer Engineering Science and Viscoelasticity: An Introduction*, Springer, 2010.

[7] Z. Chen, G. Huan, and Y. Ma, *Computational Methods for Multiphase Flows in Porous Media*, Computational Science and Engineering, SIAM, 2006.

[8] D. Cohen and A. B. White, Jr., *Sharp fronts due to diffusion and viscoelastic relaxation in polymers*, SIAM Journal on Applied Mathematics, 51 (1991), pp. 472–483.

[9] J. Crank and G. S. Park, *Diffusion in Polymers*, Academic Press, 1968.

[10] D. A. Edwards and D. S. Cohen, *A mathematical model for a dissolving polymer*, AIChE Journal, 41 (1995), pp. 2345–2355.

[11] L. C. Evans, *Partial Differential Equations*, American Mathematical Society, 1998.

[12] J. A. Ferreira, P. de Oliveira, and P. M. Silva, *Reaction–diffusion in viscoelastic materials*, Journal of Computational and Applied Mathematics, 236 (2012), pp. 3783–3795.

[13] J. A. Ferreira, M. Grassi, E. Gudiño, and P. de Oliveira, *A 3D Model for Mechanistic Control of Drug Release*, SIAM Journal on Applied Mathematics, 74 (2014), pp. 620–633.

[14] J. A. Ferreira, M. Grassi, E. Gudiño, and P. de Oliveira, *A new look to non-Fickian diffusion*, Applied Mathematical Modelling, 39 (2015), pp. 194–204.

[15] J. A. Ferreira, E. Gudiño, and P. de Oliveira, *Analytical and Numerical Study of Memory Formalisms in Diffusion Processes*, Modelling and Simulation in Fluid Dynamics in Porous Media, Springer Proceedings in Mathematics and Statistics, J. A. Ferreira, S. Barbeiro, G. Pena and M. F. Wheeler (editors), 28 (2013), pp. 67–85.

[16] Y. C. Fung, *Biomechanics: Mechanical Properties of Living Tissues*, Springer-Verlag, 1993.

[17] B. S. Gow and C. D. Hadfield, *The elasticity of canine and human coronary arteries with reference to postmortem changes*, Circulation Research, 45 (1979), pp. 588–594.

[18] M. Grassi, G. Pontrelli, L. Teresi, G. Grassi, L. Comel, A. Ferluga, and L. Galasso, *Novel design of drug delivery in stented arteries: a numerical comparative study*, Mathematical Biosciences and Engineering, 6 (2009), pp. 493–508.

[19] F. Hecht, *freeFEM++, Third Edition, Version 3.20*, tech. report.

[20] T. Khamdaeng, J. Luo, J. Vappou, P. Terdtoon, and E. E. Konofagou, *Arterial stiffness identification of the human carotid artery using the stress-strain relationship in vivo*, Ultrasonics, 52 (2012), pp. 402–411.

[21] M. Kohandel, S. Sivaloganathan, and G. Tenti, *Estimation of the quasi-linear viscoelastic parameters using a genetic algorithm*, Mathematical and Computer Modelling, 47 (2008), pp. 266–270.

[22] Q. Liu and D. Kee, *Modeling of diffusion through polymeric membranes*, Rheologica Acta, 44 (2004), pp. 287–294.

[23] Q. Liu, X. Wang, and D. De Kee, *Mass transport through swelling membranes*, International Journal of Engineering Science, 43 (2005), pp. 1464–1470.

[24] F. Migliavacca, F. Gervaso, M. Prosi, P. Zunino, S. Minisini, L. Formaggia, and G. Dubini, *Expansion and drug elution model of a coronary stent*, Computer Methods in Biomechanics and Biomedical Engineering, 10 (2007), pp. 63–73.

[25] F. Migliavacca, L. Petrini, V. Montanari, I. Quagliana, F. Auricchio, and G. Dubini, *A predictive study of the mechanical behaviour of coronary stents by computer modelling*, Medical Engineering & Physics, 27 (2005), pp. 13–18.

[26] S. Minisini, *Mathematical and Numerical Modeling of Controlled drug release*, PhD thesis, Politecnico di Milano, 2009.

[27] A. Muliana and K. R. Rajagopal, *Changes in the response of viscoelastic solids to changes in their internal structure*, Acta Mechanica, 217 (2010), pp. 297–316.

[28] A. H. Muliana and K. R. Rajagopal, *On the response of viscoelastic biodegradable polymeric solids*, Mechanics Research Communications, 39 (2012), pp. 51–58.

[29] A. Nekouzadeh, K. M. Pryse, E. L. Elson, and G. M. Genin, *A simplified approach to quasi-linear viscoelastic modeling*, Journal of Biomechanics, 40 (2007), pp. 3070–3078.

[30] I. Ozolanta, G. Tetere, B. Purinya, and V. Kasyanov, *Changes in the mechanical properties, biochemical contents and wall structure of the human coronary arteries with age and sex*, Medical Engineering & Physics, 20 (1998), pp. 523–533.

[31] G. Pontrelli, *The role of the arterial prestress in blood flow dynamics*, Medical Engineering & Physics, 28 (2006), pp. 6–12.

[32] G. Pontrelli and F. de Monte, *Mass diffusion through two-layer porous media: an application to the drug-eluting stent*, International Journal of Heat and Mass Transfer, 50 (2007), pp. 3658–3669.

[33] ——, *A multi-layer porous wall model for coronary drug-eluting stents*, International Journal of Heat and Mass Transfer, 53 (2010), pp. 3629–3637.

[34] S. Prabhu and S. Hossainy, *Modeling of degradation and drug release from a biodegradable stent coating*, Journal of Biomedical Materials Research. Part A, 80 (2007), pp. 732–741.

[35] A. Raval, J. Parikh, and C. Engineer, *Mechanism of controlled release kinetics from medical devices*, Brazilian Journal of Chemical Engineering, 27 (2010), pp. 211–225.

[36] J. N. Reddy, *An Introduction to the Finite Element Method*, McGraw-Hill; 3rd edition, 2005.

[37] J. M. Schakenraad, M. J. Hardonk, J. Feijen, I. Molenaar, and P. Nieuwenhuis, *Enzymatic activity toward poly(L-lactic acid) implants*, Journal of Biomedical Materials Research, 24 (1990), pp. 529–545.

[38] J. Siepmann and A. Göpferich, *Mathematical modeling of bioerodible, polymeric drug delivery systems*, Advanced Drug Delivery Reviews, 48 (2001), pp. 229–247.

[39] J. S. Soares, *Constitutive Modeling for Biodegradable Polymers Application in Endovascular Stents*, PhD thesis, Mechanical Engineering, Texas A&M University, 2008.

[40] J. S. Soares, J. E. Moore, and K. R. Rajagopal, *Modeling of deformation accelerated breakdown of polylactic acid biodegradable stents*, Journal of Medical Devices, 4 (2010), p. 41007.

[41] Y. Tao, *Nonlinear Viscoelastic Properties and Constitutive Modeling of Blood Vessel*, Master's thesis, National University of Singapore, 2009.

[42] K. L. Troyer, D. Estep, and C. M. Puttlitz, *Viscoelastic effects during loading play an integral role in soft tissue mechanics*, Acta Biomaterialia, 8 (2012), pp. 234–243.

[43] V. Tuoi, *Mathematical Analysis of Some Models for Drug Delivery*, PhD thesis, National University of Ireland, 2012.

[44] C. Vergara and P. Zunino, *Multiscale boundary conditions for drug release from cardiovascular stents*, Multiscale Modeling & Simulation, 7 (2008), pp. 565–588.

[45] F. Zhang, M. Fath, R. Marks, and R. Linhardt, *A highly stable covalent conjugated heparin biochip for heparin-protein interaction studies*, Analytical Biochemistry, 304 (2002), pp. 271–273.

[46] P. Zunino, *Multidimensional pharmacokinetic models applied to the design of drug-eluting stents*, Cardiovascular Engineering, 4 (2004), pp. 181–191.